

Organic Geochemistry
Incorporation of water-derived hydrogen into methane during artificial maturation of source rock under hydrothermal conditions
--Manuscript Draft--

Manuscript Number:	OG-5031R2
Article Type:	Research Paper
Keywords:	methane; natural gas generation kinetics; D/H ratios; kerogen; clumped isotopologues; hydrogen isotope exchange; water isotopes
Corresponding Author:	David T. Wang, Ph.D. ExxonMobil Upstream Research Company Spring, Texas UNITED STATES
First Author:	David T. Wang, Ph.D.
Order of Authors:	David T. Wang, Ph.D. Jeffrey S. Seewald Eoghan P. Reeves Shuhei Ono Sean P. Sylva
Abstract:	To investigate the origin of C–H bonds in thermogenic methane (CH ₄), a solvent-extracted sample of organic-rich Eagle Ford shale was reacted with heavy water (D ₂ O) under hydrothermal conditions (350 bar) in a flexible Au-TiO ₂ cell hydrothermal apparatus at a water-to-rock ratio of approximately 5:1. Temperature was increased from 200 to 350 °C over the course of one month and the concentrations of aqueous species and methane isotopologues were quantified as a function of time. In general, production of hydrogen, CO ₂ , alkanes, and alkenes increased with time and temperature. Methane formed during the early stages of the experiment at 200 °C was primarily C ₁ H ₄ with some CH ₃ D. With progressively higher temperatures, increasing proportions of deuterated isotopologues were produced. Near the end of the experiment, the concentration of CD ₄ exceeded that of all other isotopologues combined. These results suggest that competition between rates of kerogen-water isotopic exchange and natural gas generation may govern the D/H ratio of thermogenic gases. Furthermore, hydrogenation of kerogen by water may be responsible for hydrocarbon yields in excess of those predicted by conventional models of source rock maturation in which hydrocarbon generation is limited by the amount of organically-bonded hydrogen.

Highlights

- Substantial amounts of deuterium are incorporated into generated methane when source rock is heated in the presence of D₂O under hydrothermal conditions.
- Much of the H in thermogenic natural gases may derive from water.
- Gas generation may not be limited by the HI of sedimentary organic matter.

1 Title:

2 Incorporation of water-derived hydrogen into methane during artificial maturation of source rock under
3 hydrothermal conditions

4

5 Submitted to *Organic Geochemistry* on 05 February 2022. Revised manuscript submitted 13 July 2022.

6

7

8 Authors and affiliations:

9 David T. Wang^{a,b*}, Jeffrey S. Seewald^b, Eoghan P. Reeves^c, Shuhei Ono^a, and Sean P. Sylva^b

10 ^aDepartment of Earth, Atmospheric and Planetary Sciences, Massachusetts Institute of Technology, Cambridge, Massachusetts 02139, USA.

11 ^bMarine Chemistry and Geochemistry Department, Woods Hole Oceanographic Institution, Woods Hole, Massachusetts 02543, USA.

12 ^cDepartment of Earth Science, University of Bergen, Bergen N-5007, Norway.

13

14 * Corresponding author. Present address: Esso Exploration and Production Guyana Ltd, 86 Duke Street,
15 Georgetown, Guyana. *E-mail address:* dtw@alum.mit.edu (D.T. Wang).

16

17 *Keywords:*

18 methane, natural gas generation kinetics, D/H ratios, kerogen, clumped isotopologues, hydrogen isotope
19 exchange, water isotopes

20

21 **Abstract**

22 To investigate the origin of C–H bonds in thermogenic methane (CH_4), a solvent-extracted sample of organic-rich
23 Eagle Ford shale was reacted with heavy water (D_2O) under hydrothermal conditions (350 bar) in a flexible Au-
24 TiO_2 cell hydrothermal apparatus at a water-to-rock ratio of approximately 5:1. Temperature was increased from
25 200 to 350 °C over the course of one month and the concentrations of aqueous species and methane isotopologues
26 were quantified as a function of time. In general, production of hydrogen, CO_2 , alkanes, and alkenes increased
27 with time and temperature. Methane formed during the early stages of the experiment at 200 °C was primarily
28 C^1H_4 with some CH_3D . With progressively higher temperatures, increasing proportions of deuterated
29 isotopologues were produced. Near the end of the experiment, the concentration of CD_4 exceeded that of all other
30 isotopologues combined. These results suggest that competition between rates of kerogen-water isotopic
31 exchange and natural gas generation may govern the D/H ratio of thermogenic gases. Furthermore,
32 hydrogenation of kerogen by water may be responsible for hydrocarbon yields in excess of those predicted by
33 conventional models of source rock maturation in which hydrocarbon generation is limited by the amount of
34 organically-bonded hydrogen.

35

36 Abstract: 194 words

37 Main Text: 6923 words

38

39

40

41 1. INTRODUCTION

42 Variation in D/H ratios (δD values) of thermogenic natural gases is often attributed to kinetically-controlled
43 fractionation during pyrolysis of kerogen or petroleum. A number of studies have investigated how D/H ratios of
44 methane and other hydrocarbons evolve with increasing thermal maturity (Sackett, 1978; Berner et al., 1995;
45 Sackett and Conkright, 1997; Tang et al., 2005; Ni et al., 2011; Reeves et al., 2012). However, kinetic isotope
46 effects involving hydrogen addition or abstraction are often large and by themselves do not explain the
47 geologically-reasonable apparent equilibrium temperatures of ~150 to 220 °C obtained for reservoir gases that
48 have been studied for their clumped isotopologue compositions (Stolper et al., 2014, 2015; Wang et al., 2015;
49 Douglas et al., 2017; Young et al., 2017; Shuai et al., 2018; Giunta et al., 2019; Labidi et al., 2020; Thiagarajan et
50 al., 2020). There is also evidence that δD values of CH_4 approach values expected for isotopic equilibrium
51 between CH_4 and H_2O in formation waters at temperatures characterizing reservoirs and/or mature source rocks
52 (~150 to 250 °C) (Clayton, 2003; Wang et al., 2015; Xie et al., 2021), although findings of insignificant hydrogen
53 exchange occurring under these conditions also exist (Yeh and Epstein, 1981). In order for methane samples to
54 have approached or attained equilibrium values of $\Delta^{13}\text{CH}_3\text{D}$ and $\Delta^{12}\text{CH}_2\text{D}_2$ —parameters that describe the
55 abundances of clumped isotopologues relative to a stochastic population of molecules containing isotopes
56 randomly distributed amongst them—there must be a pathway by which either (i) isotopes can be exchanged
57 amongst methane isotopologues alone, (ii) methane isotopologues exchange hydrogen with water or other organic
58 molecules, or (iii) methane isotopologues are derived from methyl moieties which contain C–H bonds that have
59 previously exchanged with water prior to forming methane (Hoering, 1984; Smith et al., 1985; Schimmelmann et
60 al., 1999, 2006; Lis et al., 2006).

61 Here, we study the origin of C–H bonds in thermogenic methane by heating a powdered solvent-extracted source
62 rock in the presence of D_2O , and examining the degree of deuteration in the generated methane. This experiment
63 is conceptually very similar to ones conducted by Hoering (1984), Lewan (1997), and Schimmelmann et al.
64 (2001). The experiments in those studies were designed to track incorporation of D into bitumen and kerogen,
65 and none specifically quantified the extent of deuteration in the produced natural gases.

66 2. MATERIALS AND METHODS

67 2.1. Experimental materials and equipment

68 Experiments were conducted in a gold-titanium reaction cell housed within a flexible cell hydrothermal apparatus
69 (Seyfried et al., 1987) at the Woods Hole Oceanographic Institution (WHOI). Prior to use, the titanium surfaces in
70 contact with the reaction cell contents were heated in air for 24 h at 400 °C to form a more inert TiO_2 surface
71 layer. The reaction cell was further pre-treated prior to loading by soaking in concentrated HCl for 4 hours,
72 followed by rinsing with water to pH neutral and drying in the oven. The exit tube of the apparatus was cleaned
73 by forcing ~20 ml of MilliQ deionized water (18.2 MΩ) through, followed by ~20 ml concentrated HCl, ~100 ml
74 water, ~20 ml concentrated HNO_3 , and then ~100 ml of water until the pH tested 7 using pH paper.

75 The source material for this experiment was a hand sample of Upper Cretaceous Eagle Ford Shale taken from an
76 outcrop in Uvalde County, Texas, USA (Hentz and Ruppel, 2010). There is no known oil or gas production from
77 the Eagle Ford in Uvalde County (Tian et al., 2013; *IHS Markit Well Database*, 2019). The Eagle Ford here is
78 thermally-immature ($R_o = 0.40\text{--}0.55\%$, Cardneaux, 2012; Cardneaux and Nunn, 2013; Harbor, 2011). The sample
79 was powdered to <250 µm and Soxhlet-extracted to remove bitumen and free hydrocarbons. In a subsequent step,
80 the solvent-extracted residue was subjected to hydrochloric acid treatment to remove carbonate minerals.

81 Elemental analysis (**Table 1**) of the original rock sample (UNEX), the Soxhlet-extracted rock sample (EX), and
82 the decalcified+extracted rock sample (DECA) indicates a total organic carbon (TOC) content of ~2.5% and a
83 carbonate content of ~80% by weight. The H/C atomic ratio of the decalcified rock is 2.4. This value is probably
84 several tens of percent higher than the actual H/C ratio of isolated kerogen (not determined) given that substantial
85 amounts of H are likely borne by clays and other minerals that were not removed (Whelan and Thompson-Rizer,
86 1993; Baskin, 1997).

87 Geochemical data for the Eagle Ford sample can be drawn from neighboring Kinney County, Texas, where
88 complete sections of immature Eagle Ford have been recovered by the U.S. Geological Survey (drill core GC-3;
89 French et al., 2020) and Shell (Iona-1 drill core; Eldrett et al., 2014, 2015; Sun et al., 2016); there, the Eagle Ford
90 also crops out, is immature, and is presumed to be geochemically similar. The high calcium carbonate content
91 and relatively lower organic enrichment is consistent with data from the Upper Eagle Ford in the Shell Iona-1
92 core from neighboring Kinney County, Texas (Eldrett et al., 2015).

93 The reaction cell was loaded with 10.03 grams of the EX powder. The starting fluid used was heavy water (D_2O ,
94 99% purity, Cambridge Isotope Laboratories, Inc.) containing NaCl (0.497 mol/kg). The NaCl was added to allow
95 for detection of any leaks in the reaction cell, as dilution of the starting fluid by deionized water from the
96 surrounding pressure vessel would decrease observed Cl concentrations. The reaction cell was loaded with 55.03
97 g of this starting fluid, sealed with a small argon-purged headspace (to allow for expansion of the starting fluid at
98 conditions), and then pressurized and brought to initial condition (200 °C, 350 bar) in approximately 2 h. Several
99 milliliters of fluid were bled during heat-up to purge the exit tube, leaving an estimated 52.6 g of fluid in the cell
100 at the beginning of the experiment (**Table 2**).

101 2.2. Analytical methods

102 To monitor the fluid composition and the extent of deuteration with time, sample aliquots of fluid were withdrawn
103 through the capillary exit tube into gastight glass/PTFE syringes. Immediately prior to a sampling event, a small
104 amount (~0.5 g) of fluid was removed and discarded to flush the exit tube. A fluid sample was taken at the
105 beginning and end of each temperature stage. One additional sample (#4) was drawn in the middle of the second
106 temperature stage (300 °C). At time point #6, two aliquots were drawn, each in separate syringes and sampled
107 into separate vials.

108 Deuterium (D_2) is likely to be the main form of molecular hydrogen (H_2) in our experiment due to rapid exchange
109 between water and dissolved hydrogen (Lécluse and Robert, 1994; Wang et al., 2018). The concentration of H_2
110 was determined after headspace extraction using a gas chromatograph (GC) supplied with nitrogen carrier gas and
111 equipped with a molecular sieve 5Å column and thermal conductivity detector. Concentrations reported in
112 **Table 2** have been corrected for the difference in thermal conductivity between D_2 and 1H_2 (see note *a* of
113 **Table 2**), assuming that all dissolved hydrogen is as D_2 . Analytical reproducibility of H_2 concentration data is
114 ±10% or better (2σ).

115 Concentrations of total dissolved inorganic carbon (ΣCO_2) and C₁ to C₆ hydrocarbons (alkanes and alkenes) were
116 determined using a purge-and-trap cryofocusing device coupled to a gas chromatograph equipped with a Porapak
117 Q column and serially-connected thermal conductivity and flame ionization detectors. Analytical procedures were
118 as described in Reeves et al. (2012). Analytical reproducibility on duplicate samples was ±5% or better (2σ). The
119 C₅ and C₆ compounds could not be quantified accurately due to their semi-volatile nature; however, C₅ and C₆
120 were detected at all sampling points.

At each sampling, a separate ~1 to 2 ml aliquot was injected directly into a pre-weighed, evacuated serum vial capped with boiled blue butyl rubber stoppers, for analysis of the extent of deuteration of methane. A Hewlett-Packard (HP) 6890 gas chromatography-mass spectrometry (GC-MS) system equipped with a 5Å molecular sieve column (HP-PLOT 30 m × 0.32 mm × 12.0 μm) coupled to an HP 5973 mass selective detector was used to determine the amount of deuteration in CH₄. Mass spectrometer source and quadrupole analyzer temperatures were 230 and 150 °C, respectively, and mass spectra were recorded with an electron impact (EI) ionization energy of 70 eV. Ion currents were monitored at integral masses between *m/z* 10 and 50. Extracted ion currents were quantified at *m/z* 14 through 20 for methane. Expected fragmentation patterns of the five methane-*d_n* isotopologues (C¹H₄, CH₃D, CH₂D₂, CHD₃, and CD₄) were determined by analysis of commercial synthetic standards (>98% purity, Cambridge Isotope Laboratories, Inc.). We refer to the fully protiated methane isotopologue as C¹H₄ in the text when it is necessary to specifically distinguish it from bulk CH₄.

3. RESULTS AND DISCUSSION

3.1. Temperature and thermal maturity

Temperatures logged during the experiment are shown in **Fig. 1A**. Using the temperature history, we calculated thermal maturity as a function of time in units of vitrinite reflectance (%R_o) using EASY%Ro (Sweeney and Burnham, 1990). The estimated thermal maturities are plotted in **Fig. 1B**. While the model predicts maturities of ~0.20 to 0.34% R_o-equivalent for time points #1 and 2 (respectively) and the data are plotted at these calculated maturities, the actual maturity at these time points can be no less than 0.4–0.5% (the initial maturity of the Eagle Ford rock sample, see §2.1). The difference between the plotted and actual %R_o values is somewhat immaterial; what is key is that time points #1 and 2 represent source rock that has undergone only incipient organic metamorphism. Maturities encountered in the remainder of the experiment spanned the entire range of the oil window (ca. 0.5% to 1.3% R_o-equivalent; Burnham, 2019). The modeled maturity at the final time point (#9) is 1.27% R_o.

3.2. Concentrations of aqueous species

3.2.1. Inorganic species

Measured concentrations of aqueous species are shown in **Fig. 2**. Concentrations of aqueous H₂ increased from below detection (<13 μmol/kg) to up to 1.1 mmol/kg at the end of the experiment, and increased with each temperature step. The H₂ concentration also rose slightly between the beginning and end of each temperature stage of the experiment.

The concentration of ΣCO₂ increased during the early stages of the experiment, and leveled off at ~50 mmol/kg at 350 °C. The plateauing inorganic carbon concentration suggests that the aqueous solution reached saturation with carbonate minerals (Seewald et al., 1998), a result of CO₂ production during hydrothermal alteration of kerogen (Seewald, 2003), and dissolution of carbonate minerals initially present in the Eagle Ford shale.

3.2.2. Alkanes and alkenes

Concentrations of methane increased in every successive time step, as did concentrations of detected *n*-alkanes. Except for the beginning of the experiment, molar concentrations of C₁ and ΣC_{2–4} were very similar and increased almost in unison.

158 Alkenes (ethylene and propylene, **Fig. 2D–E**) rose in concentration with every increase in temperature, indicating
159 generation of unsaturated hydrocarbons via thermolytic processes. While concentrations of *n*-alkanes increased
160 monotonically from beginning to end of each temperature stage, the concentrations of alkenes remained
161 constant—or in the 350 °C stage, trended downwards—with time during each stage. Concentrations of alkenes
162 consistent with thermodynamic equilibrium at measured H₂ concentrations are on the order of ~10^{-7.4} and ~10^{-6.6}
163 mol/kg for ethylene and propylene, respectively, at 350 °C (Shock et al., 1989; Shock and Helgeson, 1990).
164 Measured concentrations of alkenes were ~2 orders of magnitude higher than alkane-alkene equilibrium
165 predictions, indicating strong disequilibrium in the relative concentration of alkenes and alkanes. Some portion of
166 the ~10^{-6.5} mol/kg of these alkenes present at time point #1 could have been indigenous to the source rock (i.e.,
167 adsorbed and leached out during initial heating).

168 Evidence from hydrothermal experiments suggests that metastable, reversible alkane/alkene equilibrium should
169 be attained under hydrothermal conditions with half-equilibration times of several hundred hours or less at
170 temperatures of 325 to 350 °C (Seewald, 1994, 2001). Failure to achieve thermodynamic equilibrium within
171 these timescales indicates that generation of thermogenic alkenes occurs concurrently with alkane/alkene
172 hydrogen exchange. Various pyrolysis experiments have reported alkene production (Huizinga et al., 1987; Leif
173 and Simoneit, 2000), lending further support to the hypothesis that continued production of alkenes competes with
174 their conversion into alkanes via hydrogenation at these temperatures and timescales and under redox conditions
175 characterizing hydrothermal maturation of organic-rich mudrocks.

176 Unlike the C₂₊ alkanes, methane cannot dehydrogenate to form an alkene. Hence, hydrogen exchange of methane
177 requires that the very stable C–H bond be broken. Under certain conditions, generally requiring the absence of
178 water or other catalyst poisons, methane exchanges hydrogen over certain catalytic materials such as γ-alumina at
179 room temperature over hours to days (Sattler, 2018, and refs. therein) or with organometallic catalysts under even
180 colder conditions (Golden et al., 2001). However, such catalysts in their active forms are not known to occur
181 naturally in aqueous environments. Experiments conducted by Reeves et al. (2012) with aqueous methane in the
182 presence of iron-bearing minerals in similar flexible-cell Au-TiO₂ reaction vessels revealed only minimal
183 potential exchange over several months, even at temperatures as high as 323 °C. Recently, Turner et al. (2022)
184 conducted a set of experiments in flexible gold-cell hydrothermal reactors with CH₄ dissolved in supercritical
185 water at 376 to 420 °C to specifically constrain the rate of CH₄–H₂O hydrogen isotope exchange. Their results
186 confirm that exchange occurs over timescales of hundreds of years at 300 °C and tens of years at 350 °C (half-
187 exchange time, τ_{1/2}), much longer than the duration of our experiment.

188 3.3. Production of deuterated methane isotopologues

189 Mass spectra collected for standards are shown in **Fig. 3A**. Relative fragment intensities were similar to those
190 determined in early studies from the U.S. National Bureau of Standards (Dibeler and Mohler, 1950; Mohler et al.,
191 1958). Mass spectra of samples are shown in **Fig. 3B**. No methane peaks of usable size could be obtained for
192 time point #1. All other time points yielded quantifiable extracted ion chromatogram peaks.

193 The mass spectra of commercial standards were used to fit the sample data using a constrained linear least-squares
194 solver (LSQNONNEG) implemented in MATLAB.¹ Estimated fractional abundances of methane-*d* isotopologues at

¹ This deconvolution scheme has been used to derive concentrations of methane-*d* isotopologues from mass spectral data for a separate experimental exchange study (A. Sattler, pers. comm.).

each time point are shown in **Fig. 4A**.² While it is not straightforward to quantify the uncertainty in these fractional abundances, comparison of the calculated results for samples #6(1) and 6(2) suggests the random error is unlikely to be so large as to affect our interpretation of the overall trends below. Some systematic error is likely present as we did not correct the mass spectra for the ^{13}C isotope or for isotopic impurities in the standards. Fractional abundances for each of the isotopologues were converted into absolute abundances (**Fig. 4B**) by multiplying by the methane concentration. The proportion of D in methane-bound hydrogen, calculated from the relative isotopologue abundances, is shown in **Fig. 5**.

Methane formed during the early stages of the experiment at 200 °C was primarily C^1H_4 with some CH_3D , whereas at higher temperatures the isotopologues produced consisted almost exclusively of CD_4 , CHD_3 , and CH_3D (**Fig. 4A** and **Fig. 5**). These results suggest that at relatively lower temperatures of ~200 °C, the rate of methane generation approaches or exceeds the rate of D/H exchange between water and kerogen, whereas at higher temperatures, extensive D/H exchange between kerogen (or petroleum, if it is also a precursor of methane) and water occurs prior to methane generation. CD_4 became the dominant methane species at temperatures of 300 °C and above, suggesting that more than 50% of all labile, methane-generating sites on kerogen were fully deuterated by this time. As discussed above, uncatalyzed CH_4 – D_2O isotopic exchange at this temperature occurs over a much longer timescales than the short (~1 month) duration of our laboratory experiment. There is a possibility of mineral catalysis on the surfaces of the source rock powder used in the experiment, which we cannot rule out given the setup of our experiment. However, the minimal degree of isotopic exchange observed by Reeves et al. (2012) at temperatures of 323 °C and timescales of ~1 year in the presence of redox-active minerals (pyrite, pyrrhotite, and magnetite) suggests that direct exchange of CH_4 with D_2O in our experiment is probably unimportant.³

Production of C^1H_4 in the first stage of the experiment (200 °C) indicates that the earliest “capping” hydrogen derives from kerogen or other H-containing species in the rock as opposed to from the H atoms of water. This can only be the case if kerogen has not yet undergone D/H exchange.⁴ While constraints on timescales of D/H exchange at 200 °C are sparse, the available literature supports this assertion. Experiments conducted with model hydrocarbons indicate that D/H exchange of carbon-bound H at 200 °C takes at least several decades, much longer than the heating time in our experiment (Sessions et al., 2004; Schimmelmann et al., 2006; Sessions, 2016; and refs. therein).

Production of C^1H_4 and CH_3D appeared to cease by midway through the 300 °C stage (time point #4, 284 hours), or was overshadowed by the generation of much larger quantities of the higher isotopologues. Continued (though relatively minor) production of methane that was not fully-deuterated (CHD_3 and CH_3D , **Fig. 4B**) suggests that the kerogen (or petroleum) from which methane was generated still did not fully exchange before methane formed.

² Results of this experiment were first presented in the appendix of a Ph.D. thesis (Wang, 2017). That earlier analysis contained a mathematical error (neglected to divide by the relative peak areas of the pure isotopologue standards). As a result, Fig. B.3 of that thesis appears different than **Fig. 4** in this paper.

³ While it is not an important factor in exchange between CH_4 and D_2O , the source rock matrix is likely important as a catalyst for the exchange of kerogen-bound H with D_2O (prior to methane generation), a process discussed in §3.4.2 and in Alexander et al. (1984).

⁴ It is conceivable that the C^1H_4 observed at time point #2 may have been gas originally present but sorbed to a solid phase at the start of the experiment and later leached into the fluid, but we consider this unlikely because Soxhlet extraction should have removed nearly all of the CH_4 initially sorbed. Furthermore, the concentration of methane tripled between time points #1 (19 h) and #2 (164 h). Release of sorbed gases was probably nearly complete by 19 h.

If significant exchange were to occur, either between water and kerogen, or between water and methane generated by thermal degradation of longer chain products, and this exchange occurs sequentially, the predominant isotopologue would be expected to follow the progression $\text{C}^1\text{H}_4 \rightarrow \text{CH}_3\text{D} \rightarrow \text{CH}_2\text{D}_2 \rightarrow \text{CHD}_3 \rightarrow \text{CD}_4$. Instead, CH_2D_2 represents a smaller fraction of the methane isotopologues than either CH_3D or CHD_3 at all times, and calculated proportions of CH_2D_2 do not exceed 10% at any point in the experiment (**Fig. 4A**). A possible explanation is that various CH_x moieties (e.g., aromatic C vs. methylene C vs. heteroatom-bound C) of the kerogen or generated petroleum have significantly different propensities to undergo exchange and hydrogenation (Schimmelmann et al., 2006). Thermal degradation that occurs much slower or faster than exchange may yield either fully-deuterated kerogen (e.g., $-\text{CD}_3$) or singly-deuterated methane, respectively, hence leading to an absence of CH_2D_2 . Alternatively (or possibly in addition), D/H exchange of partially-deuterated longer-chain hydrocarbon molecules with water may be faster than degradation, such that the production of CH_2D_2 is bypassed. The selective production of deuterated methane isotopologues is additional evidence that exchange between water/methane or methane/methane at temperatures of 200 to 350 °C is slow on timescales relevant to laboratory experiments.⁵

Comparison of our results with those of Wei et al. (2019), who examined CH_4 generation from petroleum source rock heated under hydrothermal conditions, reveals similar thermal maturity trends for the extent of CH_4 deuteration (**Fig. 5A**). Both studies yielded methane with an increasing percentage of water-derived hydrogen as thermal maturity increased. The deuteration vs. maturity trends are sub-parallel to each other. The observed offset between the Wei et al. experimental results and ours (**Fig. 5A**) is probably due to the different source rocks and experimental conditions, including the use of D_2O instead of normal water as the aqueous medium in our experiments. By the middle of the oil window (0.75–0.9% R_o), methane in both studies contained more than 50% of its hydrogen content derived from water.

In a differently-constructed study, Dias et al. (2014) evaluated incorporation of aqueous hydrogen into gaseous products during hydrous pyrolysis of bituminous coal samples taken from the same coal seam along a transect at various distances away from an igneous intrusion (and hence with different initial R_o values ranging from 0.5 to 6.8%). After hydrous pyrolysis, measured R_o values ranged from 1.4 to 6.9%. An observed dependence of δD of CH_4 to δD of water allowed them to differentiate native (sorbed or trapped) and newly-generated (via hydrous pyrolysis) hydrocarbon gases, with almost all (>90%) of CH_4 generated from coals with initial $R_o < 2.0\%$ being of newly-generated origin. While the design of their experiment did not allow for quantification of the fractional contribution of water-derived H to the hydrogen content (and hence cannot be plotted on Fig. 5A), their results are consistent with incorporation of aqueous hydrogen into hydrocarbon gases generated by maturation of thermally-immature organic matter.

The percentage of methane deuteration as a function of cumulative CH_4 generated is shown in **Fig. 5B**.⁶ Because approximately 100 μmol of CH_4 was generated in total, the x -axis of this panel can be read as % of cumulative methane generation. At 50% deuteration, less than 10% of methane has been generated. Stated another way, for 90% of the total methane generated in the experiment, more than half of its H content comes from water. From **Fig. 4A**, the fully-deuterated isotopologue CD_4 predominates towards the end of the experiment (time points #7–9). These late time points mark the end of the oil window (EASY%Ro between 0.9 and 1.3%) (**Fig. 5A**), suggesting that the immediate precursors of methane have already fully-exchanged their hydrogens with water.

⁵ This might be verified by heating normal water (${}^1\text{H}_2\text{O}$) in the presence of an initial charge of CD_4 and monitoring for any increase in the δD value of water.

⁶ Calculated as $[\text{CH}_4] \times V_{\text{remaining}} + \sum([\text{CH}_4] \times V_{\text{withdrawn}})$.

267 The fourth (capping) H in methane may come directly from water or may be abstracted from deuterated kerogen
268 (Dong et al., 2021).

269 **3.4. Interpretation of D/H and clumped isotope signatures of thermogenic CH₄**

270 Efforts to understand the D/H ratios of natural gas hydrocarbons have generally been focused on determining the
271 influence of thermal maturity, organic-inorganic interactions, catalysts, and/or biological processes on the
272 fractionation of hydrogen isotopes in these molecules during their generation, alteration, and/or destruction in
273 source rocks and reservoirs of sedimentary basins. There exist multiple examples of quantitatively-based
274 numerical models for predicting δD values of natural gases, each grounded in different levels of theory or
275 empiricism (Sackett, 1978; Berner et al., 1995; Clayton, 2003; Tang et al., 2005; Lu et al., 2011, 2021; Ni et al.,
276 2011, 2012).

277 Correct interpretation of δD values and clumped isotope signatures of CH₄ depends on understanding the relative
278 kinetics of (a) methane generation from kerogen maturation or cracking of high-molecular weight hydrocarbons;
279 (b) hydrogen exchange of methane precursor molecules with other organic molecules and/or water; and (c) direct
280 or indirect hydrogen exchange between CH₄ and H₂O in the various rock elements of a petroleum system.
281 Timescales of all of these processes range between years to tens of billions of years at the peak hydrocarbon-
282 generating temperatures of 100 to 200 °C, hence the relative importance of these three processes broadly governs
283 the amount of organic-derived and water-derived H in CH₄. These three processes are evaluated separately here
284 with respect to the experimental results and how they apply to the interpretation of isotope and isotopologue ratios
285 of CH₄.

286 *3.4.1. Fractionation and inheritance during methane generation*

287 Methane is generated directly during catagenesis via cleavage of methyl groups from kerogen or bitumen in
288 source rocks. It is also produced as a product of the thermal destruction of high- and low-molecular weight free
289 or bound hydrocarbons, low-molecular weight organic acids, and other organic molecules in source rocks and/or
290 high-temperature reservoirs. Thermogenic methane production has been reported over a very wide range of
291 temperatures, with some reports of commercial volumes of thermogenic natural gas generated at temperatures
292 lower than 86 °C (Laplante, 1974), perhaps even lower than 62 °C (Rowe and Muehlenbachs, 1999). Thermal
293 maturities of corresponding source rocks of putative low-temperature hydrocarbon gases and condensates were
294 estimated to be as low as ~0.25 to 0.4% *R_o*-equivalent (Laplante, 1974; Stahl, 1977; Purcell et al., 1979; Connan
295 and Cassou, 1980; Snowdon, 1980; Jenden et al., 1993; Muscio et al., 1994; Rowe and Muehlenbachs, 1999;
296 Ramaswamy, 2002). Kerogen moieties will not have undergone much D/H exchange at these low thermal
297 maturities (Dawson et al., 2005; Maslen et al., 2012; Vinnichenko et al., 2021), and thus CH₄ generated from
298 immature or marginally-mature source rocks will partially inherit its hydrogen and their corresponding C–H
299 linkages from the precursor organic matter. Since methyl groups of wood (and presumably other naturally-
300 occurring organic matter) carry clumped isotope values that deviate from equilibrium (Lloyd et al., 2021), and
301 because equilibrium methyl group clumping values [Δ(¹³CH₂D–R) values] are quite similar to Δ¹³CH₃D values of
302 CH₄ at these temperatures (within several tenths of a permil; Wang et al., 2015; Lloyd et al., 2021), CH₄ generated
303 from sedimentary organic matter at low levels of thermal stress can be expected to carry non-equilibrated
304 clumping values inherited from methane precursors (**Fig. 6A**). The process of terminating the CH₃· radical with a
305 H· radical may be an additional source of disequilibrated clumped methane signatures (Dong et al., 2021; Xie et
306 al., 2021). Under hydrothermal conditions, water is known to provide capping hydrogens to methane via a free

307 radical mechanism (He et al., 2019). Secondary isotope effects from the breaking of C–C bonds adjacent to intact
308 C–H bonds will also be incorporated (Ni et al., 2011).

309 *3.4.2. D/H exchange in precursor organic molecules*

310 In maturing and thermally-mature source rocks, kerogens can be expected to have exchanged part of their organic
311 hydrogen pool with ambient waters. In experiments on source rocks heated to 310–381 °C for up to 6 days with
312 deuterium-enriched and deuterium-depleted waters, Schimmelmann et al. (1999) found that 45 to 79% of carbon-
313 bound hydrogen was derived from water after pyrolysis to equivalent maturities as high as ~1.3% (as
314 EASY%Ro). Aliphatic Type I kerogen, containing large amounts of alkyl groups, were noted to be more
315 isotopically-conservative than kerogens with greater amounts of NSO-containing moieties such as Type IIS
316 kerogen.

317 Exchange of *n*-alkyl hydrogens is slow relative to hydrogen exchange at other positions such as at the α -carbons
318 of C=O groups (Sessions et al., 2004). However, exchange rates for aliphatic hydrogens are not zero. Exchange
319 may proceed via hydrogen transfer to a relatively stable tertiary carbocation-containing intermediate from
320 adjacent methyl or methylene groups (Alexander et al., 1984), or via the reversible dehydration of alkanes to form
321 alkenes under conditions of metastable equilibrium (Seewald, 1994; Reeves et al., 2012). In the absence of
322 significant direct CH₄–H₂O exchange, the formation of large amounts of CD₄ during our experiment suggests that
323 the hydrogen at methyl groups of kerogen (or in other alkyl precursors) exchanges with water under thermal
324 conditions compatible with the generation of petroleum (**Fig. 6B–C**). Water is abundant within most source
325 rocks, with even source rocks with very low water saturation containing up to several percent water by weight
326 (Kazak and Kazak, 2019). Hence, substantial incorporation of water-derived H into CH₄ is likely to occur in
327 actively-generating source rocks so long as water is in contact with sedimentary organic matter. Water dissolved
328 in bitumen generated from kerogen decomposition may participate in CH₄ generation (Lewan and Roy, 2011), as
329 well as water located in pore spaces that are at least partially-lined with organic matter (see §3.5). Equilibrium
330 D/H fractionation between organics and water is likely to be readily attained in at least several functional groups
331 during kerogen or bitumen maturation. While different equilibrium fractionation factors characterize the various
332 H positions in different normal and branched alkanes, the average D/H fractionation for *n*-alkanes trends in the
333 same direction as methane (i.e., alkane δ D lower than water) (Wang et al., 2009). The progressive incorporation
334 of pre-equilibrated alkyl H into thermogenic methane during natural gas generation may explain in part the
335 approach towards apparent equilibrium with formation water seen in CH₄ of increasing thermal maturity (Clayton,
336 2003; Wang et al., 2018; Turner et al., 2021).

337 *3.4.3. D/H exchange between methane and water in conventional vs. unconventional reservoirs*

338 Timescales of direct hydrogen exchange between CH₄ and ambient H₂O based on experiments conducted in the
339 absence of a catalyst range from hundreds of thousands of years at temperatures around 200 °C, up to hundreds of
340 millions of years at temperatures below 150 °C (Koepp, 1978; Reeves et al., 2012; Wang et al., 2018; Beaudry et
341 al., 2021; Turner et al., 2022).

342 In a conventional petroleum system, hydrocarbons are generated within an organic-rich source rock, expelled
343 from the source rock into permeable carrier beds, and transported along carrier beds to a reservoir or seep.
344 Generation of oil typically occurs at 80–160 °C (the 'oil window'; **Fig. 7A**). Oil remains within the organic matrix
345 until the amount of retained oil exceeds the expulsion threshold (typically considered a function of organic
346 richness) prior to being expelled from the source rock (Sandvik et al., 1992). Oil-prone source rocks will tend to
347 expel most of their generated hydrocarbons relatively soon after generation, whereas in leaner source rocks with

less generative potential, generated oil mostly remains trapped in the source rock (Cooles et al., 1986). In the latter case, larger hydrocarbon compounds (C_{15+}) will have ample time to both undergo exchange of its carbon-bound H (Sessions et al., 2004) and degrade to smaller compounds such as CH_4 that can more easily escape the source rock (Cooles et al., 1986). Expulsion of light hydrocarbons (C_{15} or below, including the C_1 – C_5 gases) is geologically rapid, particularly if the source rock comprises relatively thin (meter-scale) organic-rich beds interbedded with permeable silts or sands (Mackenzie et al., 1983). Secondary migration (from source rock to reservoir) is likely fast as well, even if such migration occurs over long lateral distances (~25 km) (<200,000 years for the L.A. Basin; Jung et al., 2015; see also Hindle, 1997; Eichhubl and Boles, 2000). Given that reservoirs are most often cooler than the source rocks, the C–H bonds in CH_4 will have been 'frozen' at or near the point of generation for methane generated at temperatures below ~170 °C. This is easily demonstrated using forward models of isotopic exchange such as those shown by Wang (2017, their Appendix A) for clumped isotopologues of CH_4 in conventional gases under conservative assumptions about cooling during migration. **Fig. 8A** shows that under a cooling rate of 50 °C/Myr—roughly 5× slower cooling than that implied by the migration timescale study of Jung et al. (2015)—and applying the CH_4 – H_2O exchange kinetics determined by Turner et al. (2022), closure of methane isotopic exchange should occur around ~170 °C.⁷ Methane generated in source rocks at temperatures above the oil window (>160 °C) will be more likely to approach D/H equilibrium with water, even if it migrates immediately after generation. The dataset presented by Clayton (2003) showing a leveling-off of $\delta D(CH_4)$ values at around –140 to –150‰ in higher thermal maturity, conventional, oil-associated gases while $\delta^{13}C(CH_4)$ continues to increase is very supportive of exchange having occurred at temperatures of >170 °C within or proximal to the source rocks.

By contrast, extensive hydrogen exchange in CH_4 likely occurs following generation for unconventional petroleum systems where the source rocks are also the reservoirs. In these self-sourced systems, CH_4 that remains entrapped in pore spaces will probably have exchanged hydrogens with surrounding organics or with any available water as long as the rock has been exposed to temperatures of at least ~130 °C at maximum burial for several million years (**Fig. 8B**). This is supported with observations that at elevated thermal maturities, CH_4 approaches isotopic equilibrium with co-existing formation waters in unconventional reservoirs such as the Utica, Marcellus, and Eagle Ford, consistent with transfer of H from paleo-groundwaters to methane (Wang et al., 2015; Xie et al., 2021). In source-rock reservoirs which are no longer at maximum burial depths, methane may undergo retrograde isotopic exchange during cooling. Closure in these cases is highly sensitive to rates of exhumation (Reiners and Brandon, 2006), particularly as the rock passes through the range of temperatures between 130 and 160 °C (**Fig. 8B**).

3.5. Generation potential of natural gas

Volumetric calculations based on source rock extent, type, richness, and thermal maturity are used to estimate the mass of hydrocarbons generated by source rocks undergoing thermal maturation. These calculations are the basis of estimates of potential resources when assessing frontier basins when only coarse constraints on source rock presence and character are available (Schmoker, 1994). They are also formalized as programmatic subroutines embedded in modern basin modeling packages (Tissot and Espitalié, 1975; Cooles et al., 1986; Pepper and Corvi, 1995; Tissot, 2003; Freund et al., 2007; Hantschel and Kauerauf, 2009; Stainforth, 2009; Fjellanger et al., 2010) which take spatially-resolved hydrogen index (HI) values of source horizons as a key input constraint.

⁷ More comprehensive discussions of closure (quenching) temperatures for D/H exchange reactions of CH_4 can be found in Wang et al. (2018), Turner et al. (2022), and references therein.

387 In a series of experiments, Wenger and Price (1991) heated shale source rocks and coals in the presence of water
388 for 30 days at temperatures of 150 to 500 °C. They observed that HI values often increased with experimental
389 temperature, instead of declining as would be expected for simple depletion of initial kerogen via cracking
390 reactions. Furthermore, more hydrocarbons were generated in some experiments than the theoretical maximum
391 yield expected if H in generated petroleum was only derived from organic matter (Price, 2001, their Figure 3).
392 This excess hydrocarbon yield was attributed to incorporation of H₂O-derived hydrogen during the hydrolytic
393 disproportionation of kerogen into CO₂ + CH₄ and other small paraffins, consistent with theoretical and
394 experimental constraints on petroleum degradation in aqueous environments (Helgeson et al., 1993, 2009;
395 Seewald, 1994, 2001, 2003).

396 Evidence from our results and the other studies discussed above suggest that hydrocarbon generation in source
397 rocks may not be limited by the organic hydrogen content of source rocks. Hence, if H availability is not limiting,
398 and water participates in the formation of hydrocarbons, the upper bound on the amount of hydrocarbons that can
399 be generated is the availability of water to petroleum-generating reactions up to the point of TOC exhaustion.
400 This has been repeatedly suggested by several authors in years past (Lewan, 1992; Helgeson et al., 1993, 2009;
401 Price, 1994, 2001; Seewald, 1994, 2003). If correct, kinetic models of petroleum formation employed in basin
402 modeling that limit hydrocarbon yields based on HI values (Tissot et al., 1987; Tissot, 2003; Hantschel and
403 Kauerauf, 2009) may significantly underpredict the true natural gas resource potential in many of the world's
404 sedimentary basins (**Fig. 7**).

405 Chemical kinetic models employed in the upstream oil and gas industry for exploration purposes invariably use
406 simple, pseudo-first-order reactions. Many parallel reactions may be simulated at once to simulate different
407 classes of kerogen or petroleum breakdown products; however, all reactions are, without exception, pseudo-first-
408 order in the mass of remaining precursor. However, as noted in Xie et al. (2022), the rate coefficients of these
409 notionally unimolecular reactions can be pressure-dependent, because a third-body collision may be required to
410 remove excess energy from the excited intermediates. Therefore, an algorithmic reaction mechanism generator
411 (RMG; Allen et al., 2012)—operating from a database of elementary reaction kinetics—may be used to determine
412 the important reactions involved in the breakdown of kerogen and petroleum, and to estimate their rate
413 coefficients under typical subsurface pressure & temperature conditions in active source rocks. Furthermore,
414 water is almost invariably excluded as a reactant from computational studies of the thermal decomposition of
415 organic matter because of the computational burden involved. Examples include Class (2015) and Gao (2016)
416 wherein geological oil-to-gas cracking was studied by using RMG to simulate individual radical reactions
417 involved in the pyrolysis of model organic compounds under dry (water-absent) conditions. Very recent
418 developments in RMG now allow it to handle gas- and liquid-phase heterogeneous reactions (Liu et al., 2021). In
419 the future it may therefore be possible to extend the aforementioned studies on pyrolysis of model compounds to
420 include H₂O as a reactant.

421 Several important differences between experimental hydrothermal pyrolysis of source rock powder and
422 maturation of source rocks in nature bear discussing. Most obviously, laboratory experiments substitute higher
423 temperatures to permit hydrocarbons to be generated within much shorter timescales than in nature. Hence, for
424 extrapolation from laboratory to geologic conditions, it is implicitly assumed that the same chemical reactions
425 occur in the same proportions at high and low temperatures. Experiments indicate that this is not often the case,
426 particularly for individual compositional groups (Snowdon, 1979; Ungerer and Pelet, 1987; Dieckmann et al.,
427 2000; Schenk and Dieckmann, 2004). Results of experimental studies, including this one, must be interpreted
428 with this in mind.

The availability of water to natural gas-generating reactions may also differ between experiment and nature. Our experiment was set up with a comparatively high water:rock ratio (5:1) to allow ease of sampling, to maintain single-phase conditions, and to prevent dilution of the deuterium content of the water by exchange with rock. The water:carbon ratio was concomitantly high, approximately 200:1 given the TOC of 2.5% and ignoring mineral carbon which is assumed not to participate in the generation of thermogenic methane. Grinding the Eagle Ford rock sample to rock powder allowed water to readily access exposed sedimentary organic matter with ease. By contrast, water:rock ratios for shales existing in nature (0.003:1 to 0.23:1; Bern et al., 2021) are several orders of magnitude lower than those used in experiments. Petrophysical studies of the structure of pore systems within clay-rich, organic-rich, overmature gas shales suggest that much of the water is bound to the surfaces of clay minerals and contained predominantly in interstices between clay mineral grains (see Figure 30 in Passey et al., 2010). This clay-adsorbed "irreducible water" is considered immobile and cannot be produced during extraction of hydrocarbons, whereas free or capillary-bound water is mobile and comes comingled with gas and oil during production. Using a rastering scanning electron microscopy (SEM) technique, Passey et al. (2010) imaged overmature shale source rocks in 3D, finding abundant small (<0.1 μ m) bubble-shaped pore spaces within the organic matter and observing that this intra-organic porosity tended to be interconnected yet isolated from the water-bearing intergranular matrices.

While the physical separation of gas-containing pockets from water-bearing interstitial spaces alone might suggest that contact between water and organic material is limited, two processes must be considered. Firstly, much of the oil and gas generated at or near grain boundaries probably underwent primary migration and was expelled out of the source rock long before the present day (Mackenzie et al., 1983; Coopes et al., 1986; Sandvik et al., 1992). Hence, the absence of gas in contact with water does not necessarily indicate that water was unavailable during oil and gas generation. This is supported by more recent SEM work suggesting that a substantial amount of the water fraction in shale source rocks may have direct contact with organic matter that commonly exists within interstices of clay minerals (Gupta et al., 2018). A residual water monolayer on clay particles, if present, might be responsible for some of the undeuterated methane in the early stages of our experiment. If this is the case, using crushed rock instead of rock powder in the experiment might yield yet higher proportions of C¹H₄ in the earlier samples.

The second consideration is that trapped water may have been initially present and was quantitatively consumed during the generation of the gas now present in the organic porosity. This is analogous to water trapped within mineral interstices in partially-serpentized peridotitic rock at mid-ocean ridges reacting with the olivine minerals that surround it, resulting in often dry (waterless), H₂- and CH₄-rich gas secondary fluid inclusions (Klein et al., 2019; Grozeva et al., 2020). Each individual fluid inclusion (or gas-filled shale pore space), then, is a remnant micro-reactor within which all water initially present was consumed in generating the gases now present. Therefore, the activity of water in such pockets of shale source rock isolated from the broader clastic matrix may be sufficiently high to allow for hydration of kerogen at much a lower water:rock ratio in nature than used in our experiment.

465 4. CONCLUSIONS

466 Four features in the dataset are notable: (i) the production of undeuterated C¹H₄ under incipient catagenic
467 conditions; (ii) the predominance of CD₄ towards the end of the experiment, coinciding with the late oil window;
468 (iii) the lack of direct methane-water isotopic exchange even at 350 °C; and (iv) the near-absence of CH₂D₂ during
469 the experiment. These observations suggest that while some –CH_x moieties in kerogen or longer-chain

470 hydrocarbons undergo exchange more readily than cracking, some other moieties or compound classes are much
471 less prone to exchange.

472 Carefully-controlled, temperature-programmed hydrous deuteration (deuterous pyrolysis or deutothermal
473 pyrolysis) experiments on additional source rocks and organic matter types may reveal systematic differences in
474 the kinetics of exchangability vs. hydrocarbon generation. Such experiments have the potential to improve
475 prediction of generative yields and hydrocarbon composition in basins where timing and quality of charge are key
476 uncertainties.

477 Data from this study support the hypothesis that much of the H in thermogenic natural gases may derive from
478 water, implying that the hydrogen content of organic matter may not limit gas generation. In general, the
479 volumetric significance of the water hydrogen reservoir hence may be underappreciated in estimations of the
480 natural gas resource potential on Earth.

481 5. ACKNOWLEDGMENTS

482 Financial support from the U.S. National Science Foundation (NSF awards EAR-1250394 to S.O.), the Alfred P.
483 Sloan Foundation via the Deep Carbon Observatory (to S.O. and J.S.S.), a Shell-MIT Energy Initiative
484 Fellowship, and the Kerr-McGee Professorship at MIT (to S.O.) is acknowledged. E.P.R was supported by the
485 Norwegian Research Council through the Centre for Geobiology (SFF Project #179560). We are grateful to Keith
486 F. M. Thompson (PetroSurveys, Inc.) for providing the Eagle Ford rock sample, Carl Johnson (WHOI) for the
487 elemental analyses, Aaron Sattler (ExxonMobil Research and Engineering) for advice on inverting mass spectral
488 data, Michael Lewan (USGS) for comments on the thesis chapter from which this work originated, and Chris
489 Clayton (CCGS) for an email exchange that inspired this study. We thank Daniel Dawson and an anonymous
490 reviewer for helpful feedback on the manuscript, and Cliff Walters, Joe Curiale, and Lloyd Snowdon for editorial
491 handling and additional comments. The data presented in this paper were collected while the primary author was
492 a Ph.D. student in the MIT/WHOI Joint Program.

493
494 *Conflict of interest statement:* None.

6. REFERENCES

- Alexander, R., Kagi, R.I., Larcher, A.V., 1984. Clay catalysis of alkyl hydrogen exchange reactions—reaction mechanisms. *Organic Geochemistry* 6, 755–760.
- Allen, J.W., Goldsmith, C.F., Green, W.H., 2012. Automatic estimation of pressure-dependent rate coefficients. *Phys. Chem. Chem. Phys.* 14, 1131–1155.
- Baskin, D.K., 1997. Atomic H/C ratio of kerogen as an estimate of thermal maturity and organic matter conversion. *AAPG Bulletin* 81, 1437–1450.
- Beaudry, P., Stefánsson, A., Fiebig, J., Rhim, J.H., Ono, S., 2021. High temperature generation and equilibration of methane in terrestrial geothermal systems: Evidence from clumped isotopologues. *Geochimica et Cosmochimica Acta* 309, 209–234.
- Bern, C.R., Birdwell, J.E., Jubb, A.M., 2021. Water-rock interaction and the concentrations of major, trace, and rare earth elements in hydrocarbon-associated produced waters of the United States. *Environmental Science: Processes & Impacts*, 23(8), 1198–1219.
- Berner, U., Faber, E., Scheeder, G., Panten, D., 1995. Primary cracking of algal and landplant kerogens: kinetic models of isotope variations in methane, ethane and propane. *Chemical Geology* 126, 233–245.
- Burnham, A.K., 2019. Kinetic models of vitrinite, kerogen, and bitumen reflectance. *Organic Geochemistry* 131, 50–59.
- Cardneaux, A., Nunn, J.A., 2013. Estimates of maturation and TOC from log data in the Eagle Ford Shale, Maverick Basin of South Texas. *Gulf Coast Association of Geological Societies Transactions* 63, 111–124.
- Cardneaux, A.P., 2012. Mapping of the oil window in the Eagle Ford shale play of southwest Texas using thermal modeling and log overlay analysis (Masters Thesis). Louisiana State University.
- Clayton, C., 2003. Hydrogen isotope systematics of thermally generated natural gas. International Meeting on Organic Geochemistry, 21st, Kraków, Poland, Book Abstr. Part I, 51–52.
- Class, C.A., 2015. Predicting organosulfur chemistry in fuel sources (PhD Thesis). Massachusetts Institute of Technology.
- Connan, J., Cassou, A.M., 1980. Properties of gases and petroleum liquids derived from terrestrial kerogen at various maturation levels. *Geochimica et Cosmochimica Acta* 44, 1–23.
- Cooles, G., Mackenzie, A., Quigley, T., 1986. Calculation of petroleum masses generated and expelled from source rocks. *Organic Geochemistry* 10, 235–245.
- Dawson, D., Grice, K., Alexander, R., 2005. Effect of maturation on the indigenous δD signatures of individual hydrocarbons in sediments and crude oils from the Perth Basin (Western Australia). *Organic Geochemistry* 36, 95–104.
- Dias, R.F., Lewan, M.D., Birdwell, J.E. and Kotarba, M.J., 2014. Differentiation of pre-existing trapped methane from thermogenic methane in an igneous-intruded coal by hydrous pyrolysis. *Organic Geochemistry* 67, 1–7.
- Dibeler, V.H., Mohler, F.L., 1950. Mass spectra of the deuteromethanes. *J. Research Nat. Bur. Standards* 45, 441–444.
- Dieckmann, V., Horsfield, B., Schenk, H.J., 2000. Heating rate dependency of petroleum-forming reactions: implications for compositional kinetic predictions. *Organic Geochemistry* 31, 1333–1348.
- Dong, G., Xie, H., Formolo, M., Lawson, M., Sessions, A., Eiler, J., 2021. Clumped isotope effects of thermogenic methane formation: insights from pyrolysis of hydrocarbons. *Geochimica et Cosmochimica Acta*. doi:10.1016/j.gca.2021.03.009
- Douglas, P.M., Stolper, D.A., Eiler, J.M., Sessions, A.L., Lawson, M., Shuai, Y., Bishop, A., Podlaha, O.G., Ferreira, A.A., Neto, E.V.S., others, 2017. Methane clumped isotopes: Progress and potential for a new isotopic tracer. *Organic Geochemistry* 113, 262–282.
- Eichhubl, P., Boles, J.R., 2000. Rates of fluid flow in fault systems; evidence for episodic rapid fluid flow in the Miocene Monterey Formation, coastal California. *American Journal of Science* 300, 571.
- Eldrett, J.S., Ma, C., Bergman, S.C., Lutz, B., Gregory, F.J., Dodsworth, P., Phipps, M., Hardas, P., Minisini, D., Ozkan, A., Ramezani, J., Bowring, S.A., Kamo, S.L., Ferguson, K., Macaulay, C., Kelly, A.E., 2015. An

- astronomically calibrated stratigraphy of the Cenomanian, Turonian and earliest Coniacian from the Cretaceous Western Interior Seaway, USA: Implications for global chronostratigraphy. *Cretaceous Research* 56, 316–344.
- Eldrett, J.S., Minisini, D., Bergman, S.C., 2014. Decoupling of the carbon cycle during Ocean Anoxic Event 2. *Geology* 42, 567–570.
- Fjellanger, E., Kontorovich, A.E., Barboza, S.A., Burshtein, L.M., Hardy, M.J., Livshits, V.R., 2010. Charging the giant gas fields of the NW Siberia basin, in: Vining, B.A., Pickering, S.C. (Eds.), *Petroleum Geology: From Mature Basins to New Frontiers – Proceedings of the 7th Petroleum Geology Conference*. Geological Society of London, pp. 659–668.
- French, K.L., Birdwell, J.E., Lewan, M.D., 2020. Trends in thermal maturity indicators for the organic sulfur-rich Eagle Ford Shale. *Marine and Petroleum Geology* 118, 104459.
- Freund, H., Walters, C.C., Kelemen, S.R., Siskin, M., Gorbaty, M.L., Curry, D.J., Bence, A.E., 2007. Predicting oil and gas compositional yields via chemical structure–chemical yield modeling (CS-CYM): Part 1 – Concepts and implementation. *Organic Geochemistry* 38, 288–305.
- Gao, C.W., 2016. Automatic reaction mechanism generation (PhD Thesis). Massachusetts Institute of Technology.
- Giunta, T., Young, E.D., Warr, O., Kohl, I., Ash, J.L., Martini, A., Mundle, S.O., Rumble, D., Pérez-Rodríguez, I., Wasley, M., LaRowe, D.E., Gilbert, A., Sherwood Lollar, B., 2019. Methane sources and sinks in continental sedimentary systems: New insights from paired clumped isotopologues $^{13}\text{CH}_3\text{D}$ and $^{12}\text{CH}_2\text{D}_2$. *Geochimica et Cosmochimica Acta* 245, 327–351.
- Glasoe, P.K., Long, F.A., 1960. Use of glass electrodes to measure acidites in deuterium oxide. *The Journal of Physical Chemistry* 64, 188–190.
- Golden, J.T., Andersen, R.A., Bergman, R.G., 2001. Exceptionally low-temperature carbon–hydrogen/carbon–deuterium exchange reactions of organic and organometallic compounds catalyzed by the $\text{Cp}^*(\text{PMe}_3)\text{IrH}(\text{ClCH}_2\text{Cl})^+$ cation. *Journal of the American Chemical Society* 123, 5837–5838.
- Grozeva, N.G., Klein, F., Seewald, J.S., Sylva, S.P., 2020. Chemical and isotopic analyses of hydrocarbon-bearing fluid inclusions in olivine-rich rocks. *Philosophical Transactions of the Royal Society A: Mathematical, Physical and Engineering Sciences* 378, 20180431.
- Gupta, I., Jernigen, J., Curtis, M., Rai, C., Sondergeld, C., 2018. Water-wet or oil-wet: Is it really that simple in shales? *Petrophysics - The SPWLA Journal of Formation Evaluation and Reservoir Description* 59, 308–317.
- Hantschel, T., Kauerauf, A.I., 2009. Petroleum Generation, in: *Fundamentals of Basin and Petroleum Systems Modeling*. Springer Berlin Heidelberg, Berlin, Heidelberg, pp. 151–198.
- Harbor, R.L., 2011. Facies characterization and stratigraphic architecture of organic-rich mudrocks, Upper Cretaceous Eagle Ford Formation, South Texas (Masters Thesis). University of Texas at Austin.
- He, K., Zhang, S., Mi, J., Fang, Y., Zhang, W., 2019. Carbon and hydrogen isotope fractionation for methane from non-isothermal pyrolysis of oil in anhydrous and hydrothermal conditions. *Energy Exploration & Exploitation* 37, 1558–1576.
- Helgeson, H.C., Knox, A.M., Owens, C.E., Shock, E.L., 1993. Petroleum, oil field waters, and authigenic mineral assemblages Are they in metastable equilibrium in hydrocarbon reservoirs. *Geochimica et Cosmochimica Acta* 57, 3295–3339.
- Helgeson, H.C., Richard, L., McKenzie, W.F., Norton, D.L., Schmitt, A., 2009. A chemical and thermodynamic model of oil generation in hydrocarbon source rocks. *Geochimica et Cosmochimica Acta* 73, 594–695.
- Hentz, T.F., Ruppel, S.C., 2010. Regional lithostratigraphy of the Eagle Ford Shale: Maverick Basin to East Texas Basin. *Gulf Coast Association of Geological Societies Transactions* 60, 325–337.
- Hindle, A.D., 1997. Petroleum Migration Pathways and Charge Concentration: A Three-Dimensional Model. *AAPG Bulletin* 81, 1451–1481.
- Hoering, T., 1984. Thermal reactions of kerogen with added water, heavy water and pure organic substances. *Organic Geochemistry* 5, 267–278.

- 594 Huizinga, B.J., Tannenbaum, E., Kaplan, I.R., 1987. The role of minerals in the thermal alteration of organic
595 matter—IV. Generation of n-alkanes, acyclic isoprenoids, and alkenes in laboratory experiments.
596 *Geochimica et Cosmochimica Acta* 51, 1083–1097.
- 597 Hunt, J.M., 1996. Petroleum geochemistry and geology, 2nd ed. WH Freeman San Francisco.
598 IHS Markit Well Database, 2019.. IHS Markit.
- 599 Jenden, P.D., Drazan, D.J., Kaplan, I.R., 1993. Mixing of thermogenic natural gases in northern Appalachian
600 basin. *AAPG Bulletin* 77, 980–998.
- 601 Jung, B., Garven, G., Boles, J.R., 2015. The geodynamics of faults and petroleum migration in the Los Angeles
602 basin, California. *American Journal of Science* 315, 412–459.
- 603 Kazak, E.S., Kazak, A.V., 2019. A novel laboratory method for reliable water content determination of shale
604 reservoir rocks. *Journal of Petroleum Science and Engineering* 183, 106301.
- 605 Klein, F., Grozeva, N.G., Seewald, J.S., 2019. Abiotic methane synthesis and serpentinization in olivine-hosted
606 fluid inclusions. *Proceedings of the National Academy of Sciences* 116, 17666.
- 607 Koepp, M., 1978. D/H isotope exchange reaction between petroleum and water: a contributory determinant for
608 D/H-isotope ratios in crude oils, in: The Fourth International Conference, Geochronology,
609 Cosmochronology, Isotope Geology USGS Open-File Report 78-701. pp. 221–222.
- 610 Labidi, J., Young, E.D., Giunta, T., Kohl, I.E., Seewald, J., Tang, H., Lilley, M.D., Früh-Green, G.L., 2020.
611 Methane thermometry in deep-sea hydrothermal systems: Evidence for re-ordering of doubly-substituted
612 isotopologues during fluid cooling. *Geochimica et Cosmochimica Acta* 288, 248–261.
- 613 Laplante, R.E., 1974. Hydrocarbon generation in Gulf Coast Tertiary sediments. *AAPG Bulletin* 58, 1281–1289.
- 614 Lécluse, C., Robert, F., 1994. Hydrogen isotope exchange reaction rates: Origin of water in the inner solar system.
615 *Geochimica et Cosmochimica Acta* 58, 2927–2939.
- 616 Leif, R.N., Simoneit, B.R., 2000. The role of alkenes produced during hydrous pyrolysis of a shale. *Organic
617 Geochemistry* 31, 1189–1208.
- 618 Lewan, M., 1992. Water as a source of hydrogen and oxygen in petroleum formation by hydrous pyrolysis. *Am.
619 Chem. Soc. Div. Fuel Chem* 37, 1643–1649.
- 620 Lewan, M., 1997. Experiments on the role of water in petroleum formation. *Geochimica et Cosmochimica Acta*
621 61, 3691–3723.
- 622 Lewan, M.D., Roy, S., 2011. Role of water in hydrocarbon generation from Type-I kerogen in Mahogany oil
623 shale of the Green River Formation. *Organic Geochemistry* 42, 31–41.
- 624 Lis, G.P., Schimmelmann, A., Mastalerz, M., 2006. D/H ratios and hydrogen exchangeability of type-II kerogens
625 with increasing thermal maturity. *Organic Geochemistry* 37, 342–353.
- 626 Lloyd, M.K., Eldridge, D.L., Stolper, D.A., 2021. Clumped $^{13}\text{CH}_3\text{D}$ and $^{12}\text{CH}_2\text{D}_2$ compositions of methyl groups
627 from wood and synthetic monomers: Methods, experimental and theoretical calibrations, and initial
628 results. *Geochimica et Cosmochimica Acta* 297, 233–275.
- 629 Liu, M., Grinberg Dana, A., Johnson, M.S., Goldman, M.J., Jocher, A., Payne, A.M., Grambow, C.A., Han, K.,
630 Yee, N.W., Mazeau, E.J., Blondal, K., West, R.H., Goldsmith, C.F., Green, W.H., 2021. Reaction
631 Mechanism Generator v3.0: Advances in Automatic Mechanism Generation. *Journal of Chemical
632 Information and Modeling* 61, 2686–2696.
- 633 Lu, S., Wang, M., Xue, H., Li, J., Chen, F., Xu, Q., 2011. The impact of aqueous medium on gas yields and
634 kinetic behaviors of hydrogen isotope fractionation during organic matter thermal degradation. *Acta
635 Geologica Sinica - English Edition* 85, 1466–1477.
- 636 Lu, S.-F., Feng, G.-Q., Shao, M.-L., Li, J.-J., Xue, H.-T., Wang, M., Chen, F.-W., Li, W.-B., Pang, X.-T., 2021.
637 Kinetics and fractionation of hydrogen isotopes during gas formation from representative functional
638 groups. *Petroleum Science* 18, 1021–1032.
- 639 Mackenzie, A.S., Leythaeuser, D., Schaefer, R.G., Bjorøy, M., 1983. Expulsion of petroleum hydrocarbons from
640 shale source rocks. *Nature* 301, 506–509.
- 641 Maslen, E., Grice, K., Dawson, D., Wang, S., Horsfield, B., 2012. Stable hydrogen isotopes of isoprenoids and n-
642 alkanes as a proxy for estimating the thermal history of sediments through geological time:, in: Harris,
643 N.B., Peters, K.E. (Eds.), *Analyzing the Thermal History of Sedimentary Basins: Methods and Case
644 Studies*. SEPM Society for Sedimentary Geology, pp. 29–43.

- 645 Mohler, F.L., Dibeler, V.H., Quinn, E., 1958. Redetermination of mass spectra of deuteromethanes. *Journal of*
646 *Research of the National Bureau of Standards* 61, 171–172.
- 647 Muscio, G.P.A., Horsfield, B., Welte, D.H., 1994. Occurrence of thermogenic gas in the immature zone—
648 implications from the Bakken in-source reservoir system. *Organic Geochemistry* 22, 461–476.
- 649 Ni, Y., Liao, F., Dai, J., Zou, C., Zhu, G., Zhang, B., Liu, Q., 2012. Using carbon and hydrogen isotopes to
650 quantify gas maturity, formation temperature, and formation age — specific applications for gas fields
651 from the Tarim basin, China. *Energy Exploration & Exploitation* 30, 273–293.
- 652 Ni, Y., Ma, Q., Ellis, G.S., Dai, J., Katz, B., Zhang, S., Tang, Y., 2011. Fundamental studies on kinetic isotope
653 effect (KIE) of hydrogen isotope fractionation in natural gas systems. *Geochimica et Cosmochimica Acta*
654 75, 2696–2707.
- 655 Passey, Q.R., Bohacs, K., Esch, W.L., Klimentidis, R., Sinha, S., 2010. From Oil-Prone Source Rock to Gas-
656 Producing Shale Reservoir - Geologic and Petrophysical Characterization of Unconventional Shale Gas
657 Reservoirs, in: SPE-131350-MS. Presented at the International Oil and Gas Conference and Exhibition in
658 China, Society of Petroleum Engineers, Beijing, China, p. 29.
- 659 Pepper, A.S., Corvi, P.J., 1995. Simple kinetic models of petroleum formation. Part I: oil and gas generation from
660 kerogen. *Marine and Petroleum Geology* 12, 291–319.
- 661 Price, L.C., 1994. Metamorphic free-for-all. *Nature* 370, 253–254.
- 662 Price, L.C., 2001. A possible deep-basin-high-rank gas machine via water-organic-matter redox reactions, in:
663 Dyman, T.S., Kuuskraa, V.A. (Eds.), *Geologic Studies of Deep Natural Gas Resources*, Digital Data
664 Series. U. S. Geological Survey.
- 665 Purcell, L.P., Rashid, M.A., Hardy, I.A., 1979. Geochemical characteristics of sedimentary rocks in Scotian basin.
666 AAPG Bulletin 63, 87–105.
- 667 Ramaswamy, G., 2002. A field evidence for mineral-catalyzed formation of gas during coal maturation. *Oil & gas*
668 journal 100, 32–36.
- 669 Reeves, E.P., Seewald, J.S., Sylva, S.P., 2012. Hydrogen isotope exchange between *n*-alkanes and water under
670 hydrothermal conditions. *Geochimica et Cosmochimica Acta* 77, 582–599.
- 671 Rowe, D., Muehlenbachs, K., 1999. Low-temperature thermal generation of hydrocarbon gases in shallow shales.
672 *Nature* 398, 61–63.
- 673 Sackett, W.M., 1978. Carbon and hydrogen isotope effects during the thermocatalytic production of hydrocarbons
674 in laboratory simulation experiments. *Geochimica et Cosmochimica Acta* 42, 571–580.
- 675 Sackett, W.M., Conkright, M., 1997. Summary and re-evaluation of the high-temperature isotope geochemistry of
676 methane. *Geochimica et Cosmochimica Acta* 61, 1941–1952.
- 677 Sandvik, E.I., Young, W.A., Curry, D.J., 1992. Expulsion from hydrocarbon sources: the role of organic
678 absorption. *Organic Geochemistry* 19, 77–87.
- 679 Sattler, A., 2018. Hydrogen/Deuterium (H/D) exchange catalysis in alkanes. *ACS Catalysis* 8, 2296–2312.
- 680 Saxena, S.C., Saxena, V.K., 1970. Thermal conductivity data for hydrogen and deuterium in the range 100–1100
681 degrees C. *Journal of Physics A: General Physics* 3, 309–320.
- 682 Schenk, H.J., Dieckmann, V., 2004. Prediction of petroleum formation: the influence of laboratory heating rates
683 on kinetic parameters and geological extrapolations. *Marine and Petroleum Geology* 21, 79–95.
- 684 Schimmelmann, A., Boudou, J.-P., Lewan, M.D., Wintsch, R.P., 2001. Experimental controls on D/H and $^{13}\text{C}/^{12}\text{C}$
685 ratios of kerogen, bitumen and oil during hydrous pyrolysis. *Organic Geochemistry* 32, 1009–1018.
- 686 Schimmelmann, A., Lewan, M.D., Wintsch, R.P., 1999. D/H isotope ratios of kerogen, bitumen, oil, and water in
687 hydrous pyrolysis of source rocks containing kerogen types I, II, IIS, and III. *Geochimica et*
688 *Cosmochimica Acta* 63, 3751–3766.
- 689 Schimmelmann, A., Sessions, A.L., Mastalerz, M., 2006. Hydrogen isotopic (D/H) composition of organic matter
690 during diagenesis and thermal maturation. *Annual Review of Earth and Planetary Sciences* 34, 501–533.
- 691 Schmoker, J.W., 1994. Volumetric calculation of hydrocarbons generated, in: Magoon, L.B., Dow, W.G. (Eds.),
692 *The Petroleum System---from Source to Trap*, AAPG Memoir. pp. 323–326.
- 693 Seewald, J.S., 1994. Evidence for metastable equilibrium between hydrocarbons under hydrothermal conditions.
694 *Nature* 370, 285–287.

- 695 Seewald, J.S., 2001. Aqueous geochemistry of low molecular weight hydrocarbons at elevated temperatures and
696 pressures: constraints from mineral buffered laboratory experiments. *Geochimica et Cosmochimica Acta*
697 65, 1641–1664.
- 698 Seewald, J.S., 2003. Organic–inorganic interactions in petroleum-producing sedimentary basins. *Nature* 426,
699 327–333.
- 700 Seewald, J.S., Benitez-Nelson, B.C., Whelan, J.K., 1998. Laboratory and theoretical constraints on the generation
701 and composition of natural gas. *Geochimica et Cosmochimica Acta* 62, 1599–1617.
- 702 Sessions, A.L., 2016. Factors controlling the deuterium contents of sedimentary hydrocarbons. *Organic*
703 *Geochemistry* 96, 43–64.
- 704 Sessions, A.L., Sylva, S.P., Summons, R.E., Hayes, J.M., 2004. Isotopic exchange of carbon-bound hydrogen
705 over geologic timescales. *Geochimica et Cosmochimica Acta* 68, 1545–1559.
- 706 Seyfried, W.E., Jr., Janecky, D.R., Berndt, M.E., 1987. Rocking autoclaves for hydrothermal experiments, II. The
707 flexible reaction-cell system. *Hydrothermal Experimental Techniques* 9, 216–239.
- 708 Shock, E.L., Helgeson, H.C., 1990. Calculation of the thermodynamic and transport properties of aqueous species
709 at high pressures and temperatures: Standard partial molal properties of organic species. *Geochimica et*
710 *Cosmochimica Acta* 54, 915–945.
- 711 Shock, E.L., Helgeson, H.C., Sverjensky, D.A., 1989. Calculation of the thermodynamic and transport properties
712 of aqueous species at high pressures and temperatures: Standard partial molal properties of inorganic
713 neutral species. *Geochimica et Cosmochimica Acta* 53, 2157–2183.
- 714 Shuai, Y., Etiope, G., Zhang, S., Douglas, P.M., Huang, L., Eiler, J.M., 2018. Methane clumped isotopes in the
715 Songliao Basin (China): New insights into abiotic vs. biotic hydrocarbon formation. *Earth and Planetary*
716 *Science Letters* 482, 213–221.
- 717 Smith, J., Rigby, D., Gould, K., Hart, G., Hargraves, A., 1985. An isotopic study of hydrocarbon generation
718 processes. *Organic Geochemistry* 8, 341–347.
- 719 Snowdon, L., 1980. Resinite—A potential petroleum source in the upper Cretaceous/Tertiary of the Beaufort–
720 Mackenzie Basin, in: Miall, A.D. (Ed.), *Facts and Principles of World Petroleum Occurrence*, CSPG
721 Special Publications. pp. 509–521.
- 722 Snowdon, L.R., 1979. Errors in extrapolation of experimental kinetic parameters to organic geochemical systems:
723 Geologic notes. *AAPG Bulletin* 63, 1128–1134.
- 724 Stahl, W.J., 1977. Carbon and nitrogen isotopes in hydrocarbon research and exploration. *Chemical Geology* 20,
725 121–149.
- 726 Stainforth, J.G., 2009. Practical kinetic modeling of petroleum generation and expulsion. *Thematic Set on Basin*
727 *Modeling Perspectives* 26, 552–572.
- 728 Stolper, D., Martini, A., Clog, M., Douglas, P., Shusta, S., Valentine, D., Sessions, A., Eiler, J., 2015.
729 Distinguishing and understanding thermogenic and biogenic sources of methane using multiply
730 substituted isotopologues. *Geochimica et Cosmochimica Acta* 161, 219–247.
- 731 Stolper, D.A., Lawson, M., Davis, C.L., Ferreira, A.A., Santos Neto, E.V., Ellis, G.S., Lewan, M.D., Martini,
732 A.M., Tang, Y., Schoell, M., Sessions, A.L., Eiler, J.M., 2014. Formation temperatures of thermogenic
733 and biogenic methane. *Science* 344, 1500–1503.
- 734 Sun, X., Zhang, T., Sun, Y., Milliken, K.L., Sun, D., 2016. Geochemical evidence of organic matter source input
735 and depositional environments in the lower and upper Eagle Ford Formation, south Texas. *Organic*
736 *Geochemistry* 98, 66–81.
- 737 Sweeney, J.J., Burnham, A.K., 1990. Evaluation of a simple model of vitrinite reflectance based on chemical
738 kinetics. *AAPG Bulletin* 74, 1559–1570.
- 739 Tang, Y., Huang, Y., Ellis, G.S., Wang, Y., Kralert, P.G., Gillaizeau, B., Ma, Q., Hwang, R., 2005. A kinetic
740 model for thermally induced hydrogen and carbon isotope fractionation of individual *n*-alkanes in crude
741 oil. *Geochimica et Cosmochimica Acta* 69, 4505–4520.
- 742 Thiagarajan, N., Xie, H., Ponton, C., Kitchen, N., Peterson, B., Lawson, M., Formolo, M., Xiao, Y., Eiler, J.,
743 2020. Isotopic evidence for quasi-equilibrium chemistry in thermally mature natural gases. *Proceedings of*
744 *the National Academy of Sciences* 117, 3989–3995.

- Tian, Y., Ayers, W.B., McCain Jr, D., 2013. The Eagle Ford Shale play, south Texas: regional variations in fluid types, hydrocarbon production and reservoir properties, in: IPTC 2013: International Petroleum Technology Conference. European Association of Geoscientists & Engineers, p. IPTC 16808.
- Tissot, B., 2003. Preliminary data on the mechanisms and kinetics of the formation of petroleum in sediments. computer simulation of a reaction flowsheet. *Oil & Gas Science and Technology - Rev. IFP* 58, 183–202.
- Tissot, B., Espitalié, J., 1975. L'évolution thermique de la matière organique des sédiments : applications d'une simulation mathématique. Potentiel pétrolier des bassins sédimentaires de reconstitution de l'histoire thermique des sédiments. *Rev. Inst. Fr. Pét.* 30, 743–778.
- Tissot, B., Pelet, R., Ungerer, P., 1987. Thermal history of sedimentary basins, maturation indices, and kinetics of oil and gas generation. *AAPG Bulletin* 71, 1445–1466.
- Turner, A.C., Korol, R., Eldridge, D.L., Bill, M., Conrad, M.E., Miller, T.F., Stolper, D.A., 2021. Experimental and theoretical determinations of hydrogen isotopic equilibrium in the system CH₄-H₂-H₂O from 3 to 200 °C. *Geochimica et Cosmochimica Acta*. doi:10.1016/j.gca.2021.04.026
- Turner, A.C., Pester, N.J., Bill, M., Conrad, M.E., Knauss, K.G., Stolper, D.A., 2022. Experimental determination of hydrogen isotope exchange rates between methane and water under hydrothermal conditions. *Geochimica et Cosmochimica Acta* 329, 231–255. doi:10.1016/j.gca.2022.04.029
- Ungerer, P., Pelet, R., 1987. Extrapolation of the kinetics of oil and gas formation from laboratory experiments to sedimentary basins. *Nature* 327, 52–54.
- Vinnichenko, G., Jarrett, A.J.M., van Maldegem, L.M., Brocks, J.J., 2021. Substantial maturity influence on carbon and hydrogen isotopic composition of n-alkanes in sedimentary rocks. *Organic Geochemistry* 152, 104171.
- Wang, D.T., 2017. The geochemistry of methane isotopologues (PhD Thesis). Massachusetts Institute of Technology and Woods Hole Oceanographic Institution. doi:10.1575/1912/9052
- Wang, D.T., Gruen, D.S., Lollar, B.S., Hinrichs, K.-U., Stewart, L.C., Holden, J.F., Hristov, A.N., Pohlman, J.W., Morrill, P.L., Könneke, M., Delwiche, K.B., Reeves, E.P., Sutcliffe, C.N., Ritter, D.J., Seewald, J.S., McIntosh, J.C., Hemond, H.F., Kubo, M.D., Cardace, D., Hoehler, T.M., Ono, S., 2015. Nonequilibrium clumped isotope signals in microbial methane. *Science* 348, 428–431.
- Wang, D.T., Reeves, E.P., McDermott, J.M., Seewald, J.S., Ono, S., 2018. Clumped isotopologue constraints on the origin of methane at seafloor hot springs. *Geochimica et Cosmochimica Acta* 223, 141–158.
- Wang, Y., Sessions, A.L., Nielsen, R.J., Goddard III, W.A., 2009. Equilibrium ²H/¹H fractionations in organic molecules. II: Linear alkanes, alkenes, ketones, carboxylic acids, esters, alcohols and ethers. *Geochimica et Cosmochimica Acta* 73, 7076–7086.
- Wei, L., Gao, Z., Mastalerz, M., Schimmelmann, A., Gao, L., Wang, X., Liu, X., Wang, Y., Qiu, Z., 2019. Influence of water hydrogen on the hydrogen stable isotope ratio of methane at low versus high temperatures of methanogenesis. *Organic Geochemistry* 128, 137–147.
- Wenger, L., Price, L., 1991. Differential petroleum generation and maturation paths of the different organic matter types as determined by hydrous pyrolysis over a wide range of experimental temperatures, in: European Association of Organic Geochemists 15th International Meeting, Advances and Applications in the Natural Environment: Organic Geochemistry. pp. 335–339.
- Whelan, J.K., Thompson-Rizer, C.L., 1993. Chemical methods for assessing kerogen and protokerogen types and maturity, in: Engel, M.H., Macko, S.A. (Eds.), *Organic Geochemistry: Principles and Applications*. Springer US, Boston, MA, pp. 289–353.
- Whisnant, C.S., Hansen, P.A., Kelley, T.D., 2011. Measuring the relative concentration of H₂ and D₂ in HD gas with gas chromatography. *Review of Scientific Instruments* 82, 024101.
- Xie, H., Dong, G., Formolo, M., Lawson, M., Liu, J., Cong, F., Mangenot, X., Shuai, Y., Ponton, C., Eiler, J., 2021. The evolution of intra- and inter-molecular isotope equilibria in natural gases with thermal maturation. *Geochimica et Cosmochimica Acta*. doi:10.1016/j.gca.2021.05.012
- Xie, H., Formolo, M., Eiler, J., 2022. Predicting isotopologue abundances in the products of organic catagenesis with a kinetic Monte-Carlo model. *Geochimica et Cosmochimica Acta* 327, 200–228.
- Yeh, H.-W., Epstein, S., 1981. Hydrogen and carbon isotopes of petroleum and related organic matter. *Geochimica et Cosmochimica Acta* 45, 753–762.

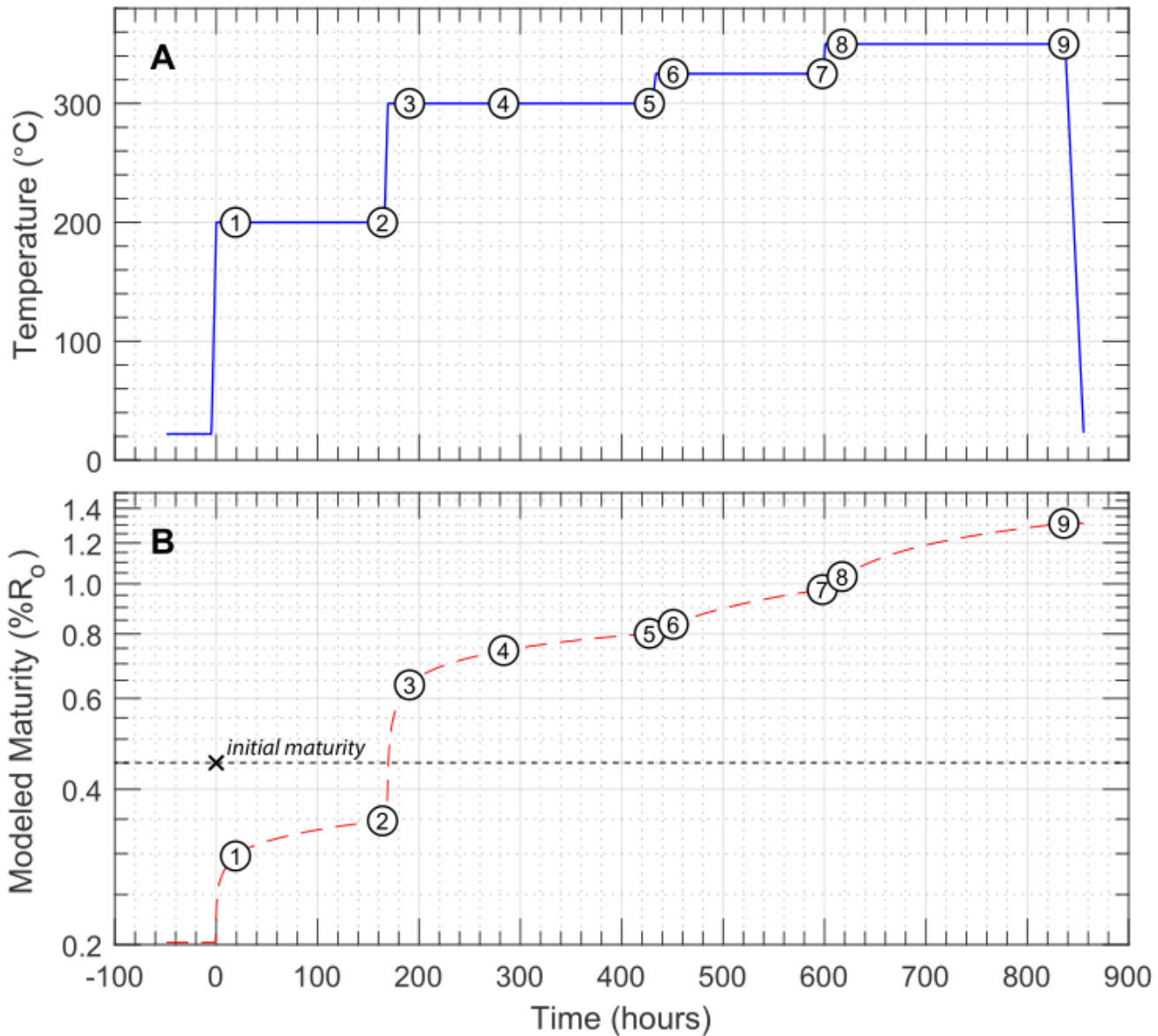
796 Young, E.D., Kohl, I.E., Lollar, B.S., Etiope, G., Rumble, D., Li, S., Haghnegahdar, M.A., Schauble, E.A.,
797 McCain, K.A., Foustoukos, D.I., Sutcliffe, C., Warr, O., Ballentine, C.J., Onstott, T.C., Hosgomez, H.,
798 Neubeck, A., Marques, J.M., Pérez-Rodríguez, I., Rowe, A.R., LaRowe, D.E., Magnabosco, C., Yeung,
799 L.Y., Ash, J.L., Bryndzia, L.T., 2017. The relative abundances of resolved $^{12}\text{CH}_2\text{D}_2$ and $^{13}\text{CH}_3\text{D}$ and
800 mechanisms controlling isotopic bond ordering in abiotic and biotic methane gases. *Geochimica et
801 Cosmochimica Acta* 203, 235–264.
802

803

804

805 **7. FIGURE CAPTIONS**

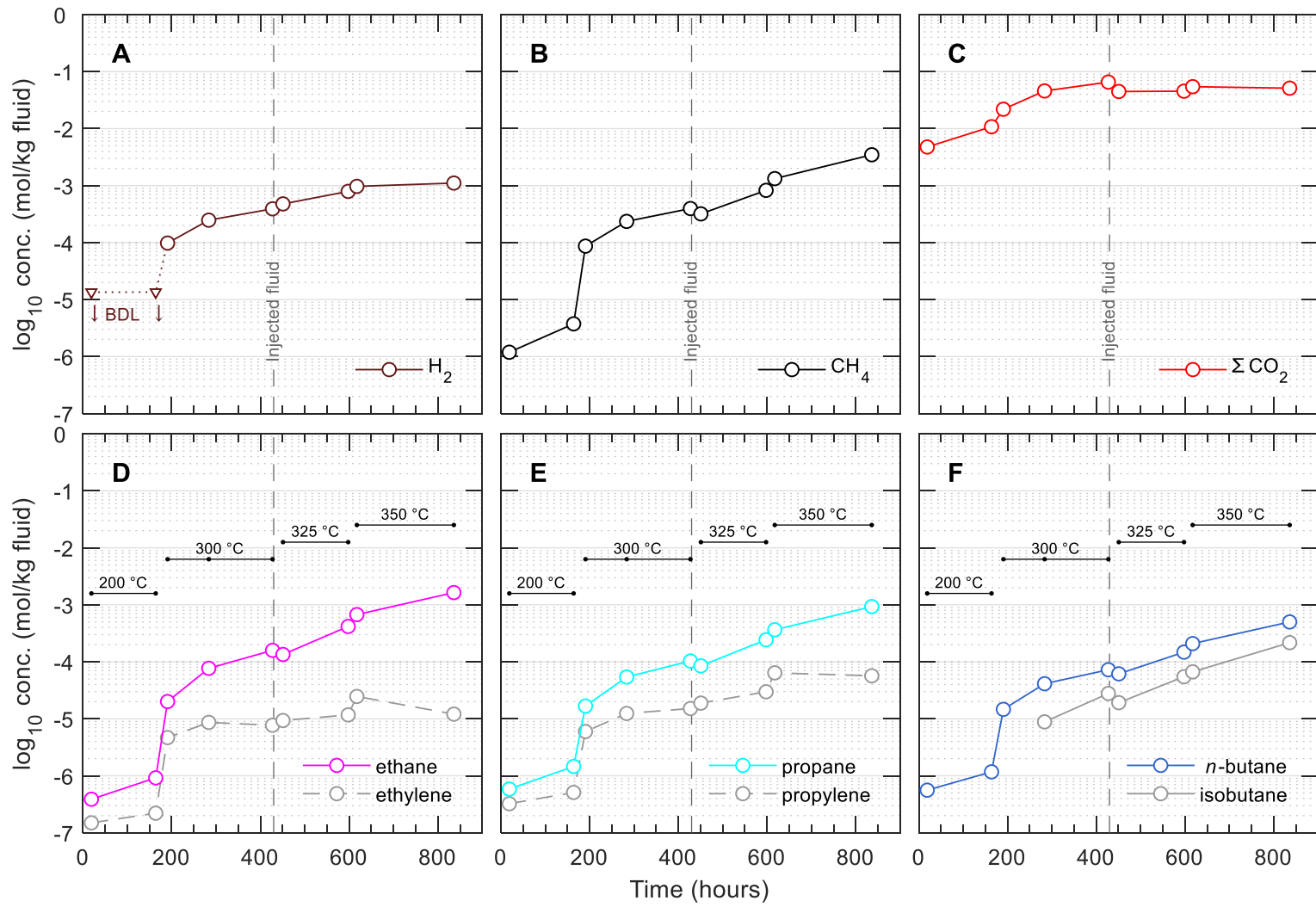
806



807

808 **Fig. 1.** Profiles of (A) temperature and (B) estimated thermal maturity (calculated using EASY%Ro) vs. time.
 809 Time zero ($t = 0$) is the time at which the experiment was brought to initial conditions (200 °C and 350 bar).
 810 Numbers in circles represent sampling points (Table 2).

811



812

813 **Fig. 2.** Concentrations of aqueous species over time during the experiment. (A) Hydrogen (H₂, measured as D₂); (B) methane (CH₄); (C) total
 814 inorganic carbon (ΣCO_2); (D) ethane and ethylene; (E) propane and propylene; and (F) n-butane and isobutane. Note that injection of additional
 815 saline D₂O at 430 hours diluted the concentration of all aqueous species by ~50%. BDL, below detection limit (<13 μ mol/kg for D₂).

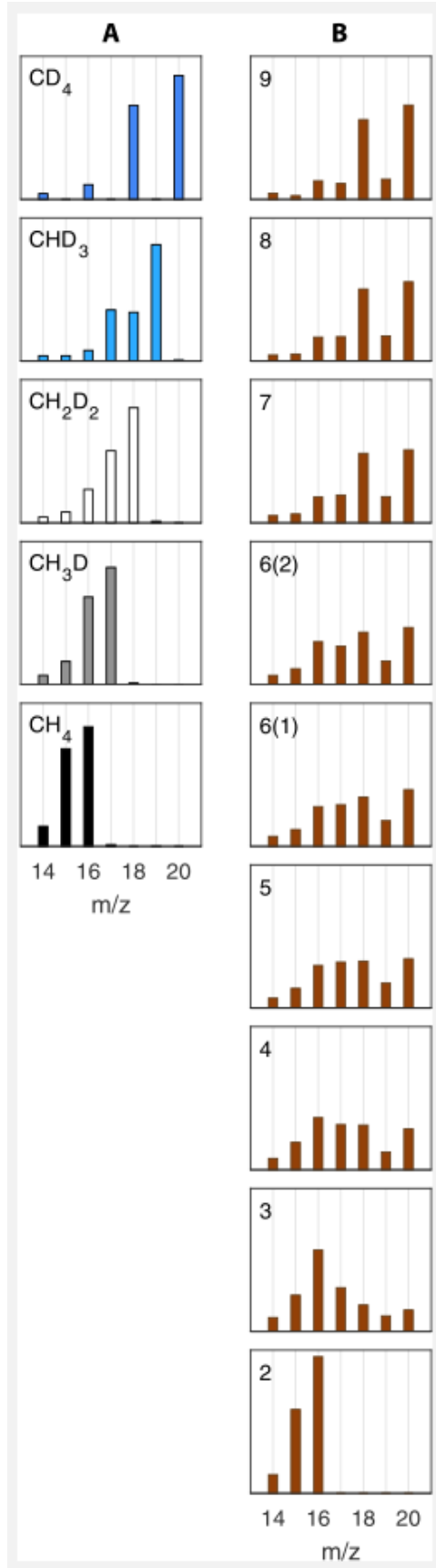
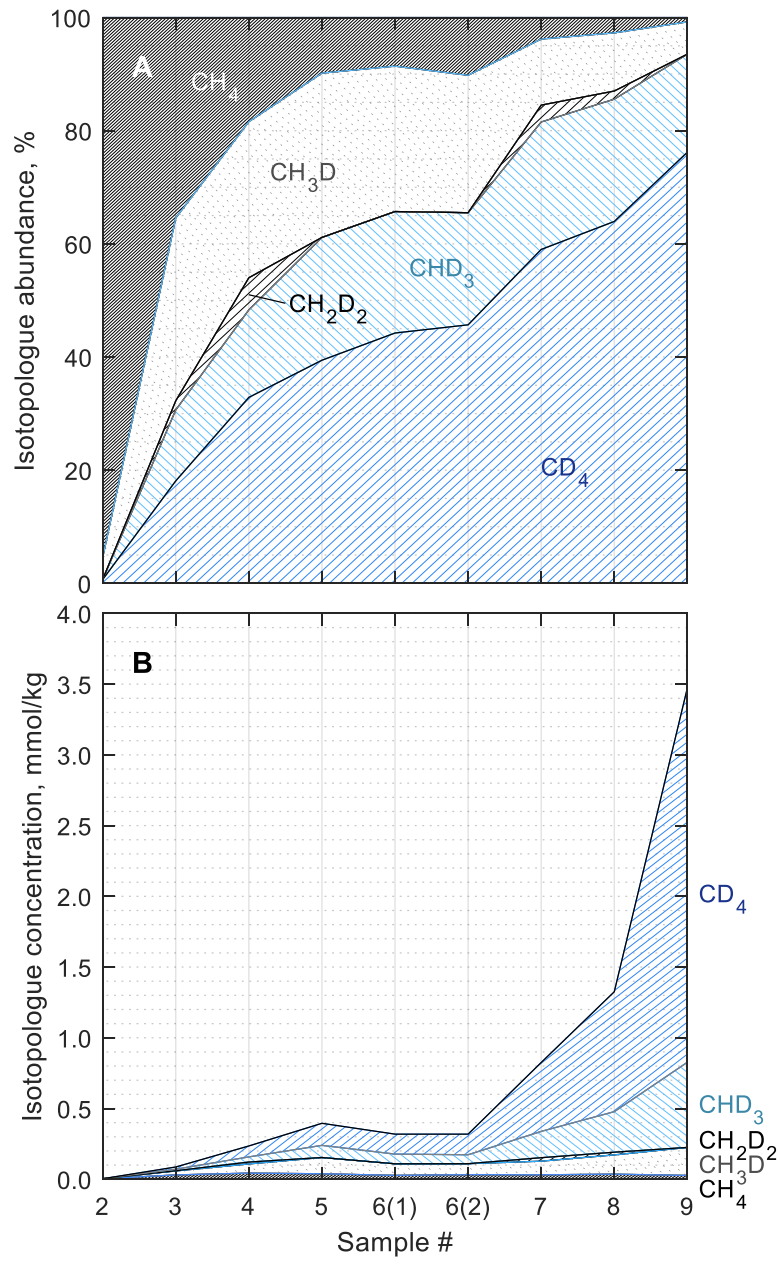
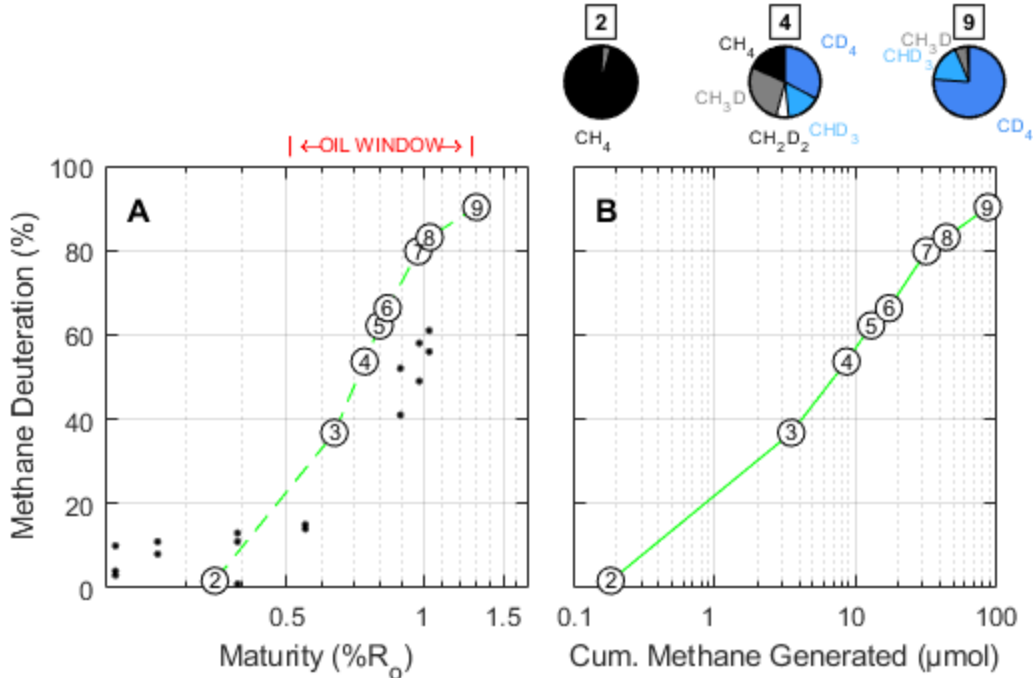


Fig. 3. Mass spectra of (A) standards and (B) samples. Isotopologue is indicated in the upper left corner of each plot. Intensities were normalized such that the m/z 14 to 20 signals sum to unity. In (B), time point is indicated in the upper left corner of each plot. Two samples were taken for time point #6, hence there are two plots. No GC-MS data were obtained for time point #1.



823

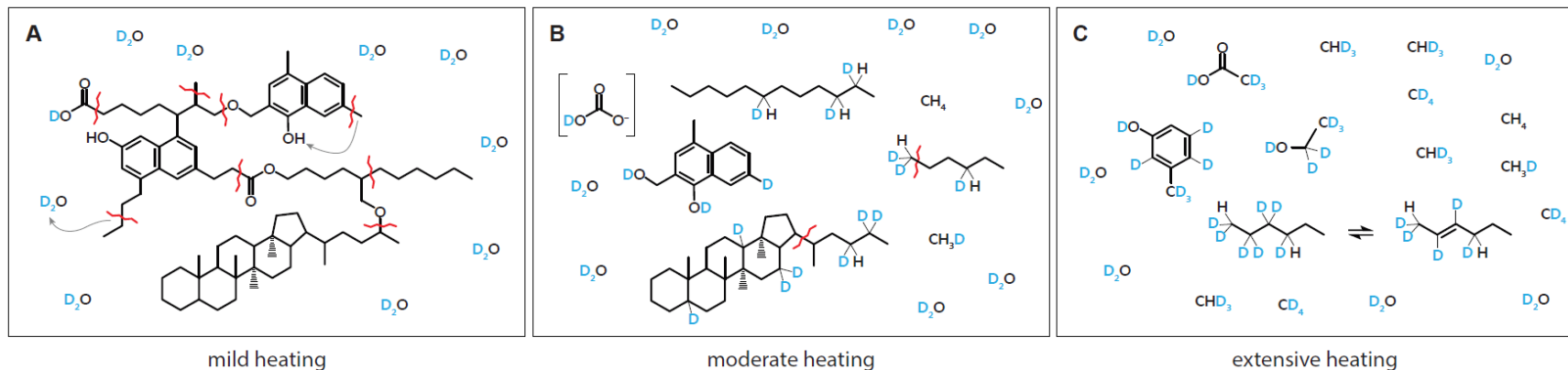
824 **Fig. 4.** Calculated (A) fractional and (B) absolute abundances of methane isotopologues.



825

826 **Fig. 5.** Extent of methane deuteration [methane-bound D/(D+H)] vs. (A) estimated maturity (via EASY%Ro) and
 827 (B) cumulative methane generated. The data shown for time point #6 is the average of the two replicate samples.
 828 Small symbols in (A) are data from Wei et al. (2019) representing percentage of water-derived H in CH₄.
 829 Thermal maturities for the Wei et al. data were calculated from a time-temperature curve reconstructed from their
 830 described experimental procedures. Pie charts above (B) represent fractional abundances of isotopologues before,
 831 during, and after peak oil generation (time points #2, 4, and 9, respectively).

832



833

mild heating

moderate heating

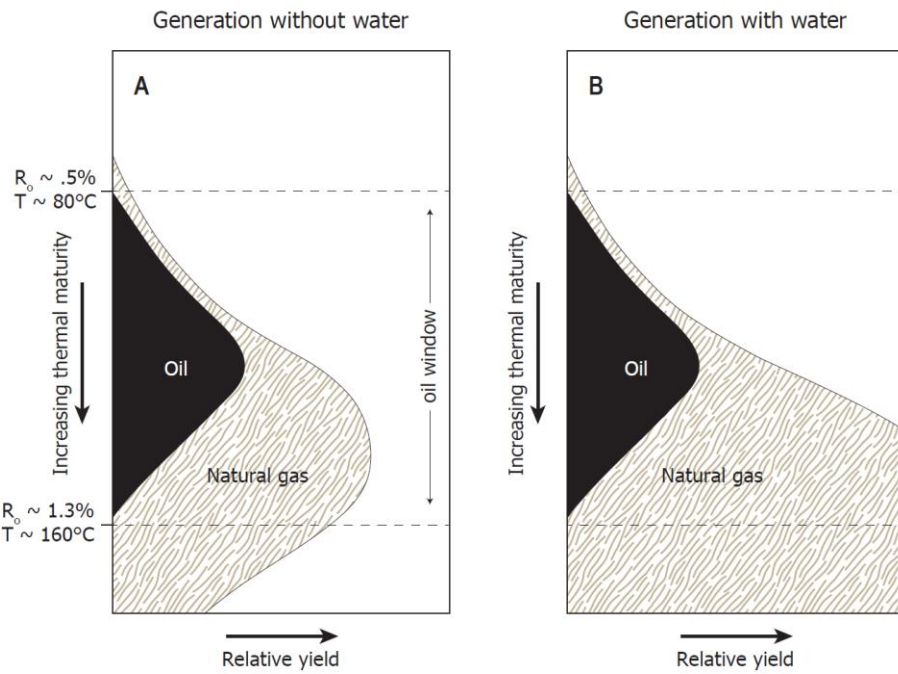
extensive heating

834

Fig. 6. Cartoon showing process of sequential deuteration of sedimentary organic matter and petroleum along with generation of deuterated methane. Snapshots shown represent stages of (A) mild heating (incipient catagenesis); (B) moderate heating (oil window); and (C) extensive heating (gas window).

835

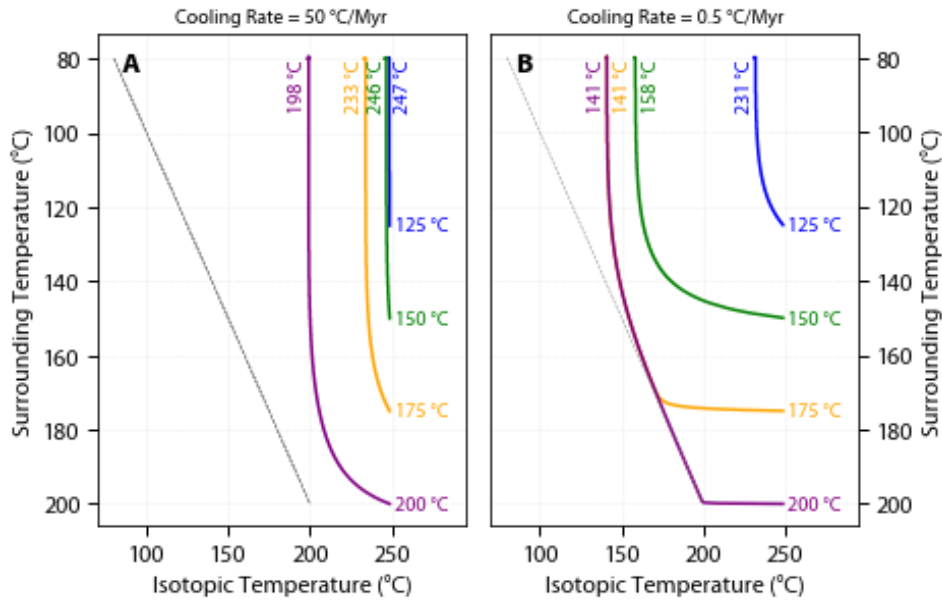
836



837

838 **Fig. 7.** Schematic yields of oil and natural gas when generation occurs from source rock in the absence (A) and
 839 presence (B) of water as a source of H. (A) Traditional model of the amount and timing of organic alteration
 840 products generated during progressive burial in sedimentary basins that assumes that H in organic alteration
 841 products is derived only from kerogen and bitumen. The form of this figure is constrained by the maturation
 842 trends shown in the Van Krevelen diagram. (B) Schematic illustration of the amount and timing of organic
 843 alteration products generated if water and minerals are allowed to contribute the requisite H for the formation of
 844 hydrocarbons. Illustration is after Seewald (2003) and Hunt (1996). Listed values of % R_o and temperature are
 845 from an EASY%Ro calculation applying a heating rate of ~0.4 °C per Myr.

846



847

848 **Fig. 8.** Influence of cooling rate on the closure temperature of hydrogen isotopic exchange between methane and water. Each fluid was cooled from an initial temperature of 125, 150, 175, or 200 °C (upright numbers at right of
849 curves) down to a final temperature of 80 °C at a rate of either (A) $-50\text{ }^{\circ}\text{C/Myr}$ (e.g., representing migration from
850 source to reservoir), or (B) $-0.5\text{ }^{\circ}\text{C/Myr}$ (e.g., representing gradual cooling of an unconventional, source-rock
851 reservoir from maximum burial). The initial methane was assigned an arbitrary isotopic temperature of 250 °C in
852 all simulations ($\Delta^{13}\text{CH}_3\text{D} \approx 2.00\text{\textperthousand}$). Curves show the predicted methane isotopic temperature assuming
853 continuous exchange with 55.5 mol/L water using the kinetic parameters for $\text{CH}_4\text{--H}_2\text{O}$ exchange from Turner et
854 al. (2022). Final methane isotopic temperatures are shown in rotated labels at the topmost ends of curves. The
855 dotted gray line is a 1:1 line representing thermal equilibrium with surrounding environment.
856

857
858
TABLES
859**Table 1**

860 Elemental analysis of Eagle Ford shale powder that was either: dried but otherwise untreated (UNEX), Soxhlet-extracted
861 (EX), or extracted + decarbonated (DECA). Values represent weight percent of the material that was ingested by the
862 elemental analyzer. Data from C. Johnson, WHOI, 1996.

(wt%)	UNEX	EX*	DECA
C	12.1	11.0	6.23
H	0.38	0.25	1.24
N	0.18	0.17	0.74
S	0.37	<0.2	2.3

863 *Used in the experiment.
864

865 **Table 2**

866 Concentration of aqueous species during heating of Soxhlet-extracted Eagle Ford shale at 200 to 350 °C and 350 bar in the
 867 presence of saline D₂O fluid.

Time Pt #	Time (h)	H ₂ (μmol/kg) ^a	CH ₄ (μmol/kg)	$\sum\text{CO}_2$ (mmol/kg)	CH ₄ / $\sum\text{C}_{2-4}$ ^b	$\sum\text{H}_2\text{S}$ (mmol/kg)	pD (25 °C) ^c
<i>Experiment begun with 52.6 g of fluid at temperature of 200 °C</i>							
1	19	BDL (<13)	1.2	4.8	0.78		
2	164	BDL (<13)	3.8	10.8	1.06		
<i>Temperature raised to 300 °C</i>							
3	191	98.0	8.7	21.9	1.68		
4	284	247	235	45.8	1.30		
5	427	392	396	65.5	1.09		
<i>Injected ~18.3 g starting fluid and raised temperature to 325 °C</i>							
6	451	477	319	44.7	1.06		
7	598	791	825	45.3	0.96		
<i>Raised temperature to 350 °C</i>							
8	617	969	1.32×10^3	54.4	1.01		
9	836	1,110	3.47×10^3	51.2	1.06	18.0	5.90

868
 869 Analytical uncertainties (2s) are ±2 °C for T; ±10% for H₂; ±5% for $\sum\text{CO}_2$, CH₄, and C₂ to C₄ hydrocarbons, ±2% for $\sum\text{H}_2\text{S}$;
 870 and ±0.05 units for pD. Concentrations are molar quantities per kg fluid.

871
 872 ^a Determined from thermal conductivity response calibrated against a known H₂ standard, and then multiplied by 1.35 to
 873 account for the difference in thermal conductivity between D₂ and ¹H₂ (Saxena and Saxena, 1970; Whisnant et al., 2011).

874 ^b Calculated as the molar ratio of methane to the sum of ethane, propane, isobutane, and n-butane.

875 ^c The listed pD value was calculated from pH measured with a glass electrode: pD = pH_{measured} + 0.41 (Glasoe and Long,
 876 1960).

1 Title:

2 Incorporation of water-derived hydrogen into methane during artificial maturation of ~~kerogen~~-source rock under
3 hydrothermal conditions

4

5 Submitted to *Organic Geochemistry* on 05 February 2022. Revised manuscript submitted 13 July 2022.

6

7

8 Authors and affiliations:

9 David T. Wang^{a,b*}, Jeffrey S. Seewald^b, Eoghan P. Reeves^c, Shuhei Ono^a, and Sean P. Sylva^b

10 ^aDepartment of Earth, Atmospheric and Planetary Sciences, Massachusetts Institute of Technology, Cambridge, Massachusetts 02139, USA.

11 ^bMarine Chemistry and Geochemistry Department, Woods Hole Oceanographic Institution, Woods Hole, Massachusetts 02543, USA.

12 ^cDepartment of Earth Science, University of Bergen, Bergen N-5007, Norway.

13

14 * Corresponding author. Present address: Esso Exploration and Production Guyana Ltd, 86 Duke Street,
15 Georgetown, Guyana. *E-mail address:* dtw@alum.mit.edu (D.T. Wang).

16

17 *Keywords:*

18 methane, natural gas generation kinetics, D/H ratios, kerogen, clumped isotopologues, hydrogen isotope
19 exchange, water isotopes

20

21 **Abstract**

22 To investigate the origin of C–H bonds in thermogenic methane (CH_4), a solvent-extracted sample of organic-rich
23 Eagle Ford shale was reacted with heavy water (D_2O) under hydrothermal conditions (350 bar) in a flexible Au-
24 TiO_2 cell hydrothermal apparatus ~~in-at~~ a water-to-rock ratio of approximately 5:1. Temperature was increased
25 from 200 to 350 °C over the course of one month and the concentrations of aqueous species and methane
26 isotopologues were quantified as a function of time. In general, production of hydrogen, CO_2 , alkanes, and
27 alkenes increased with time and temperature. Methane formed during the early stages of the experiment at 200 °C
28 was primarily C^1H_4 with some CH_3D . With progressively higher temperatures, increasing proportions of
29 deuterated isotopologues were produced. Near the end of the experiment, the concentration of CD_4 exceeded that
30 of all other isotopologues combined. These results suggest that competition between rates of kerogen-water
31 isotopic exchange and natural gas generation may govern the D/H ratio of thermogenic gases. Furthermore,
32 hydrogenation of kerogen by water may be responsible for hydrocarbon yields in excess of those predicted by
33 conventional models of source rock maturation in which hydrocarbon generation is limited by the amount of
34 organically-bonded hydrogen.

35

36 Abstract: 1942 words

37 Main Text: 6923232 words

38

39

40

41 **1. INTRODUCTION**

42 Variation in D/H ratios (δD values) of thermogenic natural gases is often attributed to kinetically-controlled
43 fractionation during pyrolysis of kerogen or ~~oils~~petroleum. A number of studies have investigated how D/H ratios
44 of methane and other hydrocarbons evolve with increasing thermal maturity (Sackett, 1978; Berner et al., 1995;
45 Sackett and Conkright, 1997; Tang et al., 2005; Ni et al., 2011; Reeves et al., 2012). However, kinetic isotope
46 effects involving hydrogen addition or abstraction are often large and by themselves do not explain the
47 geologically-reasonable apparent equilibrium temperatures of ~150 to 220 °C obtained for reservoir gases that
48 have been studied for their clumped isotopologue compositions (Stolper et al., 2014, 2015; Wang et al., 2015;
49 Douglas et al., 2017; Young et al., 2017; Shuai et al., 2018; Giunta et al., 2019; Labidi et al., 2020; Thiagarajan et
50 al., 2020). There is also evidence that δD values of CH₄ approach values expected for isotopic equilibrium
51 between CH₄ and H₂O in formation waters at temperatures characterizing reservoirs and/or mature source rocks
52 (~150 to 250 °C) (Clayton, 2003; Wang et al., 2015; Xie et al., 2021), although findings of insignificant hydrogen
53 exchange occurring under these conditions also exist (Yeh and Epstein, 1981). In order for methane samples to
54 have approached or attained equilibrium values of $\Delta^{13}\text{CH}_3\text{D}$ and $\Delta^{12}\text{CH}_2\text{D}_2$ —parameters that describe the
55 abundances of clumped isotopologues relative to a stochastic population of molecules containing isotopes
56 randomly distributed amongst them—there must be a pathway by which either (i) isotopes can be exchanged
57 amongst methane isotopologues alone, (ii) methane isotopologues exchange hydrogen with water or other organic
58 molecules, or (iii) methane isotopologues are derived from methyl moieties which contain C–H bonds that have
59 previously exchanged with water prior to forming methane (Hoering, 1984; Smith et al., 1985; Schimmelmann et
60 al., 1999, 2006; Lis et al., 2006).

61 Here, we study the origin of C–H bonds in thermogenic methane by heating ~~a kerogen~~powdered solvent-extracted
62 source rock in the presence of D₂O and examining the degree of deuteration in the generated methane. This
63 experiment is conceptually very similar to ones conducted by Hoering (1984), Lewan (1997), and Schimmelmann
64 et al. (2001). The experiments in those studies were designed to track incorporation of D into bitumen and
65 kerogen.~~N and none of these studies~~ specifically quantified the extent of deuteration in the produced natural
66 gases.

67 **2. MATERIALS AND METHODS**

68 **2.1. Experimental materials and methods/equipment**

69 Experiments were conducted in a gold-titanium reaction cell housed within a flexible cell hydrothermal apparatus
70 (Seyfried et al., 1987) at the Woods Hole Oceanographic Institution (WHOI). Prior to use, the titanium surfaces in
71 contact with the reaction cell contents were heated in air for 24 h at 400 °C to form a more inert TiO₂ surface
72 layer. The reaction cell was further pre-treated prior to loading by soaking in concentrated HCl for 4 hours,
73 followed by rinsing with water to pH neutral and drying in the oven. The exit tube of the apparatus was cleaned
74 by forcing ~20 ml of MilliQ deionized water (18.2 MΩ) through, followed by ~20 ml concentrated HCl, ~100 ml
75 water, ~20 ml concentrated HNO₃, and then ~100 ml of water until the pH tested 7 using pH paper.

76 The source material for this experiment was a hand sample of Upper Cretaceous Eagle Ford Shale taken from an
77 outcrop in Uvalde County, Texas, USA (Hentz and Ruppel, 2010). There is no known oil or gas production from
78 the Eagle Ford in Uvalde County (Tian et al., 2013; IHS Markit Well Database, 2019). The Eagle Ford here is
79 thermally-immature ($R_o = 0.40\text{--}0.55\%$, Cardneaux, 2012; Cardneaux and Nunn, 2013; Harbor, 2011). The sample
80 was powdered to <250 µm and Soxhlet-extracted to remove bitumen and free hydrocarbons. In a subsequent step,

81 the solvent-extracted residue was subjected to hydrochloric acid treatment to remove carbonate minerals.
82 Elemental analysis (**Table 1**) of the original rock sample (UNEX), the Soxhlet-extracted rock sample (EX), and
83 the decalcified+extracted rock sample (DECA) indicates a total organic carbon (TOC) content of ~2.5% and a
84 carbonate content of ~80% by weight. The H/C atomic ratio of the decalcified rock is 2.4. This value is probably
85 several tens of percent higher than the actual H/C ratio of isolated kerogen (not determined) given that substantial
86 amounts of H are likely borne by clays and other minerals that were not removed (Whelan and Thompson-Rizer,
87 1993; Baskin, 1997).

88 Geochemical data for the Eagle Ford sample can be drawn from neighboring Kinney County, Texas, where
89 complete sections of immature Eagle Ford have been recovered by the U.S. Geological Survey (drill core GC-3;
90 French et al., 2020) and Shell (Iona-1 drill core; Eldrett et al., 2014, 2015; Sun et al., 2016); there, the Eagle Ford
91 also crops out, is immature, and is presumed to be geochemically similar. The high calcium carbonate content
92 and relatively lower organic enrichment is consistent with data from the Upper Eagle Ford in the Shell Iona-1
93 core from neighboring Kinney County, Texas (Eldrett et al., 2015).

94 The reaction cell was loaded with 10.03 grams of the EX powder. The starting fluid used was heavy water (D_2O ,
95 99% purity, Cambridge Isotope Laboratories, Inc.) containing NaCl (0.497 mol/kg). The NaCl was added to allow
96 for detection of any leaks in the reaction cell, as dilution of the starting fluid by deionized water from the
97 surrounding pressure vessel would decrease observed Cl concentrations. The reaction cell was loaded with 55.03
98 g of this starting fluid, sealed with a small argon-purged headspace (to allow for expansion of the starting fluid at
99 conditions), and then pressurized and brought to initial condition (200 °C, 350 bar) in approximately 2 h. Several
100 milliliters of fluid were bled during heat-up to purge the exit tube, leaving an estimated 52.6 g of fluid in the cell
101 at the beginning of the experiment (**Table 2**).

102 **2.2. Analytical methods**

103 To monitor the fluid composition and the extent of deuteration with time, sample aliquots of fluid were withdrawn
104 through the capillary exit tube into gastight glass/PTFE syringes. Immediately prior to a sampling event, a small
105 amount (~0.5 g) of fluid was removed and discarded to flush the exit tube. A fluid sample was taken at the
106 beginning and end of each temperature stage. One additional sample (#4) was drawn in the middle of the second
107 temperature stage (300 °C). At time point #6, two aliquots were drawn, each in separate syringes and sampled
108 into separate vials.

109 Deuterium (D_2) is likely to be the main form of molecular hydrogen (H_2) in our experiment due to rapid exchange
110 between water and dissolved hydrogen (Lécluse and Robert, 1994; Wang et al., 2018). The concentration of H_2
111 was determined after headspace extraction using a gas chromatograph (GC) supplied with nitrogen carrier gas and
112 equipped with a molecular sieve 5Å column and thermal conductivity detector. Concentrations reported in
113 **Table 2** have been corrected for the difference in thermal conductivity between D_2 and 1H_2 (see note *a* of
114 **Table 2**), assuming that all dissolved hydrogen is as D_2 . Analytical reproducibility of H_2 concentration data is
115 ±10% or better (2σ).

116 Concentrations of total dissolved inorganic carbon ($\sum CO_2$) and C₁ to C₆ hydrocarbons (alkanes and alkenes) were
117 determined using a purge-and-trap cryofocusing device coupled to a gas chromatograph equipped with a Porapak
118 Q column and serially-connected thermal conductivity and flame ionization detectors. Analytical procedures were
119 as described in Reeves et al. (2012). Analytical reproducibility on duplicate samples was ±5% or better (2σ). The

120 C₅ and C₆ compounds could not be quantified accurately due to their semi-volatile nature; however, C₅ and C₆
121 were detected at all sampling points.

122 At each sampling, a separate ~1 to 2 ml aliquot was injected directly into a pre-weighed, evacuated serum vial
123 capped with boiled blue butyl rubber stoppers, for analysis of the extent of deuteration of methane. A Hewlett-
124 Packard (HP) 6890 gas chromatography-mass spectrometry (GC-MS) system equipped with a 5 Å molecular sieve
125 column (HP-PLOT 30 m × 0.32 mm × 12.0 μm) coupled to an HP 5973 mass selective detector was used to
126 determine the amount of deuteration in CH₄. Mass spectrometer source and quadrupole analyzer temperatures
127 were 230 and 150 °C, respectively, and mass spectra were recorded with an electron impact (EI) ionization energy
128 of 70 eV. Ion currents were monitored at integral masses between *m/z* 10 and 50. Extracted ion currents were
129 quantified at *m/z* 14 through 20 for methane. Expected fragmentation patterns of the five methane-*d_n*
130 isotopologues (C¹H₄, CH₃D, CH₂D₂, CHD₃, and CD₄) were determined by analysis of commercial synthetic
131 standards (>98% purity, Cambridge Isotope Laboratories, Inc.). We refer to the fully protiated methane
132 isotopologue as C¹H₄ in the text when it is necessary to specifically distinguish it from bulk CH₄.

133 3. RESULTS AND DISCUSSION

134 3.1. Temperature and thermal maturity

135 Temperatures logged during the experiment are shown in **Fig. 1A**. Using the temperature history, we calculated
136 thermal maturity as a function of time in units of vitrinite reflectance (%R_o) using EASY%Ro (Sweeney and
137 Burnham, 1990). The estimated thermal maturities are plotted in **Fig. 1B**. While the model predicts maturities of
138 ~0.20 to 0.34% R_o-equivalent for time points #1 and 2 (respectively) and the data are plotted at these calculated
139 maturities, the actual maturity at these time points can be no less than 0.4–0.5% (the initial maturity of the Eagle
140 Ford rock sample, see §2.1). The difference between the plotted and actual %R_o values is somewhat immaterial;
141 what is key is that time points #1 and 2 represent kerogen-source rock that has undergone only incipient organic
142 metamorphism. Maturities encountered in the remainder of the experiment spanned the entire range of the oil
143 window (ca. 0.5% to 1.3% R_o-equivalent; Burnham, 2019). The equivalent-modeled maturity at the final time
144 point (#9) is 1.27% R_o.

145 3.2. Concentrations of aqueous species

146 3.2.1. Inorganic species

147 Measured concentrations of aqueous species are shown in **Fig. 2**. Concentrations of aqueous H₂ increased from
148 below detection (<13 μmol/kg) to up to 1.1 mmol/kg at the end of the experiment, and increased with each
149 temperature step. The H₂ concentration also rose slightly between the beginning and end of each temperature
150 stage of the experiment.

151 The concentration of ΣCO₂ increased during the early stages of the experiment, and leveled off at ~50 mmol/kg at
152 350 °C. The plateauing inorganic carbon concentration suggests that the aqueous solution reached saturation with
153 carbonate minerals (Seewald et al., 1998), a result of CO₂ production during hydrothermal alteration of kerogen
154 (Seewald, 2003), and dissolution of carbonate minerals initially present in the Eagle Ford shale.

155 3.2.2. *Alkanes and alkenes*

156 Concentrations of methane increased in every successive time step, as did concentrations of detected *n*-alkanes.
157 Except for the beginning of the experiment, molar concentrations of C₁ and ΣC_{2–4} were very similar and increased
158 almost in unison.

159 Alkenes (ethylene and propylene, **Fig. 2D–E**) rose in concentration with every increase in temperature, indicating
160 generation of unsaturated hydrocarbons via thermolytic processes. While concentrations of *n*-alkanes increased
161 monotonically from the beginning to end of each temperature stage, the concentrations of alkenes remained
162 constant—or in the 350 °C stage, trended downwards—with time during each stage. Concentrations of alkenes
163 consistent with thermodynamic equilibrium at measured H₂ concentrations are on the order of ~10^{−7.4} and ~10^{−6.6}
164 mol/kg for ethylene and propylene, respectively, at 350 °C (Shock et al., 1989; Shock and Helgeson, 1990).
165 Measured concentrations of alkenes were ~2 orders of magnitude higher than alkane-alkene equilibrium
166 predictions, indicating strong disequilibrium in the relative concentration of alkenes and alkanes. Some portion of
167 the ~10^{−6.5} mol/kg of these alkenes present at time point #1 could have been indigenous to the source rock (i.e.,
168 adsorbed and leached out during initial heating).

169 Evidence from hydrothermal experiments suggests that metastable, reversible alkane/alkene equilibrium should
170 be attained under hydrothermal conditions with half-equilibration times of several hundred hours or less at
171 temperatures of 325 to 350 °C (Seewald, 1994, 2001). Failure to achieve thermodynamic equilibrium within
172 these timescales indicates that generation of thermogenic alkenes occurs concurrently with alkane/alkene
173 hydrogen exchange. Various pyrolysis experiments have reported alkene production (Huizinga et al., 1987; Leif
174 and Simoneit, 2000), lending further support to the hypothesis that continued production of alkenes competes with
175 their conversion into alkanes via hydrogenation at these temperatures and timescales and under redox conditions
176 characterizing hydrothermal maturation of organic-rich mudrocks.

177 Unlike the C₂₊ alkanes, methane cannot dehydrogenate to form an alkene. Hence, hydrogen exchange of methane
178 requires that the very stable C–H bond be broken. Under certain conditions, generally requiring the absence of
179 water or other catalyst poisons, methane exchanges hydrogen over certain catalytic materials such as γ-alumina at
180 room temperature over hours to days (Sattler, 2018, and refs. therein); or with organometallic catalysts under even
181 colder conditions (Golden et al., 2001). However, such catalysts in their active forms are not known to occur
182 naturally in aqueous environments. Experiments conducted by Reeves et al. (2012) with aqueous methane in the
183 presence of iron-bearing minerals in similar flexible-cell Au-TiO₂ reaction vessels revealed only minimal
184 potential exchange over several months, even at temperatures as high as 323 °C. Recently, Turner et al.
185 (unpublished / under review 2022) conducted a set of experiments in flexible gold-cell hydrothermal reactors with
186 CH₄ dissolved in supercritical water at 376 to 420 °C to specifically constrain the rate of CH₄–H₂O hydrogen
187 isotope exchange. Their results confirm that exchange occurs over timescales of hundreds of years at 300 °C and
188 tens of years at 350 °C (half-exchange time, τ_{1/2}), much longer than the duration of our experiment.

189 **3.3. Production of deuterated methane isotopologues**

190 Mass spectra collected for standards are shown in **Fig. 3A**. Relative fragment intensities were similar to those
191 determined in early studies from the U.S. National Bureau of Standards (Dibeler and Mohler, 1950; Mohler et al.,
192 1958). Mass spectra of samples are shown in **Fig. 3B4**. No methane peaks of usable size could be obtained for
193 time point #1. All other time points yielded quantifiable extracted ion chromatogram peaks.

194 The mass spectra of commercial standards were used to fit the sample data using a constrained linear least-squares
195 solver (LSQNONNEG) implemented in MATLAB.¹ Estimated fractional abundances of methane-*d* isotopologues at
196 each time point are shown in **Fig. 45A**.² While it is not straightforward to quantify the uncertainty in these
197 fractional abundances, comparison of the calculated results for samples #6(1) and 6(2) suggests the random error
198 is unlikely to be so large as to affect our interpretation of the overall trends below. Some systematic error is likely
199 present as we did not correct the mass spectra for the ¹³C isotope or for isotopic impurities in the standards.
200 Fractional abundances for each of the isotopologues were converted into absolute abundances (**Fig. 45B**) by
201 multiplying by the methane concentration. The proportion of D in methane-bound hydrogen, calculated from the
202 relative isotopologue abundances, is shown in **Fig. 56**.

203 Methane formed during the early stages of the experiment at 200 °C was primarily C¹H₄ with some CH₃D,
204 whereas at higher temperatures, the isotopologues produced consisted almost exclusively of CD₄, CHD₃, and
205 CH₃D (**Fig. 45A** and **Fig. 56**). These results suggest that at relatively lower temperatures of ~200 °C, the rate of
206 methane generation approaches or exceeds the rate of D/H exchange between water and kerogen, whereas at
207 higher temperatures, extensive D/H exchange between kerogen (or oil³ petroleum, if they are it is also a precursors
208 of methane) and water occurs prior to methane generation. CD₄ became the dominant methane species at
209 temperatures of 300 °C and above, suggesting that more than 50% of all labile, methane-generating sites on
210 kerogen were fully deuterated by this time. As discussed above, uncatalyzed CH₄–D₂O isotopic exchange at this
211 temperature occurs over a much longer timescales than the short (~1 month) duration of our laboratory
212 experiment. There is a possibility of mineral catalysis on the surfaces of the source rock powder used in the
213 experiment, which we cannot rule out given the setup of our experiment. However, the minimal degree of
214 isotopic exchange observed by Reeves et al. (2012) at temperatures of 323 °C and timescales of ~1 year in the
215 presence of redox-active minerals (pyrite, pyrrhotite, and magnetite) suggests that direct exchange of CH₄ with
216 D₂O in our experiment is probably unimportant.³

217 Production of C¹H₄ in the first stage of the experiment (200 °C) indicates that the earliest “capping” hydrogen
218 derives from kerogen or other H-containing species in the rock as opposed to from the H atoms of water. This
219 can only be the case if kerogen has not yet undergone D/H exchange.⁴ While constraints on timescales of D/H
220 exchange at 200 °C are sparse, the available literature supports this assertion. Experiments conducted with model
221 hydrocarbons indicate that D/H exchange of carbon-bound H at 200 °C takes at least several decades, much
222 longer than the heating time in our experiment (Sessions et al., 2004; Schimmelmann et al., 2006; Sessions, 2016;
223 and refs. therein).

224 Production of C¹H₄ and CH₃D appeared to cease by midway through the 300 °C stage (time point #4, 284 hours),
225 or was overshadowed by the generation of much larger quantities of the higher isotopologues. Continued (though

¹ This deconvolution scheme has been used to derive concentrations of methane-*d* isotopologues from mass spectral data for a separate experimental exchange study (A. Sattler, pers. comm.).

² Results of this experiment were first presented in the appendix of a Ph.D. thesis (Wang, 2017). That earlier analysis contained a mathematical error (neglected to divide by the relative peak areas of the pure isotopologue standards). As a result, Fig. B.3 of that thesis appears different than **Fig. 45** in this paper.

³ While it is not an important factor in exchange between CH₄ and D₂O, the source rock matrix is likely important as a catalyst for the exchange of kerogen-bound H with D₂O (prior to methane generation), a process discussed in §3.4.2 and in Alexander et al. (1984).

⁴ It is conceivable that the C¹H₄ observed at time point #2 may have been gas originally present but sorbed to a solid phase at the start of the experiment and later leached into the fluid, but we consider this unlikely because Soxhlet extraction should have removed nearly all of the CH₄ initially sorbed. Furthermore, the concentration of methane tripled between time points #1 (19 h) and #2 (164 h). Release of sorbed gases was probably nearly complete by 19 h.

Formatted: Subscript

226 relatively minor) production of methane that was not fully-deuterated (CHD_3 and CH_3D , **Fig. 45B**) suggests that
227 the kerogen (or ~~oil~~petroleum) from which methane was generated still did not fully exchange before methane
228 formed.

229 If significant exchange were to occur, either between water and kerogen, or between water and methane generated
230 by thermal degradation of longer chain products, and this exchange occurs sequentially, the predominant
231 isotopologue would be expected to follow the progression $\text{C}^1\text{H}_4 \rightarrow \text{CH}_3\text{D} \rightarrow \text{CH}_2\text{D}_2 \rightarrow \text{CHD}_3 \rightarrow \text{CD}_4$. Instead,
232 CH_2D_2 represents a smaller fraction of the methane isotopologues than either CH_3D or CHD_3 at all times, and
233 calculated proportions of CH_2D_2 do not exceed 10% at any point in the experiment (**Fig. 45A**). A possible
234 explanation is that various CH_x moieties (e.g., aromatic C vs. methylene C vs. heteroatom-bound C) of the
235 kerogen or generated petroleum ~~may~~have significantly different propensities to undergo exchange and
236 hydrogenation ([Schimmelmann et al., 2006](#)). Thermal degradation that occurs much slower or faster than
237 exchange may yield either fully-deuterated kerogen (e.g., $-\text{CD}_3$) or singly-deuterated methane, respectively, hence
238 leading to an absence of CH_2D_2 . Alternatively (or possibly in addition), D/H exchange of partially-deuterated
239 longer-chain hydrocarbon molecules with water may be faster than degradation, such that the production of
240 CH_2D_2 is bypassed~~“skipped”~~. The selective production of deuterated methane isotopologues is additional
241 evidence that exchange between water/methane or methane/methane at temperatures of 200 to 350 °C is slow on
242 timescales relevant to laboratory experiments.⁵

243 Comparison of our results with those of Wei et al. (2019), who examined CH_4 generation from petroleum source
244 rock heated under hydrothermal conditions, reveals similar thermal maturity trends for the extent of CH_4
245 deuteration (**Fig. 56A**). Both studies yielded methane with an increasing percentage of water-derived hydrogen as
246 thermal maturity increased. The deuteration vs. maturity trends are sub-parallel to each other. The observed
247 offset between the Wei et al. experimental results and ours (**Fig. 5A**) is probably due to the different source rocks
248 and experimental conditions, including the use of D_2O instead of normal water as the aqueous medium in our
249 experiments. By the middle of the oil window (0.75–0.9% R_o), methane in both studies contained more than 50%
250 of its hydrogen content derived from water.

251 [In a differently-constructed study, Dias et al. \(2014\) evaluated incorporation of aqueous hydrogen into gaseous](#)
252 [products during hydrous pyrolysis of bituminous coal samples taken from the same coal seam along a transect at](#)
253 [various distances away from an igneous intrusion \(and hence with different initial \$R_o\$ values ranging from 0.5 to](#)
254 [6.8%\). After hydrous pyrolysis, measured \$R_o\$ values ranged from 1.4 to 6.9%. An observed dependence of \$\delta\text{D}\$ of](#)
255 [\$\text{CH}_4\$ to \$\delta\text{D}\$ of water allowed them to differentiate native \(sorbed or trapped\) and newly-generated \(via hydrous](#)
256 [pyrolysis\) hydrocarbon gases, with almost all \(>90%\) of \$\text{CH}_4\$ generated from coals with initial \$R_o < 2.0\%\$ being of](#)
257 [newly-generated origin. While the design of their experiment did not allow for quantification of the fractional](#)
258 [contribution of water-derived H to the hydrogen content \(and hence cannot be plotted on Fig. 5A\), their results are](#)
259 [consistent with incorporation of aqueous hydrogen into hydrocarbon gases generated by maturation of thermally-](#)
260 [immature organic matter.](#)

261 The percentage of methane deuteration as a function of cumulative CH_4 generated is shown in **Fig. 56B**.⁶ Because
262 approximately 100 μmol of CH_4 was generated in total, the x -axis of this panel can be read as % of cumulative
263 methane generation. At 50% deuteration, ~~only~~less than 10% of methane has been generated. Stated another way,

⁵ This might be verified by heating normal water ($^1\text{H}_2\text{O}$) in the presence of an initial charge of CD_4 and monitoring for any increase in the δD value of water.

⁶ Calculated as $[\text{CH}_4] \times V_{\text{remaining}} + \sum ([\text{CH}_4] \times V_{\text{withdrawn}})$.

for 90% of the total methane generated in the experiment, more than half of its H content comes from water. From Fig. 45A, the fully-deuterated isotopologue CD₄ predominates towards the end of the experiment (time points #7–9). These late time points mark the end of the oil window (EASY%Ro between 0.9 and 1.3%) (Fig. 56A), suggesting that the immediate precursors of methane have already fully-exchanged their hydrogens with water. The fourth (capping) H in methane may come directly from water or may be abstracted from deuterated kerogen (Dong et al., 2021).

3.4. Interpretation of D/H and clumped isotope signatures of thermogenic CH₄

Efforts to understand the D/H ratios of natural gas hydrocarbons have generally been focused on determining the influence of thermal maturity, organic-inorganic interactions, catalysts, and/or biological processes on the fractionation of hydrogen isotopes in these molecules during their generation, alteration, and/or destruction in source rocks and reservoirs of sedimentary basins. There exist multiple examples of quantitatively-based numerical models for predicting δ D values of natural gases, each grounded in different levels of theory or empiricism (Sackett, 1978; Berner et al., 1995; Clayton, 2003; Tang et al., 2005; Lu et al., 2011, 2021; Ni et al., 2011, 2012).

Correct interpretation of δ D values and clumped isotope signatures of CH₄ depends on understanding the relative kinetics of (a) methane generation from kerogen maturation or cracking of high-molecular weight hydrocarbons; (b) hydrogen exchange of methane precursor molecules with other organic molecules and/or water; and (c) direct or indirect hydrogen exchange between CH₄ and H₂O in the various rock elements of a petroleum system. Timescales of all of these processes range between years to tens of billions of years at the peak hydrocarbon-generating temperatures of 100 to 200 °C, hence the relative importance of these three processes broadly governs the amount of organic-derived and water-derived H in CH₄. These three processes are evaluated separately here with respect to the experimental results and how they apply to the interpretation of isotope and isotopologue ratios of CH₄.

3.4.1. Fractionation and inheritance during methane generation

Methane is generated directly during catagenesis via cleavage of methyl groups from kerogen or bitumen in source rocks. It is also produced as a product of the thermal destruction of high- and low-molecular weight free or bound hydrocarbons, low-molecular weight organic acids, and other organic molecules in source rocks and/or high-temperature reservoirs. Thermogenic methane production ~~occurs~~ has been reported over a very wide range of temperatures, with some reports of commercial volumes of thermogenic natural gas generated at temperatures lower than 86 °C (Laplante, 1974), perhaps even lower than 62 °C (Rowe and Muehlenbachs, 1999). Thermal maturities of corresponding source rocks of putative low-temperature hydrocarbon gases and condensates were estimated to be as low as ~0.25 to 0.4% R_o-equivalent (Laplante, 1974; Stahl, 1977; Purcell et al., 1979; Connan and Cassou, 1980; Snowdon, 1980; Jenden et al., 1993; Muscio et al., 1994; Rowe and Muehlenbachs, 1999; Ramaswamy, 2002). Kerogen moieties will not have undergone much D/H exchange at these low thermal maturities (Dawson et al., 2005; Maslen et al., 2012; Vinnichenko et al., 2021), and thus CH₄ generated from immature or marginally-mature source rocks will partially inherit its hydrogen and their corresponding C–H linkages from the precursor organic matter. Since methyl groups of wood (and presumably other naturally-occurring organic matter) carry clumped isotope values that deviate from equilibrium (Lloyd et al., 2021), and because equilibrium methyl group clumping values [$\Delta(^{13}\text{CH}_3\text{D}-\text{R}$] values] are quite similar to $\Delta^{13}\text{CH}_3\text{D}$ values of CH₄ at these temperatures (within several tenths of a permil; Wang et al., 2015; Lloyd et al., 2021), CH₄ generated from sedimentary organic matter at low levels of thermal stress can be expected to carry non-equilibrated

305 clumping values inherited from methane precursors (**Fig. 67A**). The process of terminating the $\text{CH}_3\cdot$ radical with
306 a $\text{H}\cdot$ radical may be an additional source of disequilibrated clumped methane signatures (Dong et al., 2021; Xie et
307 al., 2021). Under hydrothermal conditions, water is known to provide capping hydrogens to methane via a free
308 radical mechanism (He et al., 2019). Secondary isotope effects from the breaking of C–C bonds adjacent to intact
309 C–H bonds will also be incorporated (Ni et al., 2011).

310 **3.4.2. D/H exchange in precursor organic molecules**

311 In maturing and thermally-mature source rocks, kerogens can be expected to have exchanged part of their organic
312 hydrogen pool with ambient waters. In experiments on source rocks heated to 310–381 °C for up to 6 days with
313 deuterium-enriched and deuterium-depleted waters, Schimmelmann et al. (1999) found that 45 to 79% of carbon-
314 bound hydrogen was derived from water after pyrolysis to equivalent maturities as high as ~1.3% (as
315 EASY%Ro). Aliphatic Type I kerogen, containing large amounts of alkyl groups, were noted to be more
316 isotopically-conservative than kerogens with greater amounts of NSO-containing moieties such as Type IIS
317 kerogen.

318 Exchange of *n*-alkyl hydrogens is slow relative to hydrogen exchange at other positions such as at the α -carbons
319 of C=O groups (Sessions et al., 2004). However, exchange rates for aliphatic hydrogens are not zero. Exchange
320 may proceed via hydrogen transfer to a relatively stable tertiary carbocation-containing intermediate from
321 adjacent methyl or methylene groups (Alexander et al., 1984), or via the reversible dehydration of alkanes to form
322 alkenes under conditions of metastable equilibrium (Seewald, 1994; Reeves et al., 2012). In the absence of
323 significant direct $\text{CH}_4\text{--H}_2\text{O}$ exchange, the formation of large amounts of CD_4 during our experiment suggests that
324 the hydrogen at methyl groups of kerogen (or in other alkyl precursors) exchanges with water under thermal
325 conditions compatible with the generation of petroleum (**Fig. 67B–C**). Water is abundant within most source
326 rocks, with even source rocks with very low water saturation containing up to several percent water by weight
327 (Kazak and Kazak, 2019). Hence, substantial incorporation of water-derived H into CH_4 is likely to occur in
328 actively-generating source rocks so long as water is in contact with sedimentary organic matter. Water dissolved
329 in bitumen generated from kerogen decomposition may participate in CH_4 generation (Lewan and Roy, 2011), as
330 well as water located in pore spaces that are at least partially-lined with organic matter (see §3.5). Equilibrium
331 D/H fractionation between organics and water is likely to be readily attained in at least several functional groups
332 during kerogen or bitumen maturation. While different equilibrium fractionation factors characterize the various
333 H positions in different normal n -and branched alkanes, the average D/H fractionation for *n*-alkanes trends in the
334 same direction as methane (i.e., alkane δD lower than water) (Wang et al., 2009). The progressive incorporation
335 of pre-equilibrated alkyl H into thermogenic methane during natural gas generation may explain in part the
336 approach towards apparent equilibrium with formation water seen in CH_4 of increasing thermal maturity (Clayton,
337 2003; Wang et al., 2018; Turner et al., 2021).

338 **3.4.3. D/H exchange between methane and water in conventional vs. unconventional reservoirs**

339 Timescales of direct hydrogen exchange between CH_4 and ambient H_2O based on experiments conducted in the
340 absence of a catalyst range from hundreds of thousands of years at temperatures around 200 °C, up to hundreds of
341 millions of years at temperatures below 150 °C (Koepf, 1978; Reeves et al., 2012; Wang et al., 2018; Beaudry et
342 al., 2021; Turner et al., under review2022).

343 In a conventional petroleum system, hydrocarbons are generated within an organic-rich source rock, expelled
344 from the source rock into permeable carrier beds, and transported along carrier beds to a reservoir or seep.
345 Generation of oil typically occurs at 80–160 °C (the 'oil window'; **Fig. 78A**). Oil remains within the organic

346 matrix until the amount of retained oil exceeds the expulsion threshold (typically considered a function of organic
347 richness) prior to being expelled from the source rock (Sandvik et al., 1992). Oil-prone source rocks will tend to
348 expel most of their generated hydrocarbons relatively soon after generation, whereas in leaner source rocks with
349 less generative potential, generated oil mostly remains trapped in the source rock (Coopes et al., 1986). In the
350 latter case, larger hydrocarbon compounds (C_{15+}) will have ample time to both undergo exchange of its carbon-
351 bound H (Sessions et al., 2004) and degrade to smaller compounds such as CH_4 that can more easily escape the
352 source rock (Coopes et al., 1986). Expulsion of light hydrocarbons (C_{15} or below, including the C_1 - C_5 gases) is
353 geologically rapid, particularly if the source rock comprises relatively thin (meter-scale) organic-rich beds
354 interbedded with permeable silts or sands (Mackenzie et al., 1983). Secondary migration (from source rock to
355 reservoir) is likely fast as well, even if such migration occurs over long lateral distances (~25 km) (<200,000
356 years for the L.A. Basin; Jung et al., 2015; see also Hindle, 1997; Eichhubl and Boles, 2000). Given that
357 reservoirs are most often cooler than the source rocks, the C–H bonds in CH_4 will have been 'frozen' at or near the
358 point of generation for methane generated at temperatures below ~170 °C. This is easily demonstrated using
359 forward models of isotopic exchange such as those shown by Wang (2017, *their* Appendix A) for clumped
360 isotopologues of CH_4 in conventional gases under conservative assumptions about cooling during migration.

361 **Fig. 8A shows that under a cooling rate of 50 °C/Myr—roughly 5× slower cooling than that implied by the**
362 **migration timescale study of Jung et al. (2015)—and applying the CH_4 – H_2O exchange kinetics determined by**
363 **Turner et al. (2022), closure of methane isotopic exchange should occur around ~170 °C.⁷** – Methane generated in
364 source rocks at temperatures above the oil window (>160 °C) will be more likely to approach D/H equilibrium
365 with water, even if it migrates immediately after generation. The dataset presented by Clayton (2003) showing a
366 leveling-off of $\delta D(CH_4)$ values at around –140 to –150‰ in higher *thermal* maturity, conventional, oil-associated
367 gases while $\delta^{13}C(CH_4)$ continues to increase is very supportive of exchange having occurred at temperatures of
368 >170 °C within or proximal to the source rocks.

Formatted: Font: Bold

Formatted: Font: Bold

369 By contrast, extensive hydrogen exchange in CH_4 likely ~~proceeds~~ occurs following post-generation for
370 unconventional petroleum systems where the source rocks are also the reservoirs. In these self-sourced systems,
371 CH_4 that remains entrapped in pore spaces will probably have exchanged hydrogens with surrounding organics or
372 with any available water as long as the rock has been exposed to temperatures of at least ~130 °C at maximum
373 burial *for several million years (Fig. 8B)*. This is supported with observations that at elevated *thermal* maturities,
374 CH_4 approaches isotopic equilibrium with co-existing formation waters in unconventional reservoirs such as the
375 Utica, Marcellus, and Eagle Ford, consistent with transfer of H from paleo-groundwaters to methane (Wang et al.,
376 2015; Xie et al., 2021). *In source-rock reservoirs which are no longer at maximum burial depths, methane may*
377 *undergo retrograde isotopic exchange during cooling. Closure in these cases is highly sensitive to rates of*
378 *exhumation (Reiners and Brandon, 2006), particularly as the rock passes through the range of temperatures*
379 *between 130 and 160 °C (Fig. 8B).*

380 3.5. Generation potential of natural gas

381 Volumetric calculations based on source rock extent, type, richness, and *thermal* maturity are used to estimate the
382 mass of hydrocarbons generated by source rocks undergoing thermal maturation. These calculations are the basis
383 of estimates of potential resources when assessing frontier basins when only coarse constraints on source rock
384 presence and character are available (Schmoker, 1994). They are also formalized as programmatic subroutines
385 embedded in modern basin modeling packages (Tissot and Espitalié, 1975; Coopes et al., 1986; Pepper and Corvi,

⁷ More comprehensive discussions of closure (quenching) temperatures for D/H exchange reactions of CH_4 can be found in Wang et al. (2018), Turner et al. (2022), and references therein.

386 1995; Tissot, 2003; Freund et al., 2007; Hantschel and Kauerauf, 2009; Stainforth, 2009; Fjellanger et al., 2010)
387 which take spatially-resolved hydrogen index (HI) values of source horizons as a key input constraint.

388 In a series of experiments, Wenger and Price (1991) heated shale source rocks and coals in the presence of water
389 for 30 days at temperatures of 150 to 500 °C. They observed that HI values often increased with experimental
390 temperature, instead of declining as would be expected for simple depletion of initial kerogen via cracking
391 reactions. Furthermore, more hydrocarbons were generated in some experiments than the theoretical maximum
392 yield expected if H in generated petroleum was only derived from organic matter (Price, 2001, their Figure 3).
393 This excess hydrocarbon yield was attributed to incorporation of H₂O-derived hydrogen during the hydrolytic
394 disproportionation of kerogen into CO₂ + CH₄ and other small paraffins, consistent with theoretical and
395 experimental constraints on petroleum degradation in aqueous environments (Helgeson et al., 1993, 2009;
396 Seewald, 1994, 2001, 2003).

397 Evidence from our results and the other studies discussed above suggest that hydrocarbon generation in source
398 rocks may not be limited by the organic hydrogen content of source kerogenrocks. Hence, if H availability is not
399 limiting, and water participates in the formation of hydrocarbons, the upper bound on the amount of hydrocarbons
400 that can be generated is the availability of water to petroleum-generating reactions up to the point of TOC
401 exhaustion. This has been repeatedly suggested by several authors in years past (Lewan, 1992; Helgeson et al.,
402 1993, 2009; Price, 1994, 2001; Seewald, 1994, 2003). If correct, kinetic models of petroleum formation
403 employed in basin modeling that limit hydrocarbon yields based on HI values (Tissot et al., 1987; Tissot, 2003;
404 Hantschel and Kauerauf, 2009) may significantly underpredict the true natural gas resource potential in many of
405 the world's sedimentary basins (**Fig. 7B**).

406 Chemical kinetic models employed in the upstream oil and gas industry for exploration purposes invariably use
407 simple, pseudo-first-order reactions. Many parallel reactions may be simulated at once to simulate different
408 classes of kerogen or petroleum breakdown products; however, all reactions are, without exception, pseudo-first-
409 order in the mass of remaining precursor. However, as noted in Xie et al. (2022), the rate coefficients of these
410 notionally unimolecular reactions can be pressure-dependent, because a third-body collision may be required to
411 remove excess energy from the excited intermediates. Therefore, an algorithmic reaction mechanism generator
412 (RMG; Allen et al., 2012)—operating from a database of elementary reaction kinetics—may be used to determine
413 the important reactions involved in the breakdown of kerogen and petroleum, and to estimate their rate
414 coefficients under typical subsurface pressure & temperature conditions in active source rocks. Furthermore,
415 water is almost invariably excluded as a reactant from computational studies of the thermal decomposition of
416 organic matter because of the computational burden involved. Examples include Class (2015) and Gao (2016)
417 wherein geological oil-to-gas cracking was studied by using RMG to simulate individual radical reactions
418 involved in the pyrolysis of model organic compounds under dry (water-absent) conditions. Very recent
419 developments in RMG now allow it to handle gas- and liquid-phase heterogeneous reactions (Liu et al., 2021). In
420 the future it may therefore be possible to extend the aforementioned studies on pyrolysis of model compounds to
421 include H₂O as a reactant.

422 Several important differences between experimental hydrothermal pyrolysis of source rock powder and
423 maturation of source rocks in nature bear discussing. Most obviously, laboratory experiments substitute higher
424 temperatures to permit hydrocarbons to be generated within much shorter timescales than in nature. Hence, for
425 extrapolation from laboratory to geologic conditions, it is implicitly assumed that the same chemical reactions
426 occur in the same proportions at high and low temperatures. Experiments indicate that this is not often the case,

427 particularly for individual compositional groups (Snowdon, 1979; Ungerer and Pelet, 1987; Dieckmann et al.,
428 2000; Schenk and Dieckmann, 2004). Results of experimental studies, including this one, must be interpreted
429 with this in mind.

430 The availability of water to natural gas-generating reactions may also differ between experiment and nature. Our
431 experiment was set up with a comparatively high water:rock ratio (5:1) to allow ease of sampling, to maintain
432 single-phase conditions, and to prevent dilution of the deuterium content of the water by exchange with rock. The
433 water:carbon ratio was concomitantly high, approximately 200:1 given the TOC of 2.5% and ignoring mineral
434 carbon which is assumed not to ~~not~~ participate in the generation of thermogenic methane. Grinding the Eagle
435 Ford rock sample to rock powder allowed water to readily access exposed sedimentary organic matter with ease.
436 By contrast, water:rock ratios for shales existing in nature (0.003:1 to 0.23:1; Bern et al., 2021) are several orders
437 of magnitude lower than those used in experiments. Petrophysical studies of the structure of pore systems
438 within clay-rich, organic-rich, overmature gas shales suggest that much of the water is bound to the surfaces of
439 clay minerals and contained predominantly in interstices between clay mineral grains (see Figure 30 in Passey et
440 al., 2010). This clay-adsorbed "irreducible water" is considered immobile and cannot be produced during
441 extraction of hydrocarbons, whereas free or capillary-bound water is mobile and comes comingled with gas and
442 oil during production. Using a rastering scanning electron microscopy (SEM) technique, Passey et al. (2010)
443 imaged overmature shale source rocks in 3D, finding abundant small (<0.1 µm) bubble-shaped pore spaces within
444 the organic matter and observing that this intra-organic porosity tended to be interconnected yet isolated from the
445 water-bearing intergranular matrices.

446 While the physical separation of gas-containing pockets from water-bearing interstitial spaces alone might suggest
447 that contact between water and organic material is limited, two processes must be considered. Firstly, much of
448 the oil and gas generated at or near grain boundaries probably underwent primary migration and was expelled out
449 of the source rock long before the present day (Mackenzie et al., 1983; Coopes et al., 1986; Sandvik et al., 1992).
450 Hence, the absence of gas in contact with water does not necessarily indicate that water was unavailable during oil
451 and gas generation. This is supported by more recent SEM work suggesting that a substantial amount of the water
452 fraction in shale source rocks may have direct contact with organic matter that commonly exists within interstices
453 of clay minerals (Gupta et al., 2018). A residual water monolayer on clay particles, if present, might be
454 responsible for some of the undeuterated methane in the early stages of our experiment. If this is the case, using
455 crushed rock instead of rock powder in the experiment might yield yet higher proportions of C¹H₄ in the earlier
456 samples.

Formatted: Superscript

457 The second consideration is that trapped water may have been initially present and was quantitatively consumed
458 during the generation of the gas now present in the organic porosity. This is analogous to water trapped within
459 mineral interstices in partially-serpentined peridotitic rock at mid-ocean ridges reacting with the olivine
460 minerals that surround it, resulting in often dry (waterless), H₂- and CH₄-rich gas secondary fluid inclusions
461 (Klein et al., 2019; Grozeva et al., 2020). Each individual fluid inclusion (or gas-filled shale pore space), then, is
462 a remnant micro-reactor within which all water initially present was consumed in generating the gases now
463 present. Therefore, the activity of water in such pockets of shale source rock isolated from the broader clastic
464 matrix may be sufficiently high to allow for hydration of kerogen at much a lower water:rock ratio in nature than
465 used in our experiment.

466 **4. CONCLUSIONS**

467 Four features in the dataset are notable: (*i*) the production of undeuterated C¹H₄ under incipient catagenic
468 conditions; (*ii*) the predominance of CD₄ towards the end of the experiment, coinciding with the late oil window;
469 (*iii*) the lack of direct methane-water isotopic exchange even at 350 °C; and (*iv*) the near-absence of CH₂D₂ during
470 the experiment. These observations suggest that while some –CH_x moieties in kerogen or longer-chain
471 hydrocarbons undergo exchange more readily than cracking, some other moieties or compound classes are much
472 less prone to exchange.

473 Carefully-controlled, temperature-programmed hydrous deuteration (deuterous pyrolysis or deutothermal
474 pyrolysis) experiments on additional source rocks and [kerogen-organic matter](#) types may reveal systematic
475 differences in the kinetics of exchangability vs. hydrocarbon generation. Such experiments have the potential to
476 improve prediction of generative yields and hydrocarbon composition in basins where timing and quality of
477 charge are key uncertainties.

478 Data from this study support the hypothesis that much of the H in thermogenic natural gases may derive from
479 water, implying that the hydrogen content of organic matter may not limit gas generation. In general, the
480 volumetric significance of the water hydrogen reservoir hence may be underappreciated in estimations of the
481 natural gas resource potential on Earth.

482 **5. ACKNOWLEDGMENTS**

483 Financial support from the U.S. National Science Foundation (NSF awards EAR-1250394 to S.O.), the Alfred P.
484 Sloan Foundation via the Deep Carbon Observatory (to S.O. and J.S.S.), a Shell-MIT Energy Initiative
485 Fellowship, and the Kerr-McGee Professorship at MIT (to S.O.) is acknowledged. E.P.R was supported by the
486 Norwegian Research Council through the Centre for Geobiology (SFF Project #179560). We are grateful to Keith
487 F. M. Thompson (PetroSurveys, Inc.) for providing the Eagle Ford rock sample, Carl Johnson (WHOI) for the
488 elemental analyses, Aaron Sattler (ExxonMobil Research and Engineering) for advice on inverting mass spectral
489 data, Michael Lewan (USGS) for comments on the thesis chapter from which this work originated, and Chris
490 Clayton (CCGS) for an email exchange that inspired this study. [We thank Daniel Dawson and an anonymous](#)
491 [reviewer for helpful feedback on the manuscript, and Cliff Walters, Joe Curiale, and Lloyd Snowdon for editorial](#)
492 [handling and additional comments.](#) The data presented in this paper were collected while the primary author was
493 a Ph.D. student in the MIT/WHOI Joint Program.

494

495 *Conflict of interest statement:* None.

6. REFERENCES

- Alexander, R., Kagi, R.I., Larcher, A.V., 1984. Clay catalysis of alkyl hydrogen exchange reactions—reaction mechanisms. *Organic Geochemistry* 6, 755–760.
- [Allen, J.W., Goldsmith, C.F., Green, W.H., 2012. Automatic estimation of pressure-dependent rate coefficients. *Phys. Chem. Chem. Phys.* 14, 1131–1155.](#)
- Baskin, D.K., 1997. Atomic H/C ratio of kerogen as an estimate of thermal maturity and organic matter conversion. AAPG *Bulletin* 81, 1437–1450.
- Beaudry, P., Stefánsson, A., Fiebig, J., Rhim, J.H., Ono, S., 2021. High temperature generation and equilibration of methane in terrestrial geothermal systems: Evidence from clumped isotopologues. *Geochimica et Cosmochimica Acta* 309, 209–234.
- [Bern, C.R., Birdwell, J.E., Jubb, A.M., 2021. Water-rock interaction and the concentrations of major, trace, and rare earth elements in hydrocarbon-associated produced waters of the United States. *Environmental Science: Processes & Impacts*, 23\(8\), 1198–1219.](#)
- Berner, U., Faber, E., Scheeder, G., Panten, D., 1995. Primary cracking of algal and landplant kerogens: kinetic models of isotope variations in methane, ethane and propane. *Chemical Geology* 126, 233–245.
- Burnham, A.K., 2019. Kinetic models of vitrinite, kerogen, and bitumen reflectance. *Organic Geochemistry* 131, 50–59.
- Cardneaux, A., Nunn, J.A., 2013. Estimates of maturation and TOC from log data in the Eagle Ford Shale, Maverick Basin of South Texas. *Gulf Coast Association of Geological Societies Transactions* 63, 111–124.
- Cardneaux, A.P., 2012. Mapping of the oil window in the Eagle Ford shale play of southwest Texas using thermal modeling and log overlay analysis (Masters Thesis). Louisiana State University.
- Clayton, C., 2003. Hydrogen isotope systematics of thermally generated natural gas. International Meeting on Organic Geochemistry, 21st, Kraków, Poland, Book Abstr. Part I, 51–52.
- [Class, C.A., 2015. Predicting organosulfur chemistry in fuel sources \(PhD Thesis\). Massachusetts Institute of Technology.](#)
- Connan, J., Cassou, A.M., 1980. Properties of gases and petroleum liquids derived from terrestrial kerogen at various maturation levels. *Geochimica et Cosmochimica Acta* 44, 1–23.
- Cooles, G., Mackenzie, A., Quigley, T., 1986. Calculation of petroleum masses generated and expelled from source rocks. *Organic Geochemistry* 10, 235–245.
- Dawson, D., Grice, K., Alexander, R., 2005. Effect of maturation on the indigenous δD signatures of individual hydrocarbons in sediments and crude oils from the Perth Basin (Western Australia). *Organic Geochemistry* 36, 95–104.
- [Dias, R.F., Lewan, M.D., Birdwell, J.E. and Kotarba, M.J., 2014. Differentiation of pre-existing trapped methane from thermogenic methane in an igneous-intruded coal by hydrous pyrolysis. *Organic Geochemistry* 67, 1–7.](#)
- Dibeler, V.H., Mohler, F.L., 1950. Mass spectra of the deuteromethanes. *J. Research Nat. Bur. Standards* 45, 441–444.
- Dieckmann, V., Horsfield, B., Schenk, H.J., 2000. Heating rate dependency of petroleum-forming reactions: implications for compositional kinetic predictions. *Organic Geochemistry* 31, 1333–1348.
- Dong, G., Xie, H., Formolo, M., Lawson, M., Sessions, A., Eiler, J., 2021. Clumped isotope effects of thermogenic methane formation: insights from pyrolysis of hydrocarbons. *Geochimica et Cosmochimica Acta*. doi:10.1016/j.gca.2021.03.009
- Douglas, P.M., Stolper, D.A., Eiler, J.M., Sessions, A.L., Lawson, M., Shuai, Y., Bishop, A., Podlaha, O.G., Ferreira, A.A., Neto, E.V.S., others, 2017. Methane clumped isotopes: Progress and potential for a new isotopic tracer. *Organic Geochemistry* 113, 262–282.
- Eichhubl, P., Boles, J.R., 2000. Rates of fluid flow in fault systems; evidence for episodic rapid fluid flow in the Miocene Monterey Formation, coastal California. *American Journal of Science* 300, 571.
- Eldrett, J.S., Ma, C., Bergman, S.C., Lutz, B., Gregory, F.J., Dodsworth, P., Phipps, M., Hardas, P., Minisini, D., Ozkan, A., Ramezani, J., Bowring, S.A., Kamo, S.L., Ferguson, K., Macaulay, C., Kelly, A.E., 2015. An

Formatted: English (United States)

- 546 astronomically calibrated stratigraphy of the Cenomanian, Turonian and earliest Coniacian from the
547 Cretaceous Western Interior Seaway, USA: Implications for global chronostratigraphy. *Cretaceous*
548 *Research* 56, 316–344.
- 549 Eldrett, J.S., Minisini, D., Bergman, S.C., 2014. Decoupling of the carbon cycle during Ocean Anoxic Event 2.
550 *Geology* 42, 567–570.
- 551 Fjellanger, E., Kontorovich, A.E., Barboza, S.A., Burshtein, L.M., Hardy, M.J., Livshits, V.R., 2010. Charging
552 the giant gas fields of the NW Siberia basin, in: Vining, B.A., Pickering, S.C. (Eds.), *Petroleum Geology:*
553 *From Mature Basins to New Frontiers – Proceedings of the 7th Petroleum Geology Conference*.
554 Geological Society of London, pp. 659–668.
- 555 French, K.L., Birdwell, J.E., Lewan, M.D., 2020. Trends in thermal maturity indicators for the organic sulfur-rich
556 Eagle Ford Shale. *Marine and Petroleum Geology* 118, 104459.
- 557 Freund, H., Walters, C.C., Kelemen, S.R., Siskin, M., Gorbaty, M.L., Curry, D.J., Bence, A.E., 2007. Predicting
558 oil and gas compositional yields via chemical structure–chemical yield modeling (CS-CYM): Part 1 –
559 Concepts and implementation. *Organic Geochemistry* 38, 288–305.
- 560 Gao, C.W., 2016. *Automatic reaction mechanism generation (PhD Thesis)*. Massachusetts Institute of
561 Technology.
- 562 Giunta, T., Young, E.D., Warr, O., Kohl, I., Ash, J.L., Martini, A., Mundel, S.O., Rumble, D., Pérez-Rodríguez,
563 I., Wasley, M., LaRowe, D.E., Gilbert, A., Sherwood Lollar, B., 2019. Methane sources and sinks in
564 continental sedimentary systems: New insights from paired clumped isotopologues $^{13}\text{CH}_3\text{D}$ and $^{12}\text{CH}_2\text{D}_2$.
565 *Geochimica et Cosmochimica Acta* 245, 327–351.
- 566 Glasoe, P.K., Long, F.A., 1960. Use of glass electrodes to measure acidites in deuterium oxide. *The Journal of
567 Physical Chemistry* 64, 188–190.
- 568 Golden, J.T., Andersen, R.A., Bergman, R.G., 2001. Exceptionally low-temperature carbon–hydrogen/carbon–
569 deuterium exchange reactions of organic and organometallic compounds catalyzed by the
570 $\text{Cp}^*(\text{PMe}_3)\text{IrH}(\text{ClCH}_2\text{Cl})^+$ cation. *Journal of the American Chemical Society* 123, 5837–5838.
- 571 Grozeva, N.G., Klein, F., Seewald, J.S., Sylva, S.P., 2020. Chemical and isotopic analyses of hydrocarbon-
572 bearing fluid inclusions in olivine-rich rocks. *Philosophical Transactions of the Royal Society A:
573 Mathematical, Physical and Engineering Sciences* 378, 20180431.
- 574 Gupta, I., Jernigen, J., Curtis, M., Rai, C., Sondergeld, C., 2018. Water-wet or oil-wet: Is it really that simple in
575 shales? *Petrophysics - The SPWLA Journal of Formation Evaluation and Reservoir Description* 59, 308–
576 317.
- 577 Hantschel, T., Kauerauf, A.I., 2009. Petroleum Generation, in: *Fundamentals of Basin and Petroleum Systems
578 Modeling*. Springer Berlin Heidelberg, Berlin, Heidelberg, pp. 151–198.
- 579 Harbor, R.L., 2011. Facies characterization and stratigraphic architecture of organic-rich mudrocks, Upper
580 Cretaceous Eagle Ford Formation, South Texas (Masters Thesis). University of Texas at Austin.
- 581 He, K., Zhang, S., Mi, J., Fang, Y., Zhang, W., 2019. Carbon and hydrogen isotope fractionation for methane
582 from non-isothermal pyrolysis of oil in anhydrous and hydrothermal conditions. *Energy Exploration &
583 Exploitation* 37, 1558–1576.
- 584 Helgeson, H.C., Knox, A.M., Owens, C.E., Shock, E.L., 1993. Petroleum, oil field waters, and authigenic mineral
585 assemblages: Are they in metastable equilibrium in hydrocarbon reservoirs. *Geochimica et Cosmochimica
586 Acta* 57, 3295–3339.
- 587 Helgeson, H.C., Richard, L., McKenzie, W.F., Norton, D.L., Schmitt, A., 2009. A chemical and thermodynamic
588 model of oil generation in hydrocarbon source rocks. *Geochimica et Cosmochimica Acta* 73, 594–695.
- 589 Hentz, T.F., Ruppel, S.C., 2010. Regional lithostratigraphy of the Eagle Ford Shale: Maverick Basin to East
590 Texas Basin. *Gulf Coast Association of Geological Societies Transactions* 60, 325–337.
- 591 Hindle, A.D., 1997. Petroleum Migration Pathways and Charge Concentration: A Three-Dimensional Model.
592 *AAPG Bulletin* 81, 1451–1481.
- 593 Hoering, T., 1984. Thermal reactions of kerogen with added water, heavy water and pure organic substances.
594 *Organic Geochemistry* 5, 267–278.

- 595 Huizinga, B.J., Tannenbaum, E., Kaplan, I.R., 1987. The role of minerals in the thermal alteration of organic
 596 matter—IV. Generation of n-alkanes, acyclic isoprenoids, and alkenes in laboratory experiments.
 597 *Geochimica et Cosmochimica Acta* 51, 1083–1097.
- 598 Hunt, J.M., 1996. Petroleum geochemistry and geology, 2nd ed. WH Freeman San Francisco.
 599 IHS Markit Well Database, 2019. . IHS Markit.
- 600 Jenden, P.D., Drazan, D.J., Kaplan, I.R., 1993. Mixing of thermogenic natural gases in northern Appalachian
 601 basin. *AAPG Bulletin* 77, 980–998.
- 602 Jung, B., Garven, G., Boles, J.R., 2015. The geodynamics of faults and petroleum migration in the Los Angeles
 603 basin, California. *American Journal of Science* 315, 412–459.
- 604 Kazak, E.S., Kazak, A.V., 2019. A novel laboratory method for reliable water content determination of shale
 605 reservoir rocks. *Journal of Petroleum Science and Engineering* 183, 106301.
- 606 Klein, F., Grozeva, N.G., Seewald, J.S., 2019. Abiotic methane synthesis and serpentinization in olivine-hosted
 607 fluid inclusions. *Proceedings of the National Academy of Sciences* 116, 17666.
- 608 Koepp, M., 1978. D/H isotope exchange reaction between petroleum and water: a contributory determinant for
 609 D/H-isotope ratios in crude oils, in: The Fourth International Conference, Geochronology,
 610 Cosmochronology, Isotope Geology USGS Open-File Report 78-701. pp. 221–222.
- 611 Labidi, J., Young, E.D., Giunta, T., Kohl, I.E., Seewald, J., Tang, H., Lilley, M.D., Früh-Green, G.L., 2020.
 612 Methane thermometry in deep-sea hydrothermal systems: Evidence for re-ordering of doubly-substituted
 613 isotopologues during fluid cooling. *Geochimica et Cosmochimica Acta* 288, 248–261.
- 614 Laplante, R.E., 1974. Hydrocarbon generation in Gulf Coast Tertiary sediments. *AAPG Bulletin* 58, 1281–1289.
- 615 Lécluse, C., Robert, F., 1994. Hydrogen isotope exchange reaction rates: Origin of water in the inner solar system.
 616 *Geochimica et Cosmochimica Acta* 58, 2927–2939.
- 617 Leif, R.N., Simoneit, B.R., 2000. The role of alkenes produced during hydrous pyrolysis of a shale. *Organic
 618 Geochemistry* 31, 1189–1208.
- 619 Lewan, M., 1992. Water as a source of hydrogen and oxygen in petroleum formation by hydrous pyrolysis. *Am.
 620 Chem. Soc. Div. Fuel Chem* 37, 1643–1649.
- 621 Lewan, M., 1997. Experiments on the role of water in petroleum formation. *Geochimica et Cosmochimica Acta*
 622 61, 3691–3723.
- 623 Lewan, M.D., Roy, S., 2011. Role of water in hydrocarbon generation from Type-I kerogen in Mahogany oil
 624 shale of the Green River Formation. *Organic Geochemistry* 42, 31–41.
- 625 Lis, G.P., Schimmelmann, A., Mastalerz, M., 2006. D/H ratios and hydrogen exchangeability of type-II kerogens
 626 with increasing thermal maturity. *Organic Geochemistry* 37, 342–353.
- 627 Lloyd, M.K., Eldridge, D.L., Stolper, D.A., 2021. Clumped $^{13}\text{CH}_3\text{D}$ and $^{12}\text{CH}_2\text{D}_2$ compositions of methyl groups
 628 from wood and synthetic monomers: Methods, experimental and theoretical calibrations, and initial
 629 results. *Geochimica et Cosmochimica Acta* 297, 233–275.
- 630 Liu, M., Grinberg Dana, A., Johnson, M.S., Goldman, M.J., Jocher, A., Payne, A.M., Grambow, C.A., Han, K.,
 631 Yee, N.W., Mazeau, E.J., Blodal, K., West, R.H., Goldsmith, C.F., Green, W.H., 2021. Reaction
 632 Mechanism Generator v3.0: Advances in Automatic Mechanism Generation. *Journal of Chemical
 633 Information and Modeling* 61, 2686–2696.
- 634 Lu, S., Wang, M., Xue, H., Li, J., Chen, F., Xu, Q., 2011. The impact of aqueous medium on gas yields and
 635 kinetic behaviors of hydrogen isotope fractionation during organic matter thermal degradation. *Acta
 636 Geologica Sinica - English Edition* 85, 1466–1477.
- 637 Lu, S.-F., Feng, G.-Q., Shao, M.-L., Li, J.-J., Xue, H.-T., Wang, M., Chen, F.-W., Li, W.-B., Pang, X.-T., 2021.
 638 Kinetics and fractionation of hydrogen isotopes during gas formation from representative functional
 639 groups. *Petroleum Science* 18, 1021–1032.
- 640 Mackenzie, A.S., Leythaeuser, D., Schaefer, R.G., Bjorøy, M., 1983. Expulsion of petroleum hydrocarbons from
 641 shale source rocks. *Nature* 301, 506–509.
- 642 Maslen, E., Grice, K., Dawson, D., Wang, S., Horsfield, B., 2012. Stable hydrogen isotopes of isoprenoids and n-
 643 alkanes as a proxy for estimating the thermal history of sediments through geological time:, in: Harris,
 644 N.B., Peters, K.E. (Eds.), *Analyzing the Thermal History of Sedimentary Basins: Methods and Case
 645 Studies*. SEPM Society for Sedimentary Geology, pp. 29–43.

Formatted: English (United States)

- 646 Mohler, F.L., Dibeler, V.H., Quinn, E., 1958. Redetermination of mass spectra of deuteromethanes. *Journal of*
647 *Research of the National Bureau of Standards* 61, 171–172.
- 648 Muscio, G.P.A., Horsfield, B., Welte, D.H., 1994. Occurrence of thermogenic gas in the immature zone—
649 implications from the Bakken in-source reservoir system. *Organic Geochemistry* 22, 461–476.
- 650 Ni, Y., Liao, F., Dai, J., Zou, C., Zhu, G., Zhang, B., Liu, Q., 2012. Using carbon and hydrogen isotopes to
651 quantify gas maturity, formation temperature, and formation age — specific applications for gas fields
652 from the Tarim basin, China. *Energy Exploration & Exploitation* 30, 273–293.
- 653 Ni, Y., Ma, Q., Ellis, G.S., Dai, J., Katz, B., Zhang, S., Tang, Y., 2011. Fundamental studies on kinetic isotope
654 effect (KIE) of hydrogen isotope fractionation in natural gas systems. *Geochimica et Cosmochimica Acta*
655 75, 2696–2707.
- 656 Passey, Q.R., Bohacs, K., Esch, W.L., Klimentidis, R., Sinha, S., 2010. From Oil-Prone Source Rock to Gas-
657 Producing Shale Reservoir - Geologic and Petrophysical Characterization of Unconventional Shale Gas
658 Reservoirs, in: SPE-131350-MS. Presented at the International Oil and Gas Conference and Exhibition in
659 China, Society of Petroleum Engineers, Beijing, China, p. 29.
- 660 Pepper, A.S., Corvi, P.J., 1995. Simple kinetic models of petroleum formation. Part I: oil and gas generation from
661 kerogen. *Marine and Petroleum Geology* 12, 291–319.
- 662 Price, L.C., 1994. Metamorphic free-for-all. *Nature* 370, 253–254.
- 663 Price, L.C., 2001. A possible deep-basin-high-rank gas machine via water-organic-matter redox reactions, in:
664 Dyman, T.S., Kuuskraa, V.A. (Eds.), *Geologic Studies of Deep Natural Gas Resources*, Digital Data
665 Series. U. S. Geological Survey.
- 666 Purcell, L.P., Rashid, M.A., Hardy, I.A., 1979. Geochemical characteristics of sedimentary rocks in Scotian basin.
667 AAPG Bulletin 63, 87–105.
- 668 Ramaswamy, G., 2002. A field evidence for mineral-catalyzed formation of gas during coal maturation. *Oil & gas*
669 journal 100, 32–36.
- 670 Reeves, E.P., Seewald, J.S., Sylva, S.P., 2012. Hydrogen isotope exchange between *n*-alkanes and water under
671 hydrothermal conditions. *Geochimica et Cosmochimica Acta* 77, 582–599.
- 672 Reiners, P.W., Brandon, M.T., 2006. *Using Thermochronology to Understand Orogenic Erosion*. *Annual Review*
673 *of Earth and Planetary Sciences* 34, 419–466.
- 674 Rowe, D., Muehlenbachs, K., 1999. Low-temperature thermal generation of hydrocarbon gases in shallow shales.
675 *Nature* 398, 61–63.
- 676 Sackett, W.M., 1978. Carbon and hydrogen isotope effects during the thermocatalytic production of hydrocarbons
677 in laboratory simulation experiments. *Geochimica et Cosmochimica Acta* 42, 571–580.
- 678 Sackett, W.M., Conkright, M., 1997. Summary and re-evaluation of the high-temperature isotope geochemistry of
679 methane. *Geochimica et Cosmochimica Acta* 61, 1941–1952.
- 680 Sandvik, E.I., Young, W.A., Curry, D.J., 1992. Expulsion from hydrocarbon sources: the role of organic
681 absorption. *Organic Geochemistry* 19, 77–87.
- 682 Sattler, A., 2018. Hydrogen/Deuterium (H/D) exchange catalysis in alkanes. *ACS Catalysis* 8, 2296–2312.
- 683 Saxena, S.C., Saxena, V.K., 1970. Thermal conductivity data for hydrogen and deuterium in the range 100–1100
684 degrees C. *Journal of Physics A: General Physics* 3, 309–320.
- 685 Schenk, H.J., Dieckmann, V., 2004. Prediction of petroleum formation: the influence of laboratory heating rates
686 on kinetic parameters and geological extrapolations. *Marine and Petroleum Geology* 21, 79–95.
- 687 Schimmelmann, A., Boudou, J.-P., Lewan, M.D., Wintsch, R.P., 2001. Experimental controls on D/H and
688 $\frac{\text{textsuperscript}\text{D}}{\text{C}}/\frac{\text{textsuperscript}\text{C}}{\text{D}}$ ratios of kerogen, bitumen and oil during hydrous pyrolysis. *Organic*
689 *Geochemistry* 32, 1009–1018.
- 690 Schimmelmann, A., Lewan, M.D., Wintsch, R.P., 1999. D/H isotope ratios of kerogen, bitumen, oil, and water in
691 hydrous pyrolysis of source rocks containing kerogen types I, II, IIS, and III. *Geochimica et*
692 *Cosmochimica Acta* 63, 3751–3766.
- 693 Schimmelmann, A., Sessions, A.L., Mastalerz, M., 2006. Hydrogen isotopic (D/H) composition of organic matter
694 during diagenesis and thermal maturation. *Annual Review of Earth and Planetary Sciences* 34, 501–533.
- 695 Schmoker, J.W., 1994. Volumetric calculation of hydrocarbons generated, in: Maguire, L.B., Dow, W.G. (Eds.),
696 *The Petroleum System---from Source to Trap*, AAPG Memoir. pp. 323–326.

Formatted: Superscript

Formatted: Superscript

- 697 Seewald, J.S., 1994. Evidence for metastable equilibrium between hydrocarbons under hydrothermal conditions.
698 *Nature* 370, 285–287.
- 699 Seewald, J.S., 2001. Aqueous geochemistry of low molecular weight hydrocarbons at elevated temperatures and
700 pressures: constraints from mineral buffered laboratory experiments. *Geochimica et Cosmochimica Acta*
701 65, 1641–1664.
- 702 Seewald, J.S., 2003. Organic–inorganic interactions in petroleum-producing sedimentary basins. *Nature* 426,
703 327–333.
- 704 Seewald, J.S., Benitez-Nelson, B.C., Whelan, J.K., 1998. Laboratory and theoretical constraints on the generation
705 and composition of natural gas. *Geochimica et Cosmochimica Acta* 62, 1599–1617.
- 706 Sessions, A.L., 2016. Factors controlling the deuterium contents of sedimentary hydrocarbons. *Organic*
707 *Geochemistry* 96, 43–64.
- 708 Sessions, A.L., Sylva, S.P., Summons, R.E., Hayes, J.M., 2004. Isotopic exchange of carbon-bound hydrogen
709 over geologic timescales. *Geochimica et Cosmochimica Acta* 68, 1545–1559.
- 710 Seyfried, W.E., Jr., Janecky, D.R., Berndt, M.E., 1987. Rocking autoclaves for hydrothermal experiments, II. The
711 flexible reaction-cell system. *Hydrothermal Experimental Techniques* 9, 216–239.
- 712 Shock, E.L., Helgeson, H.C., 1990. Calculation of the thermodynamic and transport properties of aqueous species
713 at high pressures and temperatures: Standard partial molal properties of organic species. *Geochimica et*
714 *Cosmochimica Acta* 54, 915–945.
- 715 Shock, E.L., Helgeson, H.C., Sverjensky, D.A., 1989. Calculation of the thermodynamic and transport properties
716 of aqueous species at high pressures and temperatures: Standard partial molal properties of inorganic
717 neutral species. *Geochimica et Cosmochimica Acta* 53, 2157–2183.
- 718 Shuai, Y., Etiope, G., Zhang, S., Douglas, P.M., Huang, L., Eiler, J.M., 2018. Methane clumped isotopes in the
719 Songliao Basin (China): New insights into abiotic vs. biotic hydrocarbon formation. *Earth and Planetary*
720 *Science Letters* 482, 213–221.
- 721 Smith, J., Rigby, D., Gould, K., Hart, G., Hargraves, A., 1985. An isotopic study of hydrocarbon generation
722 processes. *Organic Geochemistry* 8, 341–347.
- 723 Snowdon, L., 1980. Resinite—A potential petroleum source in the upper Cretaceous/Tertiary of the Beaufort-
724 Mackenzie Basin, in: Miall, A.D. (Ed.), *Facts and Principles of World Petroleum Occurrence*, CSPG
725 Special Publications. pp. 509–521.
- 726 Snowdon, L.R., 1979. Errors in extrapolation of experimental kinetic parameters to organic geochemical systems:
727 Geologic notes. *AAPG Bulletin* 63, 1128–1134.
- 728 Stahl, W.J., 1977. Carbon and nitrogen isotopes in hydrocarbon research and exploration. *Chemical Geology* 20,
729 121–149.
- 730 Stainforth, J.G., 2009. Practical kinetic modeling of petroleum generation and expulsion. *Thematic Set on Basin*
731 *Modeling Perspectives* 26, 552–572.
- 732 Stolper, D., Martini, A., Clog, M., Douglas, P., Shusta, S., Valentine, D., Sessions, A., Eiler, J., 2015.
733 Distinguishing and understanding thermogenic and biogenic sources of methane using multiply
734 substituted isotopologues. *Geochimica et Cosmochimica Acta* 161, 219–247.
- 735 Stolper, D.A., Lawson, M., Davis, C.L., Ferreira, A.A., Santos Neto, E.V., Ellis, G.S., Lewan, M.D., Martini,
736 A.M., Tang, Y., Schoell, M., Sessions, A.L., Eiler, J.M., 2014. Formation temperatures of thermogenic
737 and biogenic methane. *Science* 344, 1500–1503.
- 738 Sun, X., Zhang, T., Sun, Y., Milliken, K.L., Sun, D., 2016. Geochemical evidence of organic matter source input
739 and depositional environments in the lower and upper Eagle Ford Formation, south Texas. *Organic*
740 *Geochemistry* 98, 66–81.
- 741 Sweeney, J.J., Burnham, A.K., 1990. Evaluation of a simple model of vitrinite reflectance based on chemical
742 kinetics. *AAPG Bulletin* 74, 1559–1570.
- 743 Tang, Y., Huang, Y., Ellis, G.S., Wang, Y., Kralert, P.G., Gillaizeau, B., Ma, Q., Hwang, R., 2005. A kinetic
744 model for thermally induced hydrogen and carbon isotope fractionation of individual *n*-alkanes in crude
745 oil. *Geochimica et Cosmochimica Acta* 69, 4505–4520.

- 746 Thiagarajan, N., Xie, H., Ponton, C., Kitchen, N., Peterson, B., Lawson, M., Formolo, M., Xiao, Y., Eiler, J.,
 747 2020. Isotopic evidence for quasi-equilibrium chemistry in thermally mature natural gases. *Proceedings of*
 748 *the National Academy of Sciences* 117, 3989–3995.
- 749 Tian, Y., Ayers, W.B., McCain Jr, D., 2013. The Eagle Ford Shale play, south Texas: regional variations in fluid
 750 types, hydrocarbon production and reservoir properties, in: IPTC 2013: International Petroleum
 751 Technology Conference. European Association of Geoscientists & Engineers, p. IPTC 16808.
- 752 Tissot, B., 2003. Preliminary data on the mechanisms and kinetics of the formation of petroleum in sediments.
 753 computer simulation of a reaction flowsheet. *Oil & Gas Science and Technology - Rev. IFP* 58, 183–202.
- 754 Tissot, B., Espitalié, J., 1975. L'évolution thermique de la matière organique des sédiments : applications d'une
 755 simulation mathématique. Potentiel pétrolier des bassins sédimentaires de reconstitution de l'histoire
 756 thermique des sédiments. *Rev. Inst. Fr. Pét.* 30, 743–778.
- 757 Tissot, B., Pelet, R., Ungerer, P., 1987. Thermal history of sedimentary basins, maturation indices, and kinetics of
 758 oil and gas generation. *AAPG Bulletin* 71, 1445–1466.
- 759 Turner, A.C., Korol, R., Eldridge, D.L., Bill, M., Conrad, M.E., Miller, T.F., Stolper, D.A., 2021. Experimental
 760 and theoretical determinations of hydrogen isotopic equilibrium in the system CH₄-H₂-H₂O from 3 to
 761 200 °C. *Geochimica et Cosmochimica Acta*. doi:10.1016/j.gca.2021.04.026
- 762 Turner, A.C., Pester, N.J., Bill, M., Conrad, M.E., Knauss, K.G., Stolper, D.A., ~~unpublished / under review~~ 2022.
 763 Experimental determination of hydrogen isotope exchange rates between methane and water under
 764 hydrothermal conditions. *Geochimica et Cosmochimica Acta* [329, 231–255](#).
 765 doi:10.1016/j.gca.2022.04.029
- 766 ~~Turner, A.C., Pester, N.J., Bill, M., Conrad, M.E., Knauss, K.G., Stolper, D.A., under review. Experimental
 767 determination of hydrogen isotope exchange rates between methane and water under hydrothermal
 768 conditions. Geochimica et Cosmochimica Acta.~~
- 769 Ungerer, P., Pelet, R., 1987. Extrapolation of the kinetics of oil and gas formation from laboratory experiments to
 770 sedimentary basins. *Nature* 327, 52–54.
- 771 Vinnichenko, G., Jarrett, A.J.M., van Maldegem, L.M., Brocks, J.J., 2021. Substantial maturity influence on
 772 carbon and hydrogen isotopic composition of n-alkanes in sedimentary rocks. *Organic Geochemistry* 152,
 773 104171.
- 774 Wang, D.T., 2017. The geochemistry of methane isotopologues (PhD Thesis). Massachusetts Institute of
 775 Technology and Woods Hole Oceanographic Institution. doi:10.1575/1912/9052
- 776
- 777 Wang, D.T., Gruen, D.S., Lollar, B.S., Hinrichs, K.-U., Stewart, L.C., Holden, J.F., Hristov, A.N., Pohlman, J.W.,
 778 Morrill, P.L., Könneke, M., Delwiche, K.B., Reeves, E.P., Sutcliffe, C.N., Ritter, D.J., Seewald, J.S.,
 779 McIntosh, J.C., Hemond, H.F., Kubo, M.D., Cardace, D., Hoehler, T.M., Ono, S., 2015. Nonequilibrium
 780 clumped isotope signals in microbial methane. *Science* 348, 428–431.
- 781 Wang, D.T., Reeves, E.P., McDermott, J.M., Seewald, J.S., Ono, S., 2018. Clumped isotopologue constraints on
 782 the origin of methane at seafloor hot springs. *Geochimica et Cosmochimica Acta* 223, 141–158.
- 783 Wang, Y., Sessions, A.L., Nielsen, R.J., Goddard III, W.A., 2009. Equilibrium ²H/H fractionations in organic
 784 molecules. II: Linear alkanes, alkenes, ketones, carboxylic acids, esters, alcohols and ethers. *Geochimica
 785 et Cosmochimica Acta* 73, 7076–7086.
- 786 Wei, L., Gao, Z., Mastalerz, M., Schimmelmann, A., Gao, L., Wang, X., Liu, X., Wang, Y., Qiu, Z., 2019.
 787 Influence of water hydrogen on the hydrogen stable isotope ratio of methane at low versus high
 788 temperatures of methanogenesis. *Organic Geochemistry* 128, 137–147.
- 789 Wenger, L., Price, L., 1991. Differential petroleum generation and maturation paths of the different organic matter
 790 types as determined by hydrous pyrolysis over a wide range of experimental temperatures, in: European
 791 Association of Organic Geochemists 15th International Meeting, Advances and Applications in the
 792 Natural Environment: Organic Geochemistry. pp. 335–339.
- 793 Whelan, J.K., Thompson-Rizer, C.L., 1993. Chemical methods for assessing kerogen and protokerogen types and
 794 maturity, in: Engel, M.H., Macko, S.A. (Eds.), *Organic Geochemistry: Principles and Applications*.
 795 Springer US, Boston, MA, pp. 289–353.

Formatted: Subscript

Formatted: Subscript

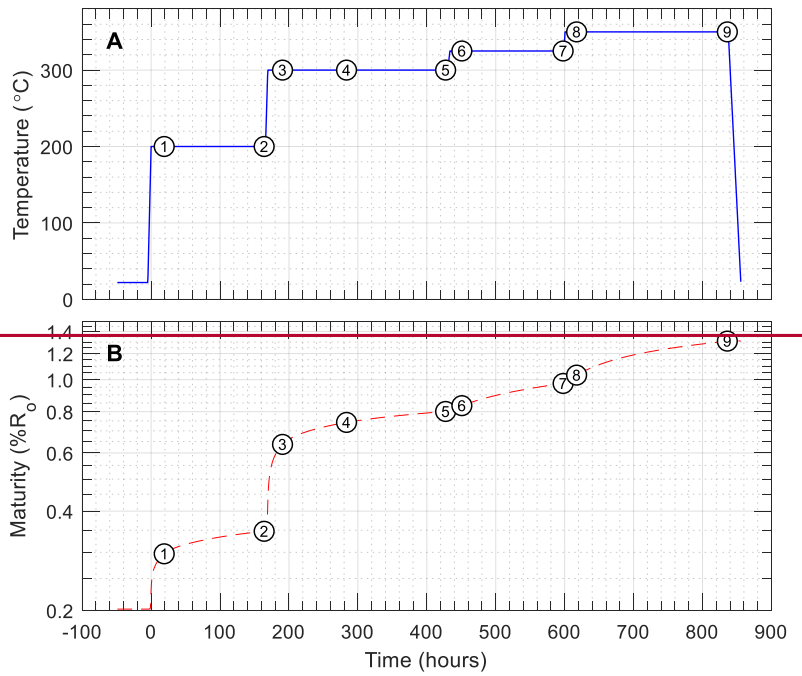
Formatted: Subscript

- 796 Whisnant, C.S., Hansen, P.A., Kelley, T.D., 2011. Measuring the relative concentration of H₂ and D₂ in HD gas
797 with gas chromatography. *Review of Scientific Instruments* 82, 024101.
- 798 Xie, H., Dong, G., Formolo, M., Lawson, M., Liu, J., Cong, F., Mangenot, X., Shuai, Y., Ponton, C., Eiler, J.,
799 2021. The evolution of intra- and inter-molecular isotope equilibria in natural gases with thermal
800 maturation. *Geochimica et Cosmochimica Acta*. doi:10.1016/j.gca.2021.05.012
- 801 [Xie, H., Formolo, M., Eiler, J., 2022. Predicting isotopologue abundances in the products of organic catagenesis
with a kinetic Monte-Carlo model. Geochimica et Cosmochimica Acta 327, 200–228.](#)
- 803 Yeh, H.-W., Epstein, S., 1981. Hydrogen and carbon isotopes of petroleum and related organic matter.
804 *Geochimica et Cosmochimica Acta* 45, 753–762.
- 805 Young, E.D., Kohl, I.E., Lollar, B.S., Etiope, G., Rumble, D., Li, S., Haghnegahdar, M.A., Schauble, E.A.,
806 McCain, K.A., Foustoukos, D.I., Sutcliffe, C., Warr, O., Ballentine, C.J., Onstott, T.C., Hosgormez, H.,
807 Neubeck, A., Marques, J.M., Pérez-Rodríguez, I., Rowe, A.R., LaRowe, D.E., Magnabosco, C., Yeung,
808 L.Y., Ash, J.L., Bryndzia, L.T., 2017. The relative abundances of resolved ¹²CH₂D₂ and ¹³CH₃D and
809 mechanisms controlling isotopic bond ordering in abiotic and biotic methane gases. *Geochimica et
810 Cosmochimica Acta* 203, 235–264.
- 811
- 812
- 813

Formatted: Spanish (Spain)

814

7. FIGURE CAPTIONS



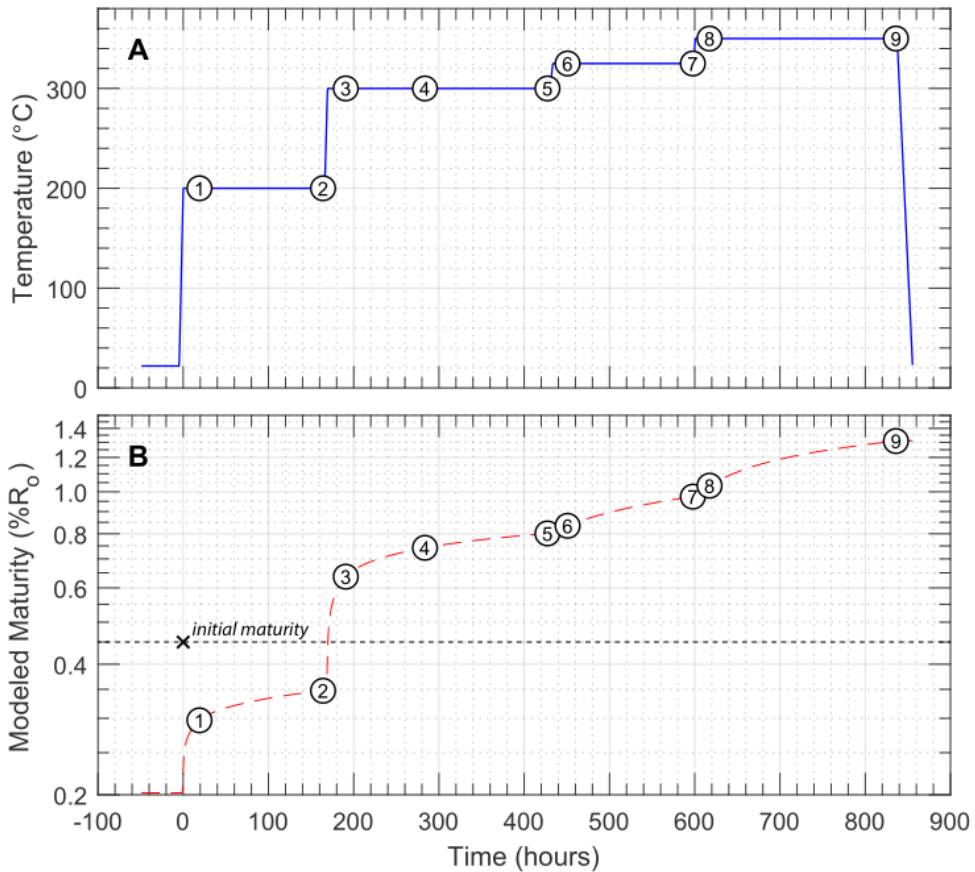
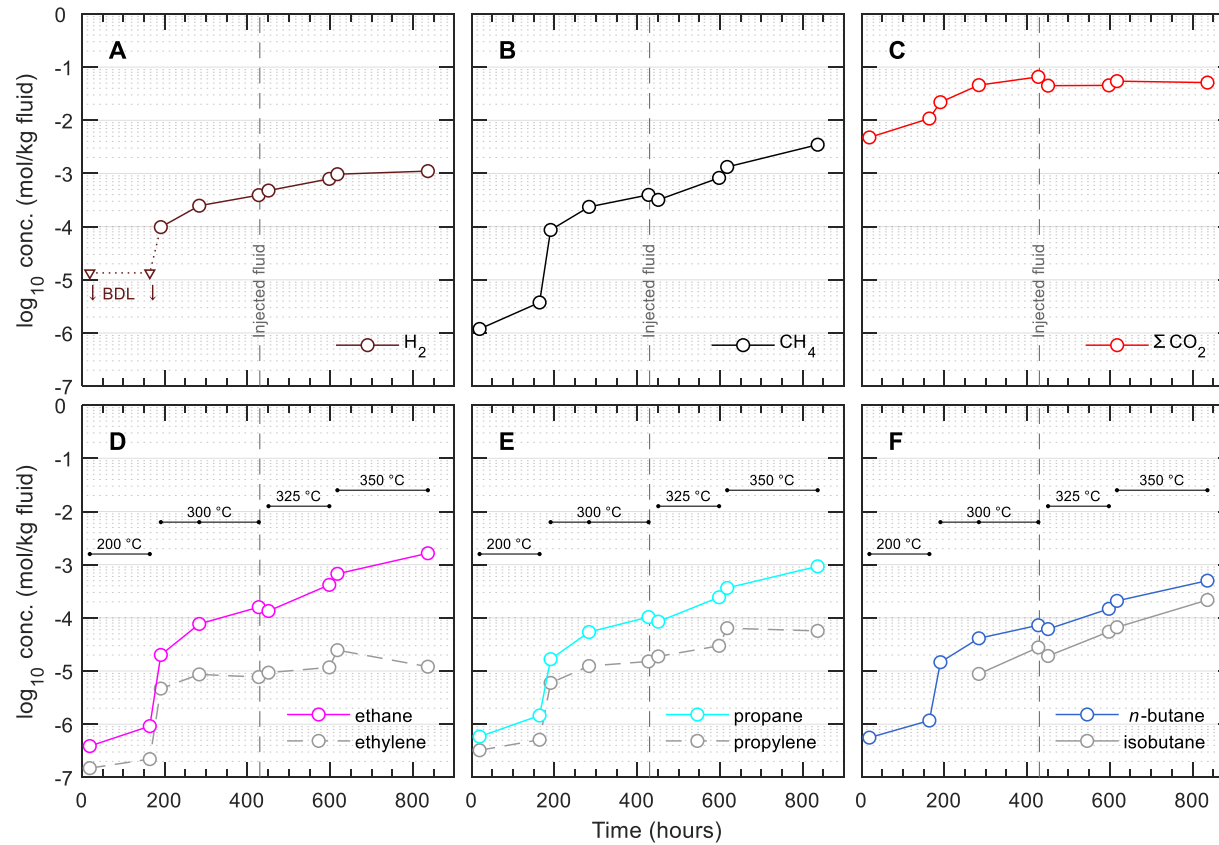


Fig. 1. Profiles of (A) temperature and (B) estimated thermal maturity (calculated using EASY%Ro) vs. time.

Time zero ($t = 0$) is the time at which the experiment was brought to initial conditions (200 °C and 350 bar).

Numbers in circles represent sampling points (Table 22).

Formatted: Font: Not Bold



821

822 **Fig. 2.** Concentrations of aqueous species over time during the experiment. (A) Hydrogen (H_2 , measured as D_2); (B) methane (CH_4); (C) total
823 inorganic carbon (ΣCO_2); (D) ethane and ethylene; (E) propane and propylene; and (F) *n*-butane and isobutane. Note that injection of additional
824 saline D_2O at 430 hours diluted the concentration of all aqueous species by ~50%. BDL, below detection limit (<13 $\mu\text{mol}/\text{kg}$ for D_2).

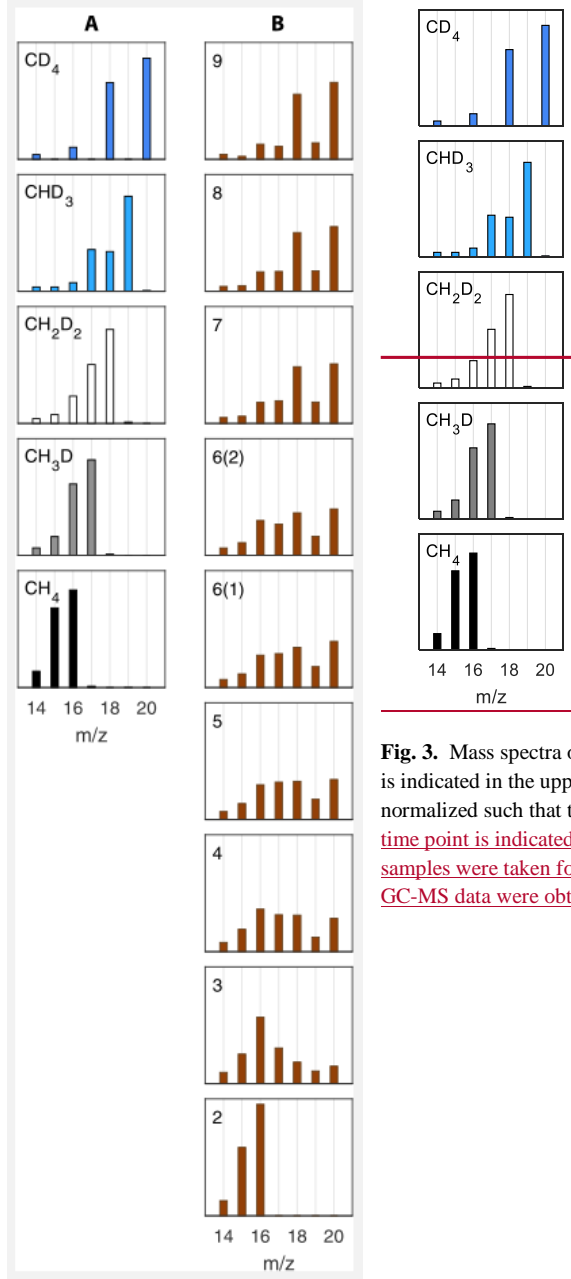


Fig. 3. Mass spectra of **(A)** standards and **(B)** samples. Isotopologue is indicated in the upper left corner of each plot. Intensities were normalized such that the m/z 14 to 20 signals sum to unity. In **(B)**, time point is indicated in the upper left corner of each plot. Two samples were taken for time point #6, hence there are two plots. No GC-MS data were obtained for time point #1.

Formatted: Font: Bold

Formatted: Font: Bold

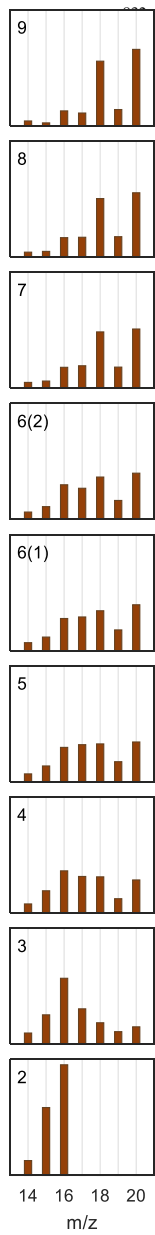
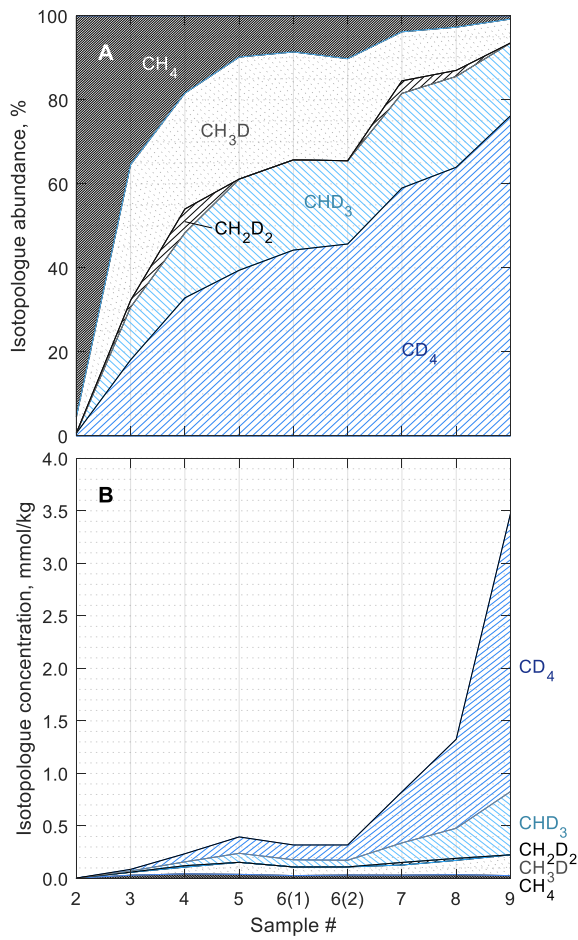
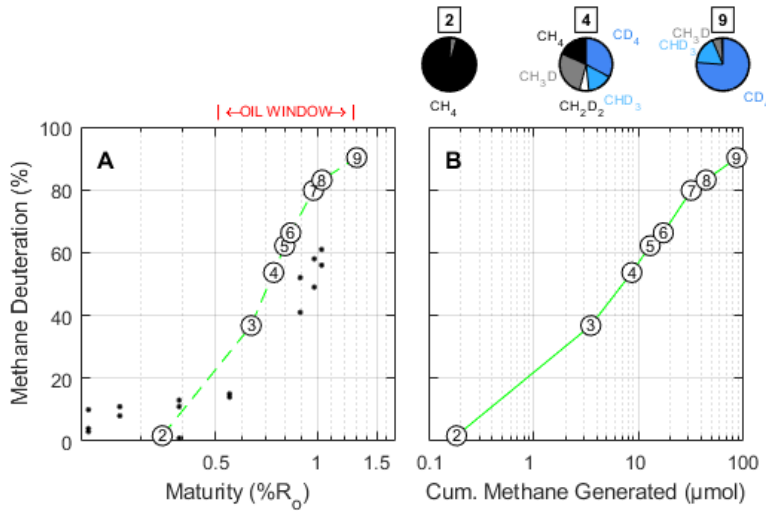


Fig. 4. Mass spectra of samples. Time point is indicated in the upper left corner of each plot. Intensities were normalized such that the m/z 14 to 20 signals sum to unity. Two samples were taken for time point #6, hence there are two plots. No GC MS data was obtained for time point #1.



837

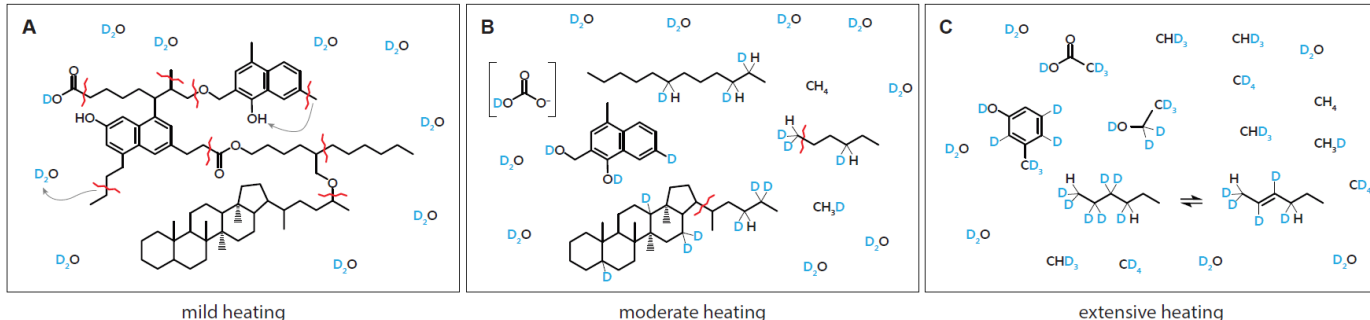
838 **Fig. 45.** Calculated (A) fractional and (B) absolute abundances of methane isotopologues.



839

840 | **Fig. 56.** Extent of methane deuteration [methane-bound D/(D+H)] vs. (A) estimated maturity (via EASY%Ro)
 841 and (B) cumulative methane generated. The data shown for time point #6 is the average of the two replicate
 842 samples. Small symbols in (A) are data from Wei et al. (2019) representing percentage of water-derived H in
 843 CH₄. Thermal maturities for the Wei et al. data were calculated from a time-temperature curve reconstructed
 844 from their described experimental procedures. Pie charts above (B) represent fractional abundances of
 845 isotopologues before, during, and after peak oil generation (time points #2, 4, and 9, respectively).

846



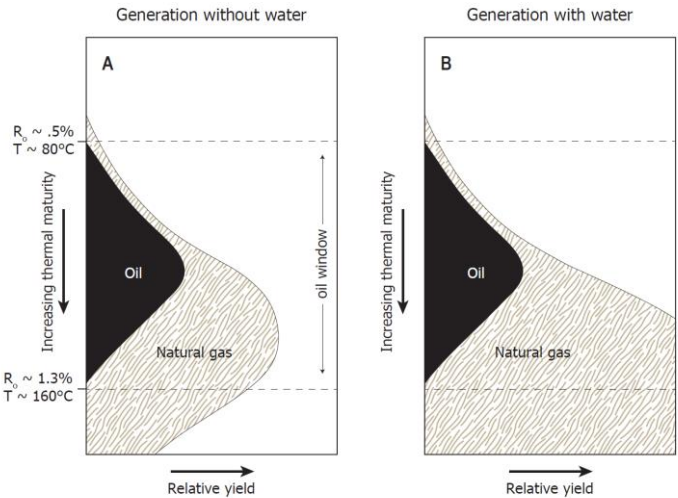
847

Fig. 67. Cartoon showing process of sequential deuteration of sedimentary kerogen and oil organic matter and petroleum along with generation of deuterated methane. Snapshots shown represent stages of (A) mild heating (incipient catagenesis); (B) moderate heating (oil generation window); and (C) extensive heating (gas window).

Formatted: Font: Bold

Formatted: Font: Bold

Formatted: Font: Bold

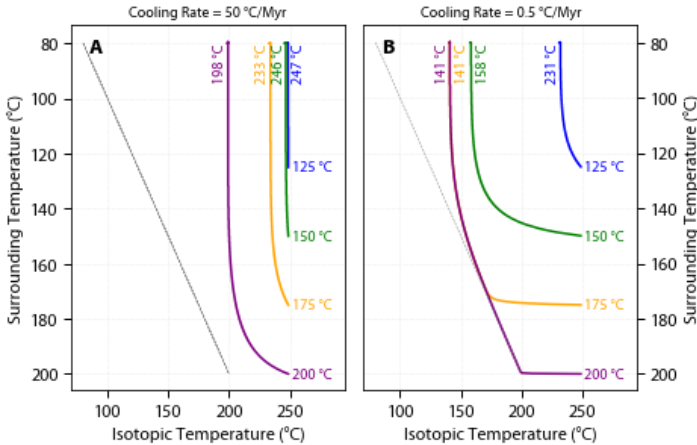


851

852 **Fig. 78.** Schematic yields of oil and natural gas when generation occurs from source rock in the absence (A) and
 853 presence (B) of water as a source of hydrogen-H. (A) Traditional model of the amount and timing of organic
 854 alteration products generated during progressive burial in sedimentary basins that assumes that hydrogen-H in
 855 organic alteration products are-is derived only from kerogen and bitumen. The form of this figure is constrained
 856 by the maturation trends shown in the Van Krevelen diagram. (B) Schematic illustration of the amount and
 857 timing of organic alteration products generated if water and minerals are allowed to contribute the requisite
 858 hydrogen-H for the formation of hydrocarbons. Illustration is after Seewald (2003) and Hunt (1996). Listed
 859 values of $\%R_o$ and temperature are from an EASY%Ro calculation applying a heating rate of $\sim 0.4^\circ\text{C}$ per Myr.

Formatted: Font: Bold

Formatted: Font: Bold



861

862 **Fig. 8.** Influence of cooling rate on the closure temperature of hydrogen isotopic exchange between methane and
 863 water. Each fluid was cooled from an initial temperature of 125, 150, 175, or 200 °C (upright numbers at right of
 864 curves) down to a final temperature of 80 °C at a rate of either (A) $-50\text{ }^{\circ}\text{C/Myr}$ (e.g., representing migration from
 865 source to reservoir), or (B) $-0.5\text{ }^{\circ}\text{C/Myr}$ (e.g., representing gradual cooling of an unconventional, source-rock
 866 reservoir from maximum burial). The initial methane was assigned an arbitrary isotopic temperature of 250 °C in
 867 all simulations ($\Delta^{13}\text{CH}_3\text{D} \approx 2.00\%$). Curves show the predicted methane isotopic temperature assuming
 868 continuous exchange with 55.5 mol/L water using the kinetic parameters for $\text{CH}_4\text{-H}_2\text{O}$ exchange from Turner et
 869 al. (2022). Final methane isotopic temperatures are shown in rotated labels at the topmost ends of curves. The
 870 dotted gray line is a 1:1 line representing thermal equilibrium with surrounding environment.

Formatted: Font: Bold

Formatted: Font: Bold

Formatted: Not Superscript/ Subscript

Formatted: Subscript

871 **TABLES**

872

873 **Table 1**

874 Elemental analysis of Eagle Ford shale powder that was either: dried but otherwise untreated (UNEX), Soxhlet-extracted
875 (EX), or extracted + decarbonated (DECA). Values represent weight percent of the material that was ingested by the
876 elemental analyzer. Data from C. Johnson, WHOI, 1996.

(wt%)	UNEX	EX*	DECA
C	12.1	11.0	6.23
H	0.38	0.25	1.24
N	0.18	0.17	0.74
S	0.37	<0.2	2.3

877 *Used in the experiment.

878

879 **Table 2**

880 Concentration of aqueous species during heating of Soxhlet-extracted Eagle Ford shale at 200 to 350 °C and 350 bar in the
 881 presence of saline D₂O fluid.

Time Pt #	Time (h)	H ₂ (μmol/kg) ^a	CH ₄ (μmol/kg)	ΣCO ₂ (mmol/kg)	CH ₄ /ΣC ₂₋₄ ^b	ΣH ₂ S (mmol/kg)	pD (25 °C) ^c
<i>Experiment begun with 52.6 g of fluid at temperature of 200 °C</i>							
1	19	BDL (<13)	1.2	4.8	0.78		
2	164	BDL (<13)	3.8	10.8	1.06		
<i>Temperature raised to 300 °C</i>							
3	191	98.0	8.7	21.9	1.68		
4	284	247	235	45.8	1.30		
5	427	392	396	65.5	1.09		
<i>Injected ~18.3 g starting fluid and raised temperature to 325 °C</i>							
6	451	477	319	44.7	1.06		
7	598	791	825	45.3	0.96		
<i>Raised temperature to 350 °C</i>							
8	617	969	1.32 × 10 ³	54.4	1.01		
9	836	1,110	3.47 × 10 ³	51.2	1.06	18.0	5.90

882
 883 Analytical uncertainties (2s) are ±2 °C for T; ±10% for H₂; ±5% for ΣCO₂, CH₄, and C₂ to C₄ hydrocarbons, ±2% for ΣH₂S;
 884 and ±0.05 units for pD. Concentrations are molar quantities per kg fluid.

885
 886 ^a Determined from thermal conductivity response calibrated against a known H₂ standard, and then multiplied by 1.35 to
 887 account for the difference in thermal conductivity between D₂ and ¹H₂ (Saxena and Saxena, 1970; Whisnant et al., 2011).
 888 ^b Calculated as the molar ratio of methane to the sum of ethane, propane, isobutane, and n-butane.

889 ^c The listed pD value was calculated from pH measured with a glass electrode: pD = pH_{measured} + 0.41 (Glasoe and Long,
 890 1960).

Figure 1

Click here to
access/download Figure; Figure 1.pdf

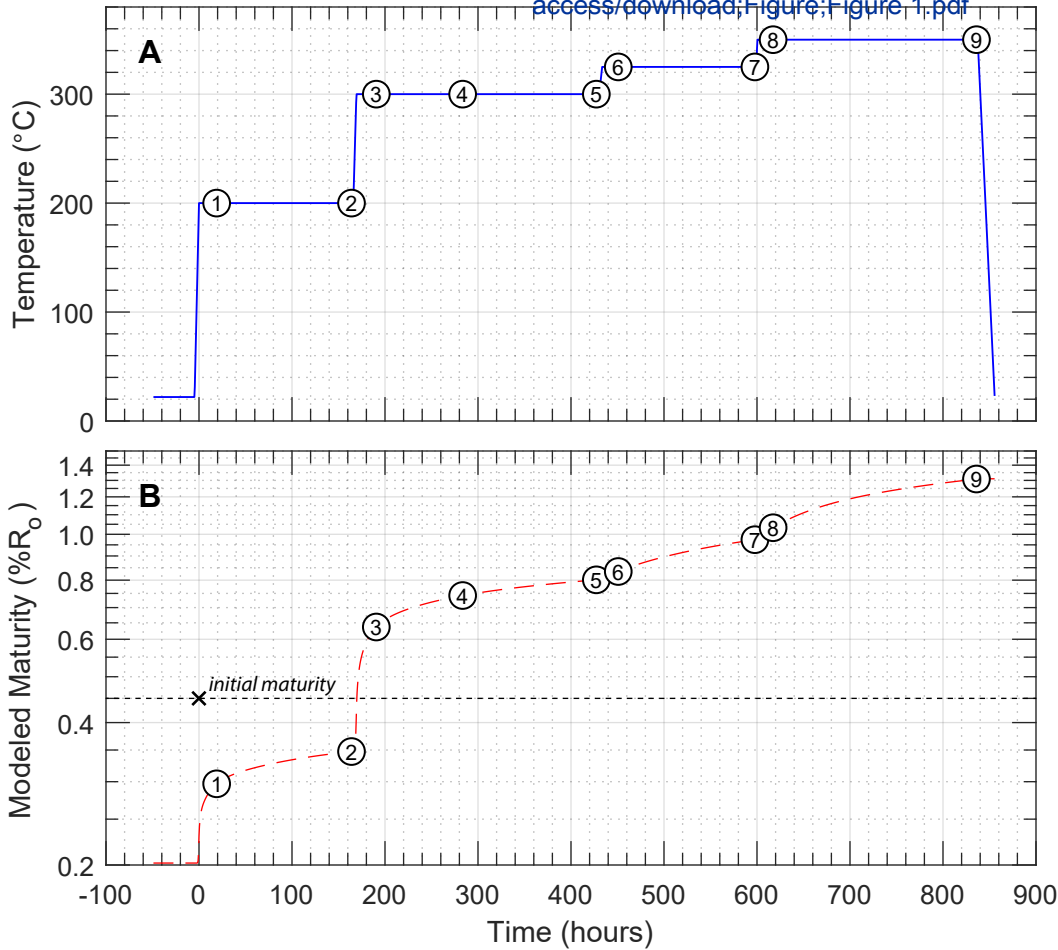


Figure 2

[Click here to access/download;Figure;Figure 2.pdf](#)

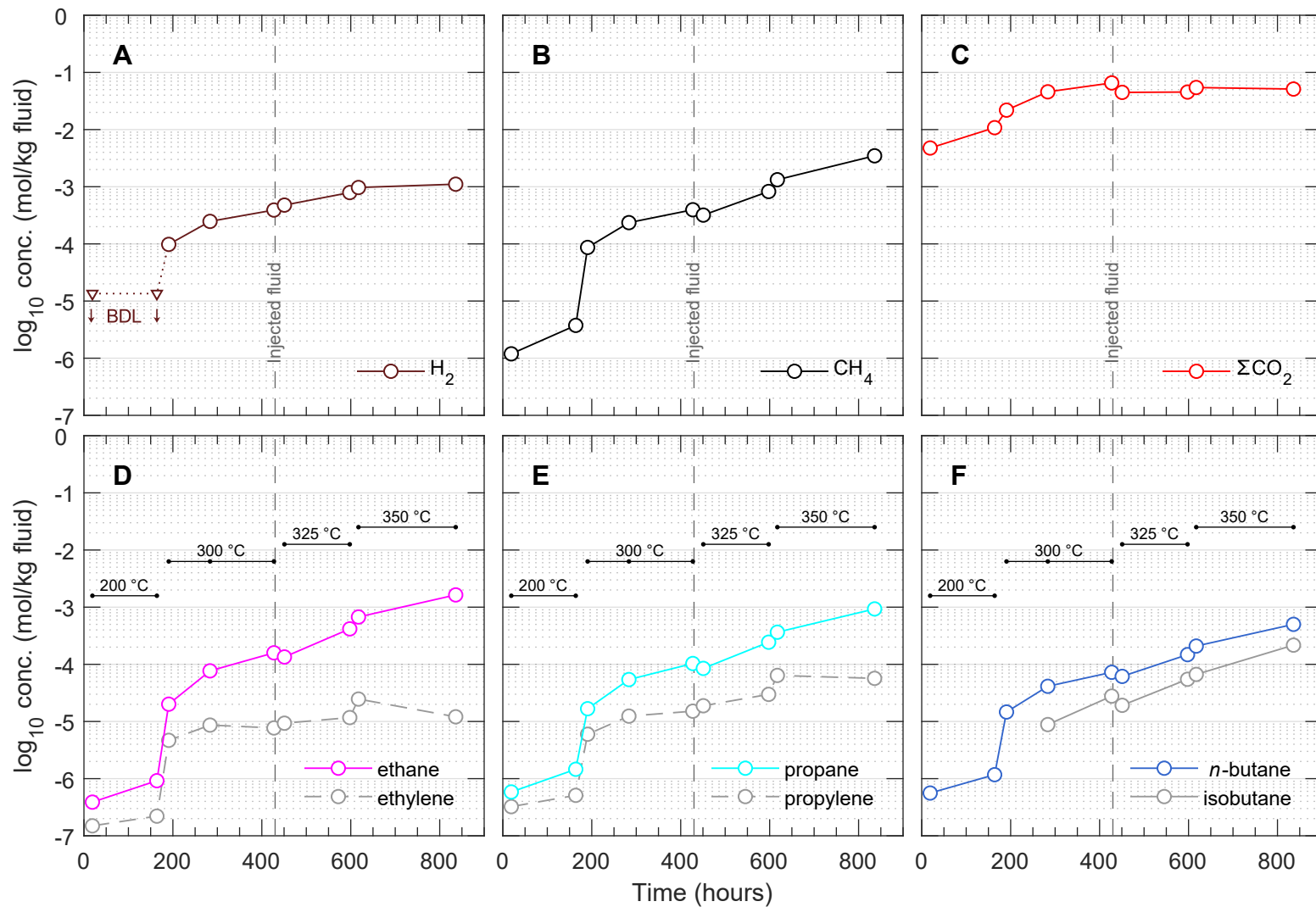
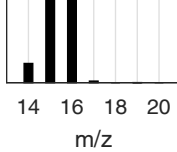
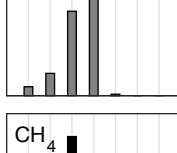
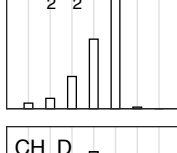
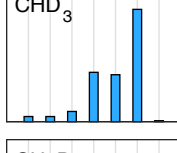
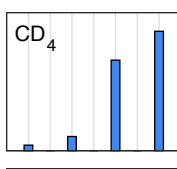


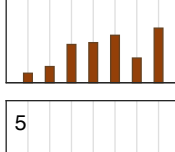
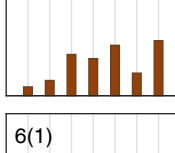
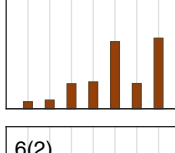
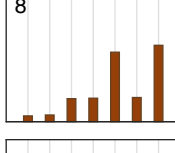
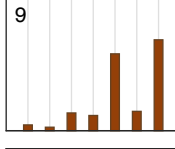
Figure 2



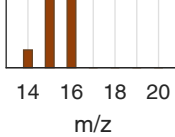
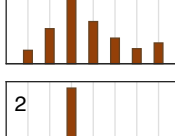
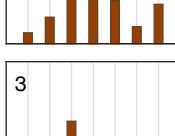
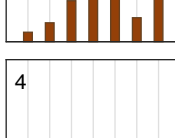
14 16 18 20

m/z

[Click here to access/download](#)



5



14 16 18 20

m/z

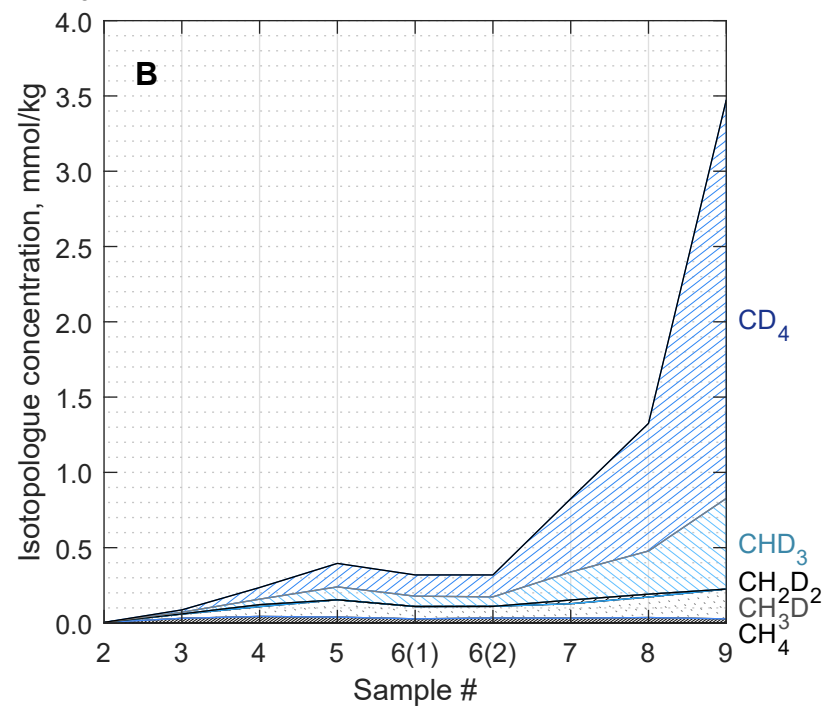
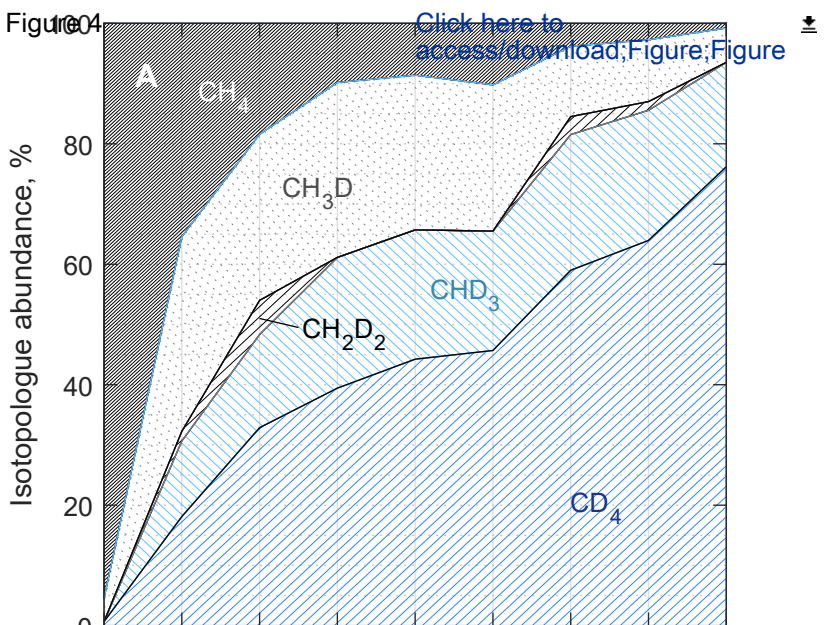


Figure 5

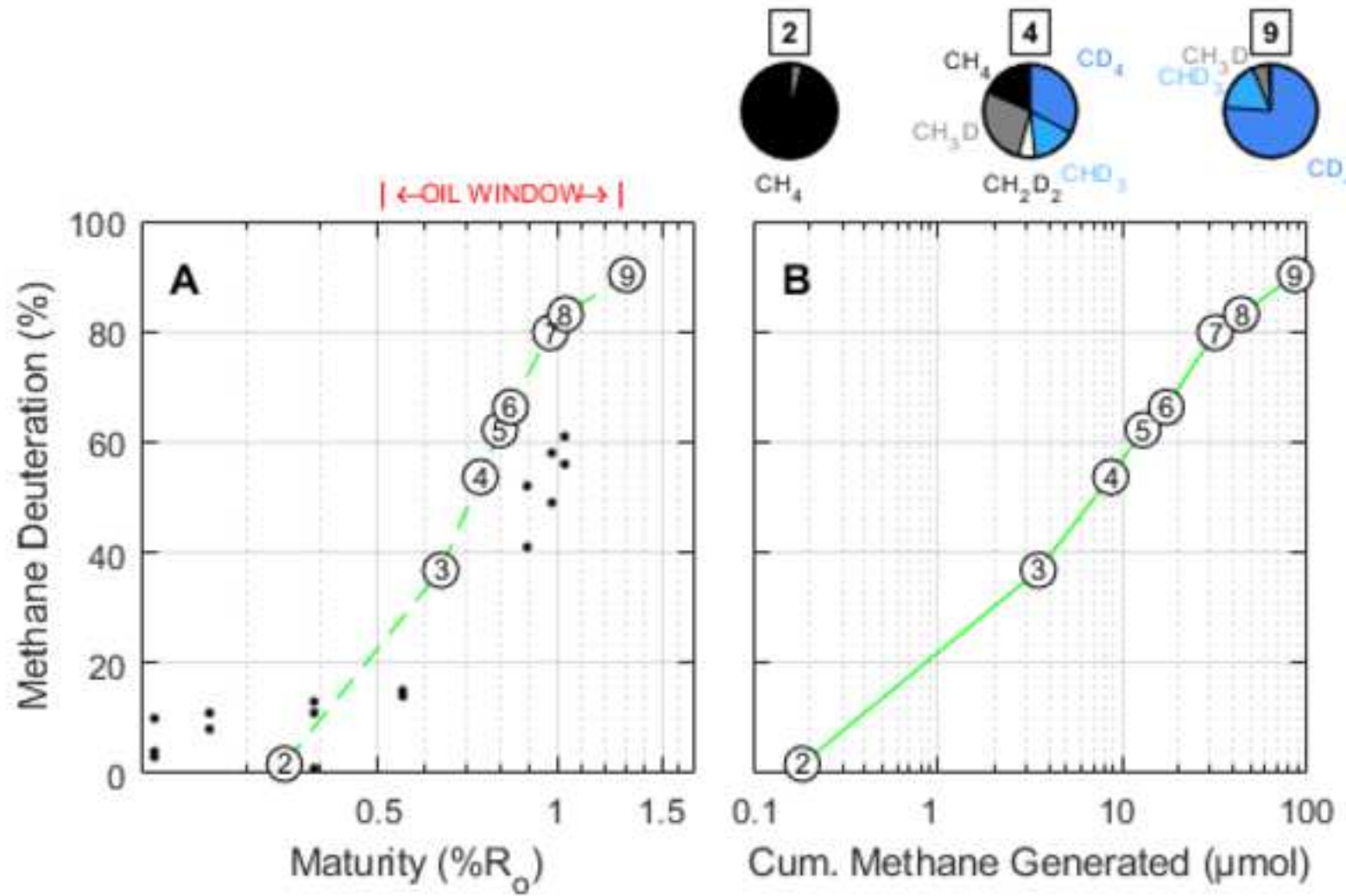
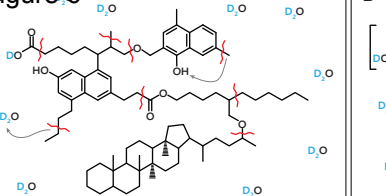
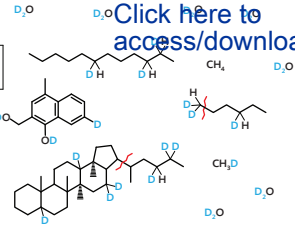
[Click here to access/download;Figure;Figure 5.png](#)

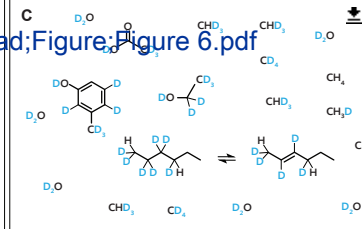
Figure 6



mild heating



moderate heating



extensive heating

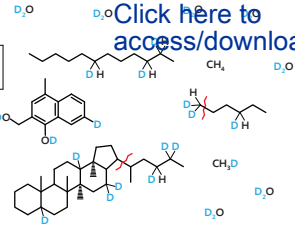


Figure 7

Generation without water

Click here to
access/download/Figure,Figure

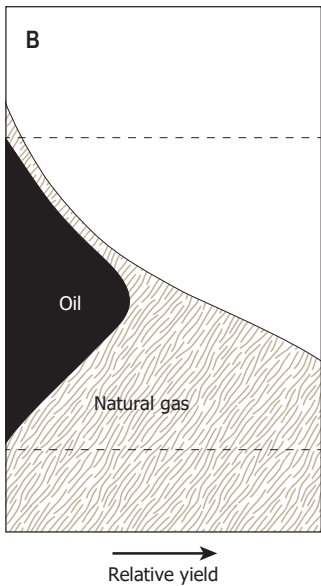
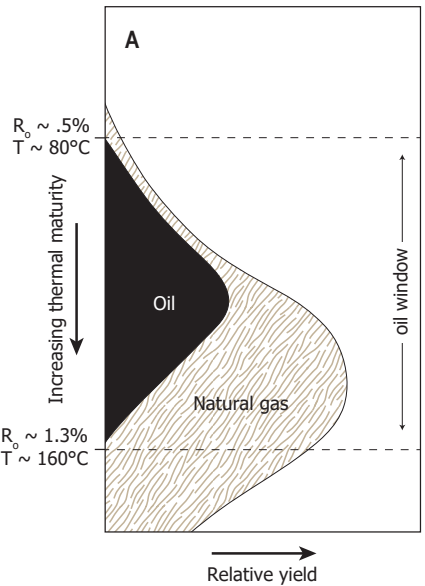
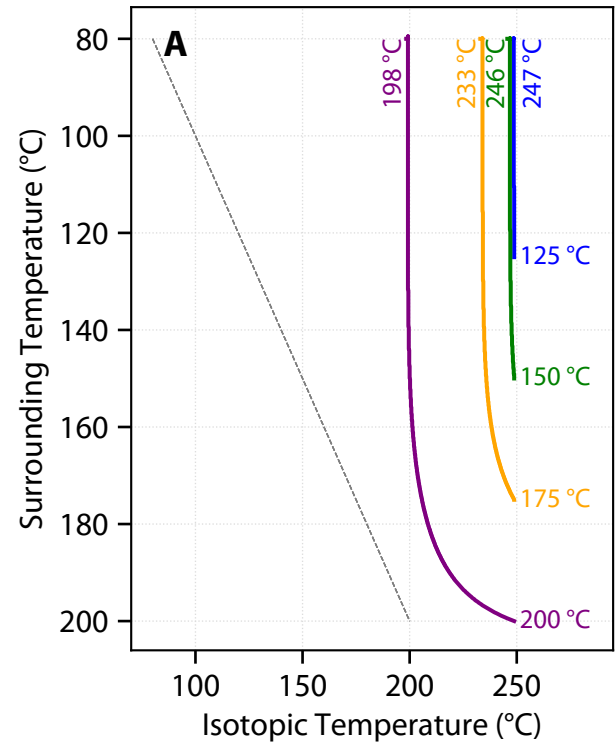


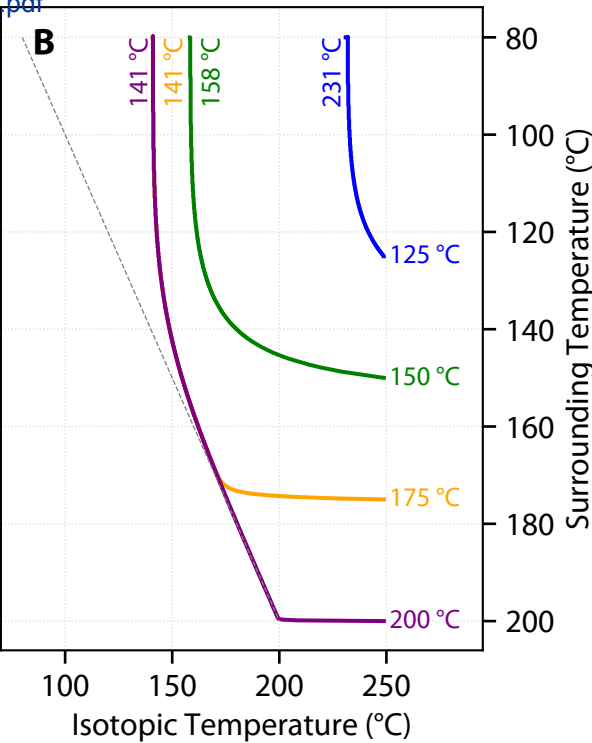
Figure 8

Cooling Rate = 50 °C/Myr



Click here to access/download Figure; Figure 8.pdf

Cooling Rate = 0.5 °C/Myr



Response to Editors

Wang et al., OG-5031R1

Ms. Ref. No.: OG-5031R1

Title: Incorporation of water-derived hydrogen into methane during artificial maturation of kerogen under hydrothermal conditions Organic Geochemistry

Dear Dr. David T. Wang,

David,

Sorry this has taken so long, but the Joe Curiale, the Associate Editor assigned to this paper, had a very difficult time getting people to agree to be reviewers. This seems to be a growing problem for all papers.

Reviewers have now commented on your paper. You will see that they are advising that you revise your manuscript. If you are prepared to undertake the work required, I would be pleased to reconsider your revised paper for publication. Reviewer #1 and the Associate Editor have attached files that you need to download from the Editorial Management system.

Authors are normally expected to provide a revised manuscript within 4 weeks. After this time the manuscript will be cleared out of the system and a "revision" after this date would have to be submitted anew and given a new tracking number. Under extenuating circumstances, the Associate Editor should be contacted with a request for an extension. Significantly delayed revisions may become superseded in the literature and require changes beyond those requested by the reviewers and Associate Editor.

For your guidance, reviewers' comments are appended below. Please note that reviewers may have uploaded files as part of the review. If this is the case, you can access the uploaded files on the Editorial Manager.

If you decide to revise the work, please submit a list of changes or a rebuttal against each point raised, a copy of the manuscript with track changes and a clean copy of the manuscript when you submit the revision. Organic Geochemistry also encourages authors to include an acknowledgement of the time and effort provided by the reviewers, whether they are anonymous or have been identified.

Yours sincerely,

Clifford C. Walters, PhD
Editor-in-Chief
Organic Geochemistry

Dear Editors,

We have addressed the comments by the AE and Reviewers below. Please see the attached revised manuscript with tracked changes, as well as a clean copy of the Manuscript. Thank you,

**David T. Wang on behalf of coauthors.
7/13/2022**

Reviewers' comments:

Associate Editor (Joe Curiale)

The original submission of your manuscript, designated OG-5031, was reviewed by Associate Editor Lloyd Snowdon prior to placing the manuscript with peer reviewers. The paper was then returned to you for revisions, which you provided. Upon receipt of the revised version – now designated OG-5031R1 – the Chief Editor placed the paper with me (J A Curiale) to serve as Associate Editor.

Before proceeding any further, let me start with an apology – for how long it has taken to get peer reviews back to you. As you may be aware, finding high-quality peer reviewers – experienced, willing and able – is tough these days; I placed more than 10 review invitations before receiving two acceptances. In the end, though, I believe we now have excellent reviews – reviews which should help you improve the paper.

Your revised version, OG-5031R1, has been reviewed by three individuals: Reviewer 1 (Daniel Dawson), Reviewer 3 (anonymous) and Reviewer 4 (J A Curiale, as Associate Editor) (not sure why a "Reviewer 2" assignment was skipped in Elsevier's Editorial Manager...). Reviewers 1 and 3 have provided comments below, and Reviewer 1 has also uploaded a marked manuscript for you to download and examine. Reviewer 4 has provided all comments on the paper directly on a marked manuscript uploaded to Editorial Manager, and available to you for download.

Reviewers 1 and 3 have recommended that the paper be "published with minor changes", and my recommendation as Reviewer 4 is essentially the same. Thus, I am recommending to the Chief Editor that the paper be revised and considered for acceptance have the revisions are examined.

All reviewers' comments are quite clear, so I will not go over them in detail here. Reviewer 1, in his marked manuscript and his comments below, makes numerous substantive and editorial suggestions, ranging from the need for consistency in units to the need for re-plotting in some cases (and combining figures) to re-wording needed for clarification. Reviewer 3 (all comments provided in detail below) also makes editorial and substantive recommendations, and provides some additional needed references. In my own review, provide on-manuscript in the uploaded file, I have made four substantive remarks as well as several editorial changes directly on the manuscript.

I encourage you to examine the reviews carefully, and hope that you are agreeable to modifying the paper by incorporating the changes recommended by the reviewers; it would certainly be a good addition to the literature, and fits well into Organic Geochemistry. Should you choose to proceed, please return (a) a track-changes version of your revisions, (b) a changes-accepted version, and (c) most importantly, a detailed cover letter describing how you have dealt with each recommendation of each reviewer. I look forward to hearing back from you, and again, apologies for the long turnaround time on this manuscript.

We appreciate the editors' efforts to locate expert reviewers and have addressed all comments individually below.

COMMENTS FROM REVIEWERS 1 AND 3 FOLLOW.

REVIEWER #1

Reviewer #1: This manuscript presents the results of an artificial source rock maturation experiment to evaluate the incorporation of water-derived hydrogen into generated methane, and discusses the implications on D/H ratios of generated thermogenic gases and hydrocarbon generation potential.

I commend the authors on submitting an extremely interesting and well written manuscript, having carried out a well conceived and designed artificial maturation experiment. I would also like to commend the authors on not only presenting their interesting experimental results in relation to H/D exchange, but also including useful and insightful commentary on the implications for natural petroleum systems. I believe this will be of significant interest to readers of Organic Geochemistry.

I have no hesitation in recommending this manuscript for publication in Organic Geochemistry, and have suggested only minor changes in the annotated PDF provided with this review. The majority of changes are cosmetic in nature, in order to follow the Organic Geochemistry style guide.

Regards,
Daniel Dawson

We appreciate Dr. Dawson's comments and have copied his comments from the uploaded PDF and address them below.

Editorial changes are made in the Word document with tracked changes.

L136: Recommend plotting the initial maturity as a horizontal line on the plot in Figure 1B.

Now plotted in revised Figure 1B.

L145: Consider using consistent units (micrmol/kg) to make it easier for the reader, i.e. 1,110 micromol/kg in this case.

Left as-is.

L180: Unpublished results

These are now published; changed to Turner et al. (2022).

L187: Consider combining Fig. 3 and 4 into a single figure

Combined into single figure. Fig 3 = new Figure 3A, and Fig 4 = new Figure 3B.

L210-211: But the source rock matrix is likely important as a catalyst for the exchange of kerogen-bound H with D₂O (prior to methane generation) - I think it's important to clarify this point.

Added as footnote 3: "While it is not an important factor in exchange between CH₄ and D₂O, the source rock matrix is likely important as a catalyst for the exchange of kerogen-bound H with D₂O (prior to methane generation), a process discussed in §3.4.2 and in Alexander et al. (1984)."

L229-230: This has been well established, recommend replacing "may have" with "have" and including some references (e.g. Schimmelman et al., 2006).

Done.

REVIEWER #3

Reviewer #3: In this study, the authors have evaluated incorporation of deuterium into C1-C6 gas products generated during closed system pyrolysis of an Eagle Ford shale sample with periodic temperature increases and sampling of a single experimental vessel. The results show that gases generated at low thermal maturities contain mostly hydrogen native to the source kerogen, but deuterium incorporation from the aqueous phase increased with increasing thermal stress. However, the pattern of deuterium incorporation followed a somewhat unexpected progression (i.e., very little CH₂D₂ relative to other isotopologues). At the highest thermal stress level, the main product was CD₄ showing substantial incorporation of aqueous hydrogen isotopes into catagenetic products. This result indicates that estimates of hydrocarbon generating potential from source rocks based on their native hydrogen content may underrepresent their true potential.

The paper is well written and presents findings that will be of great interest to the readers of Organic Geochemistry. The results are consistent with other similar pyrolysis based studies, but the focus on gas isotopologues is somewhat unique, though I refer the authors to another OG paper from Dias et al. that also showed aqueous hydrogen incorporation into generated HC gases from coal. My recommendation is that the article be Accepted after minor revisions.

We appreciate the Reviewer's comments and include several of the suggested references in the revised version.

Suggestions for edits and other comments:

Line 24: change "in" to "with"

Done.

Line 64: Dias et al. have evaluated incorporation of aqueous hydrogen into gaseous products during hydrous pyrolysis of coals to differentiate native and generated hydrocarbon gases.

We appreciate the suggested reference. The Dias et al. study is constructed differently than those cited on Line 64. The ones cited here all used D₂O as reactant, whereas the Dias et al. study used local tap water. Nevertheless, it is a study that is consistent with incorporation of water-derived hydrogen into generated thermogenic natural gases. We have added a paragraph-long discussion to the Results and Discussion section (l. 268+):

In a differently-constructed study, Dias et al. (2014) evaluated incorporation of aqueous hydrogen into gaseous products during hydrous pyrolysis of bituminous coal samples taken from the same coal seam along a transect at various distances away from an igneous intrusion (and hence with different initial R_o values ranging from 0.5 to 6.8%). After hydrous pyrolysis, measured R_o values ranged from 1.4 to 6.9%. An observed dependence of δD of CH₄ to δD of water allowed them to differentiate native (sorbed or trapped) and newly-generated (via hydrous pyrolysis) hydrocarbon gases, with almost all (>90%) of CH₄ generated from coals with initial $R_o < 2.0\%$ being of newly-generated origin. While the design of their experiment did not allow for quantification of the fractional contribution of water-derived H to the hydrogen content (and hence cannot be plotted on Fig. 5A), their results are consistent with

incorporation of aqueous hydrogen into hydrocarbon gases generated by maturation of thermally-immature organic matter.

Line 68: spell out "WHOI" on first use.

Changed.

Lines 82-85: Not sure this digression on H/C ratio of the decalcified and extracted sample is relevant.

We left this in as it gives context to the H/C ratio of the powdered source rock being elevated relative to isolated kerogen.

Line 191: Insert "it" after "While".

Done.

Line 233: consider changing ""skipped"" to "bypassed".

Done.

Line 382: How would you go about estimating the amount of additional natural gas generated by incorporation of aqueous hydrogen and what kerogen structural features do you think would be most relevant to this?

Very good question. Deuterous pyrolysis or similarly constructed experiments may shed light on ultimate yields in the presence of exogenous H donors. We also expand on the use of more sophisticated chemical kinetic simulations in l. 401-416:

Chemical kinetic models employed in the upstream oil and gas industry for exploration purposes invariably use simple, pseudo-first-order reactions. Many parallel reactions may be simulated at once to simulate different classes of kerogen or petroleum breakdown products; however, all reactions are, without exception, pseudo-first-order in the mass of remaining precursor. However, as noted in Xie et al. (2022), the rate coefficients of these notionally unimolecular reactions can be pressure-dependent, because a third-body collision may be required to remove excess energy from the excited intermediates. Therefore, an algorithmic reaction mechanism generator (RMG; Allen et al., 2012)—operating from a database of elementary reaction kinetics—may be used to determine the important reactions involved in the breakdown of kerogen and petroleum, and to estimate their rate coefficients under typical subsurface pressure & temperature conditions in active source rocks. Furthermore, water is almost invariably excluded as a reactant from computational studies of the thermal decomposition of organic matter because of the computational burden involved. Examples include Class (2015) and Gao (2016) wherein geological oil-to-gas cracking was studied by using RMG to simulate individual radical reactions involved in the pyrolysis of model organic compounds under dry (water-absent) conditions. Very recent developments in RMG now allow it to handle gas- and liquid-phase heterogeneous reactions (Liu et al., 2021). In the future it may therefore be possible to extend the aforementioned studies on pyrolysis of model compounds to include H₂O as a reactant.

As for kerogen structural features, that is beyond the scope of this work, but has been covered in various articles on AFM-IR, such as Jubb et al. (2019).

Line 420: Bern et al. have estimated water-rock ratios for shales in natural settings and found that they are several orders of magnitude lower than what is typically used in experimental shale studies.

Thanks for the reference. Added as Line 424, “By contrast, water:rock ratios for shales existing in nature (0.003:1 to 0.23:1; Bern et al., 2021) are several orders of magnitude lower than those used in experiments.”

Line 432: Referring back to my comment on Line 382, I think if you were to do similar experiments on a variety of immature kerogen isolates from different environments and containing OM from different sources that were well characterized (NMR, FTIR, XPS, etc.) this could be determined. Kelemen et al. present a range of kerogen types and spectroscopic properties that could perhaps be used in a modeling study incorporating kerogen structural modeling and simulated hydrous pyrolysis conditions.

Indeed. This is an ExxonMobil (New Jersey lab) study that is an offshoot of the same project from which CS-CYM came. Unfortunately, to my (DTW's) knowledge this kind of work is no longer done at ExxonMobil. It will have to be followed up elsewhere.

REVIEWER #4

Reviewer #4: This document contains all review comments by J A Curiale on the manuscript (Wang et al.) "Incorporation of water-derived hydrogen into methane...". Changes to the text are made in lower case on the manuscript; comments to the authors are made in UPPER CASE on the manuscript and in the numbered list below.

This paper concerns the presence of deuterium in methane generated during hydrous pyrolysis of extracted Eagle Ford rock in a D2O-rich environment, and interpretations of methane origin based on results. It adds weight to the idea that water in the petroleum system is, indeed, a critical element in natural gas generation. The paper is well-written and well-reasoned, and should be published after incorporating the minor comments suggested below as well as those of peer reviewers.

We thank Dr Curiale for his comments and have incorporated them into the revised manuscript.

1. The experiment described here was conducted on a solvent-extracted rock sample. However, the authors sometimes refer (in the text) to changes occurring in kerogen. Because 'kerogen' is, in many ways, a laboratory-created product (concentrated insoluble organic matter), I recommend that instead of referring to the experimental material as 'kerogen' it should be referred to as 'extracted rock'. Indeed, it's possible (likely?) that using actual kerogen rather than extracted rock in this experiment would have yielded different results. [It is also interesting to speculate on how your results may have differed if you had used crushed-but-not-powdered extracted rock for the experiment. As you infer a few paragraphs before your Conclusions section, a mono-layer of water on clay particles could have had a significant effect. Indeed, it may have been the origin of dominantly undeuterated methane in the early stages of the experiment.]

We have replaced or clarified a number of instances where the word 'kerogen' is used to refer to the solvent-extracted rock powder. It now appears as "powdered solvent-extracted source rock" or some variant of this, to prevent confusion with a *kerogen isolate*. We have retained the use of the term "kerogen" in its meaning as 'high-molecular weight, insoluble sedimentary organic matter'. Where appropriate, we have specified the presence of additional types of organic matter, for example: "kerogen and bitumen (or petroleum) maturation".

We have also changed the title of the manuscript to: "Incorporation of water-derived hydrogen into methane during artificial maturation of source rock under hydrothermal conditions"

We added the point about residual water contributing to undeuterated methane in lines 441-444:

A residual water monolayer on clay particles, if present, might be responsible for some of the undeuterated methane in the early stages of our experiment. If this is the case, using crushed rock instead of rock powder in the experiment might yield yet higher proportions of C¹H₄ in the earlier samples.

2. The presence of ethylene and propylene in the experimental measurement at 200C is curious – makes me wonder if these are, at least to some extent, indigenous (occluded; adsorbed) in the extracted rock from the start, rather than generated thermally in the experiment. In footnote 3,

the authors note (and discount) the analogous possibility involving methane. The measurable content of EOM recovered from solvent extraction of lab-prepped kerogen, which has already been solvent-extracted to generate the extracted rock from which the kerogen is prepared via acid treatment, suggests the inefficiency of a single round of solvent extraction of the starting rock.

It is possible that ethylene and propylene could be partially indigenous. We now note this in l. 163-165: “Some portion of the $\sim 10^{-6.5}$ mol/kg of these alkenes present at time point #1 could have been indigenous to the source rock (i.e., adsorbed and leached out during initial heating).”

3. A “blank run” (see authors’ footnote 4) would have served to address the water-methane exchange question as well as other issues (I have a vague memory that Tom Hoering tried something like this many years ago).

Yes, though this is somewhat unnecessary now given new experimental data from Turner et al. (2022) directly measuring the rate of isotopic exchange between CH₄ and H₂O (it is slow and insignificant relative to lab experiment timescales).

4. In section 3.4.3 the authors suggest that CH₄ is isotopically frozen in conventional reservoirs, given that these reservoirs are commonly at temperatures less than the source rock generation temperature. However, they appear to contrast this situation with that of unconventional reservoirs (source-rock reservoirs). Such a distinction is hard to support, though, because most commercial source-rock reservoir systems are not at maximal burial depths, indicating that generation temperatures in these systems, as for “conventionals”, are still greater than present-day reservoir temperatures.

This point requires elaboration. It is important to consider that the *cooling rate* has a substantial effect on closure temperatures of CH₄-H₂O isotopic exchange. In conventional petroleum systems where migration occurs soon after generation, “quenching” of the exchange reaction will likely occur once the temperature of the migrating fluid drops below ~170 C, because migration is likely to occur to a shallower, cooler trap within a short period of time (<0.2 Myr per Jung et al., 2018, implying a cooling rate of ~250 °C/Myr or faster). A minimum, conservative estimate of the cooling rate during migration is 50 °C/Myr (5x slower than Jung et al.). We constructed a model to simulate the cooling of a migrating natural gas as it travels from a hot source rock to a cooler, conventional reservoir using this cooling rate. The model results are shown in Fig. 8A and are reproduced below.

We also performed a similar simulation using a cooling rate of 0.5 °C/Myr, which is approximates the thermal regime experienced by source-rock reservoir that has reached maximum burial and is cooling gradually (Fig. 8B). With the longer exposure time (millions of years) a methane molecule trapped within a source-rock reservoir can remain between 160 and 130 °C, substantially more exchange is expected to occur.

We have added this discussion in l. 356-362, 375-378, and footnote 7, and reference the new Figure 8.

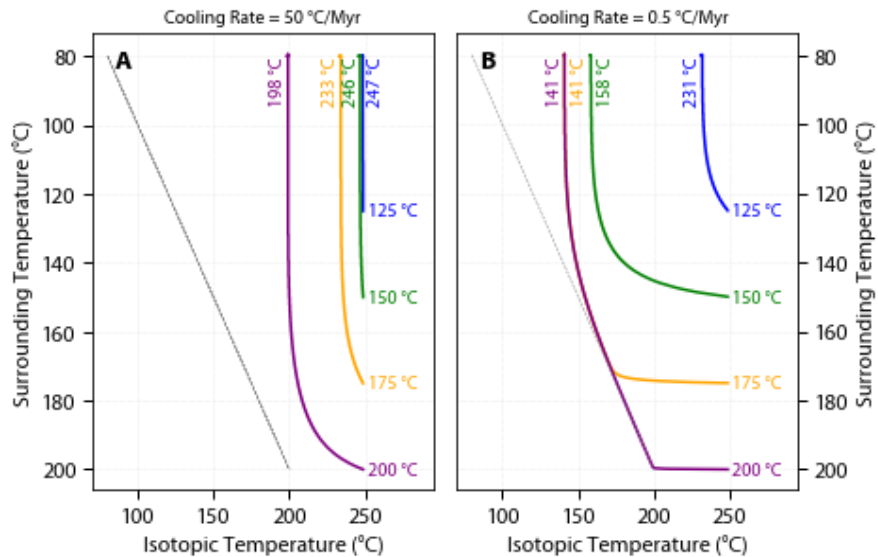


Fig. 8. Influence of cooling rate on the closure temperature of hydrogen isotopic exchange between methane and water. Each fluid was cooled from an initial temperature of 125, 150, 175, or 200 °C (upright numbers at right of curves) down to a final temperature of 80 °C at a rate of either (A) $-50\text{ }^{\circ}\text{C/Myr}$ (e.g., representing migration from source to reservoir), or (B) $-0.5\text{ }^{\circ}\text{C/Myr}$ (e.g., representing gradual cooling of an unconventional, source-rock reservoir from maximum burial). The initial methane was assigned an arbitrary isotopic temperature of 250 °C in all simulations ($\Delta^{13}\text{CH}_3\text{D} \approx 2.00\text{\textperthousand}$). Curves show the predicted methane isotopic temperature assuming continuous exchange with 55.5 mol/L water using the kinetic parameters for $\text{CH}_4\text{-H}_2\text{O}$ exchange from Turner et al. (2022). Final methane isotopic temperatures are shown in rotated labels at the topmost ends of curves. The dotted gray line is a 1:1 line representing thermal equilibrium with surrounding environment.

Declaration of interests

The authors declare that they have no known competing financial interests or personal relationships that could have appeared to influence the work reported in this paper.

The authors declare the following financial interests/personal relationships which may be considered as potential competing interests: